IOWA STATE UNIVERSITY
Digital Repository

Retrospective Theses and Dissertations

Iowa State University Capstones, Theses and Dissertations

1995

An investigation of the mechanics of rollover for cars and light trucks

Yvonne Irene Katherine Lund
Iowa State University

Follow this and additional works at: https://lib.dr.iastate.edu/rtd

 Part of the Applied Mechanics Commons

Recommended Citation
Lund, Yvonne Irene Katherine, "An investigation of the mechanics of rollover for cars and light trucks " (1995). *Retrospective Theses and Dissertations*. 10930.
https://lib.dr.iastate.edu/rtd/10930

This Dissertation is brought to you for free and open access by the Iowa State University Capstones, Theses and Dissertations at Iowa State University Digital Repository. It has been accepted for inclusion in Retrospective Theses and Dissertations by an authorized administrator of Iowa State University Digital Repository. For more information, please contact digirep@iastate.edu.

www.manaraa.com

INFORMATION TO USERS

This manuscript has been reproduced from the microfilm master. UMI films the text directly from the original or copy submitted. Thus, some thesis and dissertation copies are in typewriter face, while others may be from any type of computer printer.

The quality of this reproduction is dependent upon the quality of the copy submitted. Broken or indistinct print, colored or poor quality illustrations and photographs, print bleedthrough, substandard margins, and improper alignment can adversely affect reproduction.

In the unlikely event that the author did not send UMI a complete manuscript and there are missing pages, these will be noted. Also, if unauthorized copyright material had to be removed, a note will indicate the deletion.

Oversize materials (e.g., maps, drawings, charts) are reproduced by sectioning the original, beginning at the upper left-hand corner and continuing from left to right in equal sections with small overlaps. Each original is also photographed in one exposure and is included in reduced form at the back of the book.

Photographs included in the original manuscript have been reproduced xerographically in this copy. Higher quality 6" x 9" black and white photographic prints are available for any photographs or illustrations appearing in this copy for an additional charge. Contact UMI directly to order.

UMI

A Bell & Howell Information Company
300 North Zeeb Road, Ann Arbor, MI 48106-1346 USA
313/761-4700 800/521-0600

An investigation of the mechanics of rollover for cars and light trucks

by

Yvonne Irene Katherine Lund

A Dissertation Submitted to the

Graduate Faculty in Partial Fulfillment of the

Requirements for the Degree of

DOCTOR OF PHILOSOPHY

Department: Mechanical Engineering
Major: Mechanical Engineering

Approved:

Signature was redacted for privacy.

In Charge of Major Work

Signature was redacted for privacy.

For the Major Department

Signature was redacted for privacy.

For the Graduate College

Iowa State University
Ames, Iowa
1995

UMI Number: 9531766

UMI Microform 9531766
Copyright 1995, by UMI Company. All rights reserved.

This microform edition is protected against unauthorized
copying under Title 17, United States Code.

UMI

300 North Zeeb Road
Ann Arbor, MI 48103

TABLE OF CONTENTS

LIST OF TABLES

LIST OF FIGURES

LIST OF NOMENCLATURE

T	Track width
h	Center of gravity height
R	Distance from cg to impact corner, $\sqrt{(T/2)^2 + h^2}$
W	Total weight
W_u	Total unsprung weight
W_s	Total sprung weight
m	Total mass
M	Total mass
M_u	Total unsprung mass
M_s	Total sprung mass
g	Gravitational constant
h_1	Distance from ground to unsprung mass center
h_2	Distance from unsprung mass center to the roll center
h_3	Distance from roll center to the sprung mass center
a	Distance from sprung mass center to front wheel centerline
a	Dimensionless constant
b	Distance from sprung mass center to rear wheel centerline
b	Height of rigid block

c	Width of rigid block
$\overline{\phi}$	Roll gain
I_o	Roll moment of inertia about impact point
I_{cg}	Roll moment of inertia about center of gravity
V, v	Lateral velocity
v_{ro}	Minimum lateral velocity for curb trip rollover
v_e	Minimum lateral velocity for rollover using conservation of energy
TTR	Tilt Table Ratio
CSV	Critical Sliding Velocity
SSF	Static Stability Factor
SPR	Side Pull Ratio or Cable Pull Test
RPM	Rollover Prevention Metric
V2	Minimum lateral velocity for two-quarter turns
V2H	Minimum lateral velocity to yield two-quarter turns under hinge-impact conditions
V2I	Minimum lateral velocity to yield two-quarter turns under ice-impact conditions
A_y	Limit lateral acceleration
$\overline{A}_y$	Steady state lateral acceleration
a_{ro}	Steady state lateral acceleration for rollover
F_y	Lateral force in two-quarter-turn impact
F_z	Vertical force in two-quarter-turn impact
F_t	Tripping force in two-quarter-turn impact
N_l	Force at left tire

N_r	Force at right tire
μ, μ_y	Coefficient of friction of tire/road surface
θ	Roll angle
$\overline{\theta}$	Roll angle at take-off in two-quarter turn analysis
β	Sideslip angle
ζ	Damping constant
ϕ	Roll angle during roof impact
ϕ	Sideslope angle
$\overline{a}$	Distance that outside tire force deflects under vehicle for each g of lateral acceleration
$\overline{b}$	Distance the mass center moves to outside of turn for each g of lateral acceleration
$\overline{C}$	Total energy
$\overline{H}$	Vertical distance from cg to top
$\overline{R}$	Total distance from cg to top impact corner, $\sqrt{(T/2)^2 + \overline{H}^2}$
y_o'	Sliding distance of the contact point during rollover
H'	Distance of cg above the roll axis
K_ϕ	Sprung mass roll gradient
h_{roll}	Location of the roll axis at the longitudinal cg location
FARS	Fatal Accident Reporting System
CARS	Crash Avoidance Rollover Study
NCSS	National Crash Severity Study
NASS	National Accident Sampling System

ACKNOWLEDGEMENTS

I would like to express my gratitude to my advisor James E. Bernard for his support and encouragement in my Ph.D. program. I am also grateful to Professors Bernard, Flugrad, McConnell, Pierson, and Rogge for their input while serving on my doctoral committee.

In addition, I would like to thank my colleagues for their camaraderie. I would also like to thank my friends for their encouragement and for always being there.

Finally, I wish to thank my family for their love and support.

CHAPTER 1. INTRODUCTION

Rollover of cars and light trucks is of great interest to vehicle designers in the automotive industry and to regulators in government agencies. This interest derives in large part from the consequences of rollover accidents. For example, the Fatal Accident Reporting System (FARS) data indicates that, in 1990, about 15,900 people died in the United States in single vehicle crashes. Of these, 8100 people (51%) were fatalities which included rollover [1].

There has been interest in the topic of vehicle rollover for many years. Published work on this topic appeared as early as the 1950s and continues through today. This thesis studies the various types of rollover including smooth surface, curb tripped, and furrow tripped events. It analyzes metrics which attempt to measure rollover propensity. Simulation results based on very simple and more complex models are used as an aid in understanding rollover.

The goal of this thesis is to analyze the mechanisms behind vehicle rollover, to evaluate rollover propensity measures, and to investigate vehicle factors which may contribute to rollover behavior.

Chapter 2 presents a literature review. Chapter 3 presents background information on vehicle rollover and rollover mechanisms and motivates more detailed analyses that follow. Chapter 4 presents a study of smooth surface, untripped rollover events

including steady turns, transient maneuvers entailing turning without braking, and braking in a turn. Chapter 5 addresses curb- and furrow-tripped rollover. Models of increasing complexity shed light on the complex rollover dynamics. Particular attention is paid to recently proposed measures of roll stability, tilt table testing and critical sliding velocity calculations. These one-quarter-turn analyses are then extended to two-quarter-turn calculations, or so-called roof hit scenarios, in both the curb and furrow tripping analyses. Chapter 6 presents a sensitivity analysis on both smooth road and tripped rollover with a view toward understanding which vehicle characteristics are most important. Chapter 7 presents findings and conclusions.

CHAPTER 2. LITERATURE REVIEW

As early as the 1950s, researchers investigated the relationship between highway roadside design and vehicle rollover accidents. Stonex [2] discussed the importance of eliminating obstacles such as trees and modifying the design of standard traffic signs and lights close to the highway in order to decrease collisions. He addressed the geometry of ditches and related vehicle stability factors to the slope of the roadsides and the coefficient of friction of the roadside surfaces. He also reported on full-scale guardrail impact tests to address guardrail end installations to minimize collision damage to vehicle and to prevent vehicle rollover due to ramping.

Kemp and Neilson [3] discussed the overturn of a vehicle in braking tests on a high coefficient of friction surface. They considered rear-wheels-locked maneuvers which caused the car to spin.

Ford and Thompson [4] developed a model which quantifies the potential for a vehicle traveling on a circular track to roll. They attempted to validate their analyses using video postprocessing of vehicle tests.

In the late 1960s, Mackay and Tampen [5] investigated single vehicle rollover accidents in England. The rollovers occurred either as a result of striking an obstacle or another vehicle. The authors analyzed a sample of 89 vehicles ranging from cars to light vans. They indicated that more than half the rollovers involved no substantial

impacts either with other cars or with roadside obstacles. Approximately one-third of rollovers were generated by primary impact, usually with another vehicle.

In 1971, Larson and Liljedahl [6] presented a mathematical model for simulating sideways tractor maneuvers and to predict when rollover would occur. The model considers tire and tractor parameters as well as tractor speed and turning radius, the sideslope angle, bump height, and the lateral forces on the tires. The simulations were compared with tractor testing, with the simulations predicting tractor overturns for less severe conditions than those which were necessary to overturn the tractor. The authors believed that a better soil-tire relationship would improve the correspondence between the simulation and the test results.

In 1972, Hight, Siegel, and Nahum [7] studied the injury type, severity, body region, frequency of injury, and the injury mechanism in rollover accidents. The authors used field collision studies for 139 vehicles involved in rollover accidents in the late 60's and early 70's. They found that sixty-five percent of the rollovers were single-vehicle accidents which were generally initiated at speeds in excess of 50 mph. There was a high incidence of "broadsliding" off a highway due to locked wheel braking leading to loss of directional control. They also found that injury severity was primarily dependent on whether the occupant was ejected or remained contained in the vehicle and whether or not the vehicle hit an object during the rollover event.

Reference [7] held the view that the rollover potential was more dependent on the tripping mechanism than on vehicle dimensions. In their study the primary factor causing vehicles to roll was the lateral force at the wheels which caused the vehicles to be tripped. The secondary factors appeared to be dependent on the type of rear suspension used, the location of the center of gravity, the condition of the suspension,

springs, shock absorbers, and tires, as well as the vehicle's speed.

In 1972, Wilson and Gannon [8] gave a brief history of rollover testing including pushing vehicles down hills, performing both spiral ramp and the so-called curved rail and ramp rollover tests, and inducing smooth surface rollovers. They presented a dolly-based rollover test procedure. In investigating roof strength, they found no correlation between increased roof crush and increased head injury or overall injury.

In 1973, Jones [9] presented a simple model for a vehicle overturning upon hitting a curb. This one degree of freedom model, which neglects the vehicle suspension and tires, yielded an expression for the minimum lateral velocity for vehicle rollover resulting from curb impact. Jones also performed an analysis which included the vehicle's suspension and shock absorbers. The curb trip motion is split into three stages to take into account (1) the impulsive motion of the sprung mass rotation about the total roll center after the unsprung mass impacts the curb (the unsprung mass is assumed to be at rest without rotation about the impact point), (2) the reduced angular velocity which occurs when the springs and shocks absorb energy until the sprung mass hits the bump stop of the suspension, and (3) the motion immediately after the sprung mass strikes the bump stop. Vehicle parameters for a medium sized passenger car were substituted into the two models. The complex model yielded a roll velocity about 15% higher than the simple model.

In 1975, Jones [10] analyzed a vehicle as it hit a curb. The tangential and normal impulses were derived and used in defining the suspension compression velocity and sliding velocity of the vehicle after impact. The author then utilized a graphical method as outlined by Goldsmith [11] to predict the velocity components during and at the end of the collision based on an assumed coefficient of restitution, e, and

the coefficient of friction, μ. The results of this analytical method were favorably compared to films (48 frames/second) of a passenger car as the vehicle hit a curb and rolled over.

McHenry [12] considered the validity of relationships used for estimating vehicle speeds in rollover accidents. He addressed rollover due to curb or obstacle contact using conservation of energy and conservation of angular momentum. Momentum-based analysis yielded rollover speeds about twice as high as energy-based analysis. (Conservation of energy is inappropriate for modeling scenarios involving trip mechanisms because energy is not likely to be conserved across the impact.) McHenry also addressed rollover without obstacle contact, including the effect of suspension pre-load due to roll and buildup of yaw acceleration in lateral sliding. He presented simulation results computed using Highway-Vehicle-Object Simulation Model software, which was the most complex vehicle simulation of that era.

In 1976, Bickerstaff [13] discussed the relationship between rollover and the results of static cable pull tests. He also addressed lateral tripping velocity as postulated by Jones in Reference [9] for curb tripped rollover. Bickerstaff stated that lateral velocities calculated through this equation are too low. However, in his assumption of the mass moment of inertia about the impact point, Bickerstaff utilized the parallel axis theorem and neglected the vehicle's roll moment of inertia about its center of gravity. As a result his calculations yield velocities about 15% lower than the lateral tripping velocities calculated by Jones.

In 1978, Rice, Segal, and Jones [14, 15] reviewed the involvement of rollover in accidents and investigated untripped, smooth flat surface rollover response of automobiles. Full-scale experiments using seven vehicles were performed. (All models

were early 1970's vehicles, including a Ford Pinto and F-100 Truck, a Pontiac Trans-Am, a Dodge Coronet, an American Motors Gremlin, a Chevrolet Brookwood station wagon, and an Oldsmobile Toronado.) Four primary control input patterns, including reverse steer, reverse steer and braking, a slalom maneuver, and a trapezoidal steer input, were varied in magnitude and timing. Variations on these basic maneuvers included steering actions of fixed, free, and return-to-zero operation, test speeds ranging from 25 to 45 mph, constant and closed throttle control, a range of steering input rates, and combinations of inputs. On board instrumentation measured speed, steering input angle, lateral acceleration, roll angle, roll angular rate, and yaw rate.

The authors performed over 500 test runs varying the configuration and operation of each of the vehicles. The only vehicle which rolled over was the 1974 Ford Pinto, with its shock absorbers removed and with added roof weight, in the simple reverse steer maneuver in the speed range of 33-35mph. (This vehicle was used in more than 200 test runs, and later this rollover response could not be reproduced.) The authors stated that they could not devise a general test procedure for producing vehicle rollover under realistic flat-surface conditions. They found that they could not determine one set of operating values for speed, control input characteristics, etc., which would make all vehicle configurations roll over. But they did conclude that T/2h is closely related to vehicle rollover resistance (T is the vehicle's track width and h is the center of gravity height). Furthermore, they concluded that roll resistance can be degraded by design and operational features such as worn suspension elements (shock absorbers), short travel distance for compression bump stop contact, and spiked application of brakes at conditions of maximum cornering.

Rice et al. also simulated rollover using the Highway-Vehicle-Simulation Model

(HVOSM) and a modified version of NHTSA's Hybrid Vehicle Handling Program (HVHP) to handle large pitch and roll angles. Both software packages were unable to simulate the rollover event that was observed experimentally. The authors claimed that the tire model was insufficient and that vehicle characteristics were modified in the full-scale experiments due to the test procedures and were not taken into account in the simulations.

Fujiwara [16] discussed J-turn test results performed at the Nissan Proving ground to analyze the overturning phenomena. He noted that, in most cases, vehicle overturn occurs after a time delay in an uncontrollable skid caused by severe steering input. He also noted that the direct cause of overturn is largely due to changes in the friction coefficient of the road surface, such as hitting a curb, riding into sand, or rim contact with the road surface.

The author then gave results of full-scale testing of a Datsun 510 and 1200. Using ESV specifications for the J-turn, neither vehicle rolled over, even with a slip angle of 30 to 40 degrees on the Datsun 510. After applying weights to the roof of each vehicle, and therefore increasing the cg height, both vehicles overturned in a J-turn. The tests were run at 110 km/h (68 mph).

Macmillan [17] addressed the dynamics of vehicle collisions, ranging from frontal collisions to curb tripping. He derived an equation for the critical sliding velocity (CSV) for a vehicle impacting a rigid barrier. This analysis takes into account the coefficient of restitution of the curb impact.

Malliaris et al. [18] studied single and multiple car crash accident data of the late 1970s. Their data was based on early 1970s car model years. They used National Crash Severity Study (NCSS) data, Fatal Accident Reporting System (FARS), and

National Accident Sampling System (NASS).

The authors divided all cars into curb weight categories and normalized the data by obtaining the number of cars registered for use on U.S. roads in each weight category. They concluded that car size has an influence on crash severity and on the rate of involvement in accidents, with smaller cars having a higher rate of involvement.

They also examined three additional factors, alcohol involvement, young male drivers and older model year cars. The authors found no significant difference in their analysis when including or excluding these three factors.

The authors addressed pre-crash conditions of cars, light trucks and vans. They discussed "no control" before the accident, which includes skidding front, skidding sideways and spinning, and "straight" before running off the road conditions. The factor that distinguished the "straight" from the "no control" conditions is that in "straight" crashes the driver has the option of controlling the vehicle, while in the "no control" conditions, that option was no longer available. For their sample, the authors found that skidding and spinning collectively account for about 50 percent of pre-crash conditions in all single car accidents and in all single light truck and van accidents. They found skidding sideways to be the most frequent of the "no control" conditions and the principal contributor to side impacts and rollovers, and the incidence of the "no control" condition to be sensitive to car size and to be the principal contributor to the higher incidence of lighter cars in single car accidents. They also concluded that over 80 percent of rollovers in single vehicle accidents are initiated off the road, with curb impact involved in only 10 percent of the rollovers.

Brown, Stansifer, and Guenther [19] studied rollover as a result of sliding sideways and striking a curb. The authors examined the literature and addressed the two-

dimensional analysis postulated by McHenry [12] and Rice, Segal, and Jones [14, 15] using conservation of energy or conservation of momentum. The authors state that both of these analyses underestimate the minimum lateral velocity for rollover. They performed full-scale curb vehicle tests with a 1977 Chevrolet Chevette. The vehicle was pulled with four wheels in contact with the "road" surface angled at 15 degrees into the curb. The vehicle was released 4 feet from the curb with enough lateral velocity so that the vehicle struck the curb at 25 mph, at which time the vehicle rolled over. (Calculations based on conservation of momentum found the minimum lateral velocity to be 11.66 mph.) The authors did not run the full-scale test at velocities less than 25 mph to find the minimum trip velocity of the 1977 Chevrolet Chevette.

Orlowski, Bundorf, and Moffatt [20] investigated roof strength on rollover protection to see whether there was a relationship between increased roof strength and increased safety. The tests were conducted through eight lateral dolly rollover tests on 1983 Chevrolet Malibus at speeds of 32 mph. The basis of the study was to compare the rollover maneuvers of four of the vehicles with standard production roofs with four of the vehicles with rollcages added to the roof structure. Their results indicated that (1) roof strength was not an important factor in the mechanics of head neck injuries in rollover collisions for unrestrained occupants, (2) there was no significant difference in the occupant kinematics resulting from rollcaged and standard roof vehicles, and (3) that there was no reduction in the incidence or severity of head neck injuries in the rollcaged cars compared with the standard roof vehicles.

DeLeys and Brinkman [21] reviewed the guidelines for the design of roadside features and their modification to reduce the incidence of single vehicle rollovers. They used a modified version of the Highway-Vehicle-Object Simulation Model (HVOSM)

to simulate and predict the dynamic responses of representative small and large automobiles across various roadside terrain. Output from the modified HVOSM software was compared with full-scale testing of an instrumented VW Rabbit. The authors then simulated two small cars and one large car to examine the rollover tendencies of vehicles traversing various sideslope, fill-embankment, and ditch configurations.

The authors concluded that (1) 30% slope embankments are "marginally safe", and should be firm and smooth to prevent surface irregularities and to minimize the potential for the vehicle's tires to dig into the ground. (2) Slope breaks of roadside terrain should be rounded. (3) The modified HVOSM software, which incorporated a deformable-soil model accounting for tire sinkage in soil, has a limited ability to predict off-road vehicle behavior when the simulation has "good" tire data for the motion-resistance forces in soft soil. (4) Adequate vehicle parametric data for the severe operating regime associated with the rollover maneuver are generally lacking. The authors recommend determining force characteristics of tires for slip and camber angles ranging up to 90 degrees and for loads including extreme overload. (5) The existing accident database lacks the comprehensive and detailed information necessary to define the conditions that lead to rollover for the different vehicle types.

Rosenthal, Szostak, and Allen [22] presented a multi degree-of-freedom model for a curb-tripped rollover vehicle simulation. The degrees of freedom include vertical and horizontal translation (no forward translation), roll, pitch, and yaw. The authors developed a simple model (TRIP) without a sprung mass and a more complex version of the model (SPTRIP) which includes separate sprung mass roll, lateral translation, and heave degrees of freedom. The model includes tire sliding and normal forces, suspension springs, and a model that simulates the reaction force from the curb due

to vehicle impact.

Terhune [23] addressed rollover and ejection rates in passenger car and light truck single-vehicle crashes. The research considered the role of driver, environment, and vehicle factors in the rollover accidents, and addressed how occupants were ejected. The author used 1980-1985 NASS files for the model years 1979-1986 for passenger cars, pickups, vans, and utility vehicles. To provide additional details about roadsides, rollovers, and ejections, a special file was created by coding from 487 hard-copy NASS cases using a coding guide for rollover types including: trip-over, flip-over, turn-over, climb-over, fall-over, and bounce-over.

Terhune concluded that (1) light trucks and cars continued to exhibit little differences in driver injury rates, (2) light trucks have higher single-vehicle-crash overturn rates than cars; while driver and environmental factors play a role in elevating the overturn rates, vehicle factors also appear to play a significant role, (3) utility vehicles exhibit the highest rollover tendencies, and (4) ejection is preeminently a utility vehicle problem, and to a lesser extent, a pickup problem. He also found that sideslopes, both cut (slopes upward from road) and fill (slopes downward from road), as well as ditches, fences, and bridge rails, were associated with the greatest risk of overturn. In contrast, guardrails and curbs apparently offer relatively slight risks.

Nalecz, Bindemann, and Bare [24] used System Technology Incorporated's (STI) Tripped Rollover Vehicle Model to investigate vehicle rollover sensitivity to various parameter sets. This software is a nonlinear, eight degree of freedom model package which tracks the motion of a vehicle skidding laterally on pavement and impacting a curb. The authors modified the STI software, which makes small angle assumptions for the heading angle of the vehicle with respect to the curb, to include larger heading

angles.

The STI software was used in conjunction with the authors' sensitivity analysis to rank vehicle parameter sets associated with rollover propensity. This analysis examines the kinetic and potential energies of the vehicle to calculate the so-called Rollover Prevention Energy Reserve (RPER) which is the difference between the maximum allowable change in gravitational potential energy (V_{CRIT}) and the kinetic energy of the non-centroidal rotation (T_{NR}). (Reference [25] covers this in more detail.)

The authors' results indicated that vehicle geometric parameters are the most influential characteristics in tripped rollover scenarios. They stated that vehicle stability is most sensitive to changes in track width followed by changes in the center of gravity height of the sprung mass.

Orlowski et al. [26] discussed maneuvers, such as curb tripping and severe steering, which may lead to rollover. They discussed on-scene accident indicators such as pre-trip tire marks, speed at trip, number of rolls, and severity of car-to-ground impacts. The authors studied the deformation of accident vehicles for location of roof crush - leading or trailing edge - and for the location and direction of scratches. They also addressed site factors such as road surface coefficient, depth of pavement gouges, and depth of soil penetration. Tire/soil mechanics were also discussed by Brown [19]. DeLeys [21] presented force measurements from dragging a vehicle laterally through various soil conditions. His measurements of friction coefficient ranged from 0.43 to 0.57. (Stonex [2] reported coefficients of friction up to 1.1 on sod.)

Reference [26] stated that an average deceleration rate may be estimated from the distance from the point of trip to the point of rest. Hight [7] estimated average

decelerations of a vehicle rolling over to be 0.4 to 0.65 g. Other references ([20], [27], [28]) cite average decelerations between 0.36 to 0.61 g.

Garrott, Monk, and Chrstos [29] describe the design of the Inertia Parameter Measurement Device (IPMD) developed by the National Vehicle Research and Test Center. The IPMD measures the center of gravity height and the pitch, roll, and yaw moments of inertia of a vehicle. Specific details of how the apparatus was built and how it is operated are discussed as well as its calibration and instrumentation. The authors also compared the measured values from the IPMD with general rules of thumb used in the passenger car and light truck industry. Tables of measured values are then compared with the calculated cg height and pitch, roll, and yaw moments of inertia values. Some of these rules of thumb were modified based on the IPMD measurements and other rules of thumb, such as for the roll moment of inertia, were developed for quick estimation purposes. Equations for pitch, roll, and yaw moments of inertia for passenger cars and light trucks were given as a function of vehicle weight only and compared with the IPMD measured moments of inertia. The calculated R^2 values of these equations for passenger cars was between 0.80 and 0.89. The R^2 values for light trucks was between 0.70 and 0.73. The authors stated that segregation of vehicle type within the light truck category could improve these estimates. They also recommended that if accurate estimates were needed, that the light truck data should be measured instead of using the rules of thumb for the pitch, roll, and yaw moments of inertia.

Winn [30] presented rollover demonstrations on videotape. He demonstrated curb trip, furrow trip, flat-surface, paved surface tip-up, ice to pavement trip, tip-up of vehicles moving backward, tip-up caused by an improperly loaded trailer, and the

bootleg turn. He concluded that rollover crashes are complex and that well designed, rollover resistant vehicles can tip-up and rollover. Driver inputs, vehicle movements, and environmental interactions all affect rollover accidents. The author suggested that ejection is the primary cause of injury in rollover crashes and occupant safety should be addressed as a means to reduce the fatalities in rollover accidents.

Bernard, Shannan, and Vanderploeg [31] presented simple mathematical models which may be used to study rollover. Simple models yielded straightforward metrics related to wheel lift. The models were said to be useful in the assessment of simple maneuvers. Calculated limit lateral acceleration ranged from T/2h g's from the simplest models to as low as 0.60 T/2h g's for a typical passenger car from slightly more complex models of vehicles subject to transient overshoot during suddenly occurring lateral acceleration maneuvers. The authors called for more complex models to handle more complex maneuvers, wherein the kinematics of the unsprung masses or the front to rear timing of lateral forces are important.

Mengert et al. [32] used single vehicle accident data for the 1983-1985 CARDfile crash records from the states of Texas, Maryland, Washington, Pennsylvania, Indiana, and Michigan. The analysis included 40 make/models. The model years ranged from 1972 through 1985, with T/2h from 1.01 to 1.57. The data-set contained 39,956 single vehicle accidents of which 4910 were rollovers.

Logistic regression was performed with possible predictors of accident involvement including T/2h, wheelbase, driver age and sex, seat belt use, driver alcohol/drug use, weather conditions, road alignment such as curved or straight road, rural or urban location, pre-crash stability, steering avoidance attempt, driver error, make/model of vehicle, and model year. Factors relating to the suspension, tires, etc., were

not included in the study. The authors concluded that at both the accident and make/model level, the derived model was highly influenced by vehicle geometry, especially T/2h. Other variables, such as whether the accident occurred in an urban or rural location or whether a driver error was involved, were also of importance.

Thomas et al. [33] addressed how rollovers are initiated and how initiation mechanisms affect the subsequent vehicle rollover mechanics. The authors compare the results of curb trip rollovers with the behavior of dolly rollover testing. Tests were recorded with high speed movie cameras and converted by a computer program into data files used to calculate vehicle motion descriptors.

For five curb tests, sideways velocities of 29.3 to 30.2 mph were measured. The curb trip vehicles each had a 2.5 degree pre-impact roll angle, were released from the tow device, and hit a 6 inch square curb.

The dolly rollover test followed the procedures outlined in FMVSS 208 with the test vehicles inclined 23 degrees in roll, the contact patches of the leading tires 9 inches above the ground, and at a test speed of 30 mph. The test vehicles covered a wide range of vehicle sizes from a sub-compact automobile to a full-size van. A compact size vehicle of the same make and model as used in the curb test series was rolled in the dolly rollover test.

Two of the five curb trip test vehicles rolled over, yielding 1 and 1-1/2 revolutions over an average distance of 47 feet. The dolly-launched vehicle rolled 3 times, 70 feet from roll initiation. The curb-tripped vehicles tended to roll in a more purely lateral manner while the dolly rollover vehicle developed some yaw and end-to-end contact during the rollover sequence.

The authors found several differences between the two rollover procedures: (1)

higher deceleration rates during curb impact than in the corresponding first ground contact of the dolly-launched vehicle, (2) higher angular velocities experienced by the dolly-launched vehicle, and (3) higher initial energy in the dolly-launched vehicle due to its increase in the center of gravity elevation of approximately 1.5 feet due to the roll angle of the support base.

Cohen, Digges, and Nichols [34] studied rollover events to assess injury causation and mitigation measures. The paper presented accident data analyses focusing on the development of a crashworthiness rollover classification system and severity index as well as an analysis of the injuries of ejected occupants.

The authors used the 1982-86 NASS files to study the characteristics of rollover crashes. For the classification and severity portion of the study, single vehicle accidents were used. The authors divided passenger cars into 3 classes - small, medium, and large. Light trucks were divided into large and small classes. Vans and multipurpose vehicles were each in their own class. They found that more than 85 percent of rollovers were single vehicle accidents and that rollover frequency was inversely related to vehicle size classes for cars and pickup trucks.

The primary area of damage, extent of damage, and number of rolls were examined for different classes and sizes of vehicles. Vans exhibited less extensive top damage, and fewer quarter turns than the other vehicles. The most frequent damage area for all vehicles was the top and the extent of damage was primarily at the Collision Deformation Classification extent zones 3 and 4.

Nalecz, Bindemann, and Brewer [25] presented two computer-based models used to study tripped and untripped rollover accidents. The Intermediate Tripped Rollover Simulation (ITRS) is an 8 degree of freedom model for vehicles sliding laterally into

a curb, and the Intermediate Maneuver Induced Rollover Simulation (IMIRS) is for untripped vehicle accidents caused by sudden steering and braking inputs. IMIRS combines a 3 degree of freedom handling model and a 5 degree of freedom rollover model. A Calspan tire model is used with a friction ellipse to determine the tire limits of adhesion during the combined cornering and braking maneuvers.

The so-called Rollover Prevention Energy Reserve (RPER) function measures the difference between the potential energy required to bring the vehicle to the static tip over position and the rotational kinetic energy of the vehicle created after impact with the curb. Finite difference calculations were used to determine the sensitivity of RPER to various parameters. The authors state that this analysis indicated that the most important geometric parameters are the track width and T/2h.

Reference [25] also simulated a utility vehicle overturn in a J-turn maneuver. Sensitivity analyses indicated that the most influential geometrical parameters in this maneuver were sprung mass center of gravity height, front and rear track width, suspension track width, the distance from the front axle to the vehicle center of gravity, and the unsprung mass center of gravity heights. The sensitivity study was implemented as follows: Given a set of initial conditions and control commands, performance in a maneuver was assessed with regard to RPER. Sensitivity analysis involved finite difference measures of changes of RPER with respect to vehicle parameters. A complication of this technique is that changing vehicle parameters invariably changes the severity of the vehicle's trajectory, thus the finite difference derivatives are not partial derivatives of RPER taken for the same vehicle trajectory.

In the late 1980's, Harwin and Emery [35] developed a database called CARS (Crash Avoidance Rollover Study) which included data from about 3,000 single vehi-

cle rollover crashes in the state of Maryland over an eighteen month period. Data was collected by specially trained Maryland State Police who worked with NHTSA engineers. The authors looked at vehicle, environmental, and driver factors contributing to the accident data analysis. Their results were divided into five files: accident, vehicle, driver, passenger, and tire.

The accident file contains more than 60 variables which allow investigation of vehicle related factors in rollover crashes. For example, if the vehicle was determined to be skidding, the type of skid, such as spinning or sideslipping, was estimated. Also, an assessment was made as to whether braking or steering was the probable cause of the skid. The accident file also categorized events as tripped, untripped, or as unknown. Tripping mechanisms included curb, pavement edge, soil/flat, guardrail/barrier, ditch, embankment/slope down, and unknown. The vehicle parameter file contains 29 identifying vehicle characteristics. These measurements were performed by the Vehicle Research and Test Center (VRTC) using the Inertial Parameter Measurement Device [29]. The driver file includes more than 40 variables related to driver demographics, driver condition, driving history, and accident avoidance errors or attempts made by the driver. The passenger file contains 10 variables including injury severity, age/sex demographics, and restraint use. A tire file contains 25 variables which describe the tire tread depth, inflation pressure, and rolling radius of the crash vehicles' tires.

The authors concluded that untripped rollover is a relatively rare event, less than 10% of the database. They also found that over 50% of the skidding type of rollover accidents were caused by going around a curve in the road too fast and twenty-four percent of the rollover accidents were caused by severe steering input while on a

straight road.

Cooperrider, Thomas, and Hammoud [36] performed full-scale vehicle rollover tests including curb and soil trip tests and dolly rollover. (Much of the information in Reference [36] was presented earlier in Reference [33].) The authors calculated average deceleration rates from the initial trip to the point of first impact. These deceleration calculations are useful in identifying mechanisms of these trip methods and in addressing occupant motion and subsequent injury levels in rollover accidents.

The authors claim that the 1981 Dodge Challenger (T/2h = 1.335) had average decelerations of 12.4 g's in the curb trip, 1.62 g's in the soil trip test, and 1.3 g when rolled from the dolly. The lateral velocities during the test were 29.6 mph for the curb test, 33.7 mph for the soil trip test, and 30.2 mph for the dolly trip test. The 1979 Datsun B210 (T/2h = 1.288) had average decelerations of 13.2 g's for the curb trip and 1.71 g's for the soil trip test. The lateral velocities were 29.3 mph for the curb trip test and 27.0 mph for the soil trip test.

Significant differences were found in the mechanics of the vehicles when tripped by these different mechanisms. Very high deceleration rates, in excess of 10 g's, were produced in the curb trip tests. The soil trip results were in the 1.5 to 2.0 deceleration range and had a longer tripping force duration. The authors noted that the curb and soil tripped vehicles tended to roll in a more purely lateral manner, with damage primarily to the offside roof and A-pillar area, while the dolly rollover vehicles developed some yaw and end-to-end contact during the rollover sequence, resulting in damage to the left side front fender and the right or leading side roof and door frame area.

Three vehicle rollover tests did not result in rollover due to failure of the wheels

or axles under the curb impact loads. These were the Dodge Challenger traveling at a lateral velocity of 29.9 mph, the 1972 Chevrolet C20 Van (T/2h = 1.120) traveling at 29.6 mph, and the 1981 Chevrolet Impala (T/2h = 1.417) traveling at 30.2 mph. In curb impact, the average impact deceleration for the vehicles which did not roll were 5.4, 5.5 and 6.0 g's, respectively, about half the values found during maneuvers which yielded rollover.

The rollover testing suggested that the force duration necessary to trip a vehicle and cause rollover is characteristic of a particular vehicle and independent of the trip method. The authors then developed an expression relating the force inducing the rollover of a vehicle and the duration of the force necessary to cause rollover. They assumed that the trip force is constant during the rollover initiation phase. They derived an expression which they stated agrees favorably with their full-scale test results.

In 1990, Harwin and Brewer [37] studied rollovers per single vehicle accident using the CARDfile accident database for the states of Texas and Maryland (1984-1985), and for Washington (1983-1985). Nineteen foreign and domestic passenger cars, eight utility vehicles, and twenty-seven "twin" vehicles which have practically identical chassis designs were chosen for investigation. The authors used linear regression models to relate rollover per single vehicle accident (RO/SVA) to T/2h. They performed four separate analyses for Maryland and Texas data for 1984 and 1985 and a combined dataset for these two years for the two states. They compared these results with the 1983-1985 Washington data as well as the combined Texas, Maryland, and Washington data sets. They found R^2 values for all of these data sets to be in the range of 0.57 to 0.86. Specifically, for the combined data set of Texas,

Maryland, and Washington (with 40,000 single vehicle accidents and 5,000 rollover accidents), they found a R^2 value of 0.86 for percent RO/SVA with respect to T/2h.

The authors also performed a linear regression analysis on the Maryland and Texas data sets for (a) percent rollover accidents per 100,000 registered vehicles versus T/2h and for (b) percent single vehicle accidents per 100,000 registered vehicles versus T/2h. They stated that they found a "reasonably strong" correlation between percent rollovers per 100,000 registered vehicles and T/2h ($R^2 = 0.66$). However they found "practically no" correlation between percent SVA/100,000 registered vehicle and T/2h ($R^2 = 0.007$). The authors stated that this demonstrated that within a class of single vehicle accidents, the static stability factor (T/2h) exerted an influence on only one specific accident type, i.e. vehicle rollover.

Wormley and Inouye [38] performed an overview of light duty vehicle rollover testing and facilities in the United States through a literature survey and site visits. They also cite factors influencing vehicle performance with respect to rollover, in particular, the critical sliding velocity (CSV) and the static rollover stability factor (T/2h).

Jones and Penny [39] used Fatal Accident Reporting System (FARS) data for the years of 1981-87 together with engineering data for 11 pickup models, 16 utility vehicle models and 11 passenger car models. The data from the accident file was used to estimate the occurrence of rollover, given a single vehicle crash, as a function of engineering parameters: wheelbase, track width to cg height ratio, and wheelbase to track width ratio. The authors stated that T/2h was the strongest predictor of vehicle rollover for pickup trucks and utility vehicles, and for utility vehicles they stated that the wheelbase to track ratio was also significant. For passenger cars, they

state wheelbase was the best predictor of rollover.

Heydinger et al. [40] outlined the methodology for the validation of computer simulation software. They then performed this validation process using two simulation software packages - STI's Vehicle Dynamics Analysis Non-Linear (VDANL) and the University of Michigan's Improved Digital Simulation Fully Comprehensive (IDSFC).

The authors stressed two points about simulation validation: (1) The parameters used to describe the physical system to a simulation must be measured independently and not from the experiments that are used to obtain the simulation validation data, and (2) while validating a simulation, the parameters describing the system to a simulation must not be varied from their independently measured values to improve the accuracy of a simulation's predictions.

Terhune [41] examined single-vehicle crashes from the National Accident Sampling System (NASS) (1980-1986) and addressed how vehicle factors and roadside features interact to generate rollovers. He found: (1) Roadside features vary substantially in their tendencies to induce rollovers of vehicles; features appearing most hazardous in this aspect are descending sideslopes, ascending sideslopes steeper than 1:1, ditches of width 15 feet or less, and pavement edge-drops. (2) Vehicle factors appear most influential on rollover when vehicles are interacting with the more hazardous roadside features. (3) Wheelbase is related to overturn tendencies on roadsides, though further research is needed to determine whether other vehicle parameters explain this relationship. (4) Vehicle type appears to be important in distinguishing vehicle rollover tendencies. (5) Vehicle attributes relevant to vehicle loss of control preceding rollover should be distinguished from vehicle attributes influencing

the rollover consequences of a pre-crash mode. (6) Estimating T/2h based on roof height is inadequate for further research on the role of stability factors to vehicle overturns.

Malliaris and DeBlois [42] investigated the rollover characteristics of passenger cars for the years 1988-1990. Their data was taken from National Accident Sampling System (NASS) and Fatal Accident Reporting System (FARS). The authors found that over 87 percent of the accidents were single vehicle crashes with average speeds of 40 to 60 mph. The average travel speed was 50.1 mph for all rollover crashes and 63.4 mph for car rollovers in fatal accidents. For non-rollover crashes, they found average speeds of 27.7 mph and, in fatality crashes, 45.3 mph. They estimated seat belt use for all car occupants to be 50% with seat belt use in rollover accidents to be about 16%. They also found the primary mode of roll to be about the roll axis (96.4%).

In investigating the number of quarter turns, the authors found that 39.1% of the fatal rollover accidents involve two or three quarter turns and 43.2% involve four or more quarter turns. With respect to travel speed, they found that the number of quarter turns increases as the travel speed increases. They also found that as the number of quarter turns increases, that the rollover crash severity increases as seen in the number of passenger ejections (full and partial), roof and roof support intrusion, loss of passenger compartment integrity which includes windshield and window breakage, and harmful occupant contacts.

The authors also studied the potential for lateral slide as a likely condition for the occurrence of rollover. They studied the NASS and FARS data and looked at whether or not the car negotiated a curve or a lane change or performed a collision

avoidance maneuver. They also looked at whether there was roadway departure, loss of control, and/or loss of traction. The presence of any of these conditions increases the likelihood of the development of lateral slide potential. They found that the lateral slide potential was high in 83.2% of the rollovers and low in 16.8% of the rollovers. They stated that car travel speed in conjunction with the lateral slide potential appear to influence not only the incidence, but also the severity of rollovers.

Digges and Klisch [43] studied rollover using the STI Vehicle model for the tripped rollover, and the Articulated Total Body (ATB, [44]) Vehicle and Occupant Models. The STI tripped rollover model has 7 degrees of freedom. It simulates a skidding vehicle impact with a curb. Variables output by the STI model can be used as input to the ATB vehicle and occupant models to predict the post tripping motion of the vehicle and its occupants. Simulation results suggested that high roll rates increase the potential for ejection. The authors stated that the coefficient of surface friction has negligible influence on roof crush, but a significant influence on the rate of translational velocity loss. The translation velocity loss decreases with increasing roll rate and roof crush is relatively insensitive to roll rate.

Allen et al. [45] used measurement and simulation to assess a wide range of vehicles with respect to directional response and roll stability. They state that roll stability interacts with directional stability, and is related to center of gravity location, track width, and several other characteristics. They pay particular attention to lateral load transfer distribution, which they believe to be important due to its influence on directional response in limit turning maneuvers.

Twelve vehicles were tested. They were subject to parameter measurements, static pull testing, and full scale field tests. The authors state that vehicles mea-

suring less than 0.9 equivalent g's in the static pull tests are particularly susceptible to rollover depending on the severity of maneuvering conditions. Circle tests, together with computer simulation, yielded so-called cornering capacity, which was the estimated maximum acceleration possible on the circle. The difference between the side pull test and the cornering capacity yielded the so-called steady state rollover propensity margin.

The authors also attempted validation of the simulation based on twelve full-scale tested vehicles under three maneuvering conditions. These included steady state cornering up to limit lateral acceleration capability, low g sinusoidal inputs over a wide range of frequencies, and limit performance transient steer maneuver designed to reach the maximum lateral acceleration capability of the vehicle. All but two of the tested vehicles, a compact front wheel drive sedan and a rear wheel drive pickup, compared favorably with the computer simulation results. Reference [46] presents additional details.

The authors believe the simulations, together with the test results from the twelve test vehicles, indicate that VDANL has been validated in stable and unstable maneuvering conditions. They believe that VDANL is capable of giving insight into conditions leading to lateral and directional stability problems. They stated that spinout and rollover conditions could be investigated in terms of specific vehicle characteristics and maneuvering conditions.

Heydinger, Garrott, and Chrstos [47] developed a second-order slip angle model which they used to replace the tire dynamics used in the current VDANL software. The original VDANL tire dynamics modeled the tire side force as a first-order time lag. These modifications were made to improve the vehicle handling characteristics

and to better predict the tire time lags seen in full-scale tests.

The authors field tested four test vehicles: a 1987 Ford E-150 van, a 1987 Ford Thunderbird medium sized car, a 1987 Hyundai Excel small sized car, and a Suzuki Samurai utility vehicle. Each of these vehicles were tested in two maneuvers - the constant speed J-turn and constant speed sinusoidal sweep steering maneuvers - a total of 10 times for each maneuver. They measured lateral and longitudinal acceleration, yaw rate, roll angle, vehicle speed, and handwheel steer angle. The averaged outputs from these runs were compared with VDANL simulation runs with no tire dynamics, with the first-order tire dynamics, and then with second-order tire dynamics.

The authors focused their attention on transient yaw dynamics which they stated is crucial in vehicle modeling during crash avoidance maneuvers. They found that a second-order time lag of the tire slip angle led to simulation results which corresponded the best with the full-scale test output. They found this second-order system to be dependent on the vehicle's forward velocity and two tire parameters - the tire path frequency and tire damping ratio. They found that using a natural path frequency of 1.1 rad/ft for all forward velocities worked well. A damping ratio of 1.3 for forward velocities of 25 mph was used. However, a damping ratio of 0.8 for velocities of 50 mph was used since, based on limited experimental data in the literature, tire responses become underdamped at speeds above 25 mph.

Allen et al. [46] measured mass and weight distribution, vehicle geometry (which includes track width and wheelbase), center of gravity location, spring rates, roll stiffness, suspension geometry, steering ratio and compliance, and some tire parameters, for forty-one vehicles. They estimated the moments of inertia, heave damping, steering system natural frequency and damping, and some tire parameters as well. Phase

II of this project was to perform full-scale vehicle testing of 12 of these vehicles and then to use VDANL [48, 45, 49] to simulate the maneuvers performed on the full-scale vehicles for comparison, with a view toward predicting, rollover behavior.

The full-scale testing of the twelve vehicles was broken down into both low level and limit lateral acceleration maneuvers. Limit lateral acceleration maneuvers are high g maneuvers and are common in rollover accidents where large transients are expected. The vehicles were fully instrumented and the input steer angles during the maneuvers were saved as input to the computer simulations. Other vehicle characteristics measured and saved for comparison to computer output include yaw rate, slip angle, lateral acceleration, roll rate, and roll angle.

After completion of the full-scale testing, the authors simulated computer models of these vehicles in equivalent maneuvers. The authors found good correspondence of the computer simulation output response with the field test results for low lateral acceleration dynamic conditions, maneuvers less than 0.3 g's, where the tire side forces are in their linear range. These maneuvers included a steady state turn circle and sinusoidal steer inputs.

The full-scale field tests were then compared with the computer simulation of the limit lateral acceleration maneuvers. These conditions represented maneuver conditions of up to 0.8 g's of lateral acceleration with significant tire side force saturation. For the 12 vehicles, the authors stated that the comparisons between the full-scale testing and the computer simulation results were almost identical. However, in two of the vehicles where spinout was predicted in the full-scale test, the computer simulation results did not match.

A Honda Civic (4-door sedan) and a Toyota Pickup (4x4 Long Bed) were both

predicted to spinout with the given steer input. However, neither vehicle did. In order to match the computer simulation with the field test results, the authors modified the tire model used in the simulation for each of these vehicles. They stated that the tire model was inadequate in predicting the reduction in the rear tire/road coefficient of friction due to the lightly loaded rear axles. They modified the constant Calspan parameter, B_3, which relates limit shear force on the tires to normal load. They found that by lowering B_3 15% and lowering the throttle at the end of the reversal steer, that they could make the small four door sedan directionally unstable and spinout and therefore match the field test result.

For the Toyota Pickup, a 15 percent reduction in B_3 was used in the computer simulation. However, combining this change with the drop in throttle did not result in a spinout. They found that changing the Calspan coefficient, and keeping a constant throttle setting, was sufficient to cause the desired spinout and to validate the field test results.

The authors also note that this Toyota Pickup in simulations was highly sensitive to maneuver speed and to the timing of the steer input. For example, the authors state that the pickup spins out under a reversal steer profile at a speed of 60 ft/s (41 mph) but does not at 50 ft/s (34 mph). They also state that the spinout can be averted by modifying the steer maneuver conditions.

Hinch, Shadle, and Klein [1] stated that almost 10,000 people are fatally injured each year in rollover crashes. From data collected in the National Accident Sampling System's (NASS) for 1989, they estimated that nearly 90 percent of the rollover accidents were single-vehicle accidents and that about 92 percent of single-vehicle rollovers occurred off of the road. The 1990 Fatal Accident Reporting System (FARS)

data stated that there were 15,901 fatalities in single vehicle crashes. Of these single vehicle crashes, about 51% were fatalities in rollover crashes. The authors stated that rollover accidents produce injury and fatality rates which are higher than the average rates for all accidents. They also stated that utility vehicles and light duty pickups are more likely to roll over, given the occurrence of a single vehicle accident, than the average of all light duty vehicles involved in single vehicle accidents.

The authors then defined factors which they stated were influential in a vehicle's involvement in rollover accidents. They stated that there were basically two types of rollover phenomena - tripped and untripped rollover. Tripped rollover involves an abrupt impact with a rigid or nearly rigid object at the vehicle's tires or wheels. Untripped rollover exposes the vehicle to a gradual increase of the force at the tire/ground contact area such as when the tires gradually furrow into soft ground on a downslope or embankment. The authors determined performance characteristics which they stated were likely to correlate with accident data. For the untripped phenomenon, they selected three metrics - the static stability factor T/2h (SSF), the tilt table ratio (TTR), and the side pull ratio (SPR). For the tripped rollover phenomenon, they selected the rollover prevention metric (RPM) and critical sliding velocity (CSV) as well as the SSF, TTR, and SPR metrics. (The RPM metric is determined by obtaining the difference between the initial lateral translational kinetic energy before and the rotational kinetic energy after curb impact normalized by the initial energy.) They also included the center of gravity height, average track width, vehicle mass, and vehicle roll mass moment of inertia measurements and wheelbase, percentage of total vehicle weight on the rear axle, and braking stability in their analysis. These metrics and parameters were measured at two test facilities, the Ve-

hicle Research and Test Center (VRTC) and Systems Technology Incorporated (STI). The results of these measurements were compared to the static stability metric. They found correlation coefficients of 0.85 for SSF versus TTR, 0.88 for SSF versus SPR and for SSF versus RPM, and 0.43 for SSF versus CSV.

The authors then utilized the NASS accident data from five states - Maryland, New Mexico, Michigan, Georgia, and Utah to perform a logistic regression analysis of ten driver/roadway demographics variables and eight different vehicle metrics. They concluded that utility vehicles were significantly more likely than passenger cars to roll over, followed by vans, pickup trucks, and passenger cars (the reference group). In addition, front-wheel drive vehicles were significantly more likely to roll over than were rear-wheel drive vehicles and four-wheel drive vehicles were significantly more likely to roll over than rear-wheel drive vehicles.

Chrstos and Guenther [50] described and compared three methods of measuring static rollover metrics - the static stability factor (SSF), the side pull ratio (SPR), and the tilt table ratio (TTR) - and addressed the ease and repeatability of each of these measurements.

The authors stated that, even though results of Winkler et al. [51] found large differences in the center of gravity height measurements at various laboratories, that if the cg height measurement is made with care, repeatability of the static stability factor can be made within one percent accuracy. They estimated the side pull ratio measurement error to be about five percent. They also found the side pull test to be time consuming and to present a possibility of vehicle damage during the test procedure. They found the tilt table ratio test to be fairly simple and to have an error level of about one percent. The authors rated the tilt table ratio test as the

most favorable measurement device due to its accuracy and simplicity.

Klein [52] presented detailed results of the regression analyses of vehicle rollover metrics and parameters with the NASS accident data for the states of Georgia, Maryland, Michigan, New Mexico, and Utah, as presented in the paper by Hinch, Shadle, and Klein [1]. Results of each of the selected vehicle metrics - the tilt table ratio, the static stability factor, the side pull ratio, and the critical sliding velocity - are also given for the State of Michigan accident data with at least 25 single/vehicle accidents for each make/model. He found R^2 values of 0.65, 0.66, 0.58, and 0.57 for TTR, SSF, SPR, and CSV, respectively.

The author stated that the tilt table ratio appeared to provide the greatest predictability of rollover in single-vehicle accidents, but only by a slight margin over the static stability factor. Furthermore, he found that rural location in the rural/urban accident location variable in accident data was a strong predictor of rollover. In a stepwise logistic regression of the individual states, rural location was the first variable to enter models in four of the five states, and the second variable to enter in the fifth state. This agrees with work reported by Mengert et al. [32]. Additional metrics, including wheelbase, critical sliding velocity, and braking stability (the percentage of total vehicle weight on the rear axle), were also investigated and sometimes provided significant explanatory power, but were dropped from the immediate work since they provided less explanatory power than TTR, SSF, and SPR.

Garrott and Heydinger [53] studied various common vehicle directional response metrics such as response times, percent overshoot, etc., to try to determine whether these vehicle characteristics contribute to steering maneuver induced rollover accidents. Statistical analysis indicated that these metrics were not good predictors of

the observed rollovers per single vehicle accident.

Garrott [54] examined the variability of the Static Stability Factor (SSF) and the Tilt Table Ratio (TTR) with respect to vehicle loading and vehicle-to-vehicle variation. The vehicle loading was done by increasing the number of occupants in the vehicle and by adding cargo weight, placed either on the floor or raised a specific distance in the cargo space. Garrott found that, in general, both SSF and TTR decreased as occupants were added to a vehicle. The change in SSF and TTR per occupant was fairly consistent, with changes in TTR being more consistent. Placing ballast (cargo weight) to vehicles always decreased TTR but changes in SSF were increased for some vehicles and decreased for others.

Tests for vehicle-to-vehicle variation were performed on similar models and then on a range of submodels with a variety of options. Garrott found that some of the variability between similar make/models exceeded the expected non-repeatability of the measurement equipment but that, in general, the range of results is small and that the variability between similar models is not significant. He also found that tire size changes on a specific vehicle made significant changes to the static rollover metrics. Tires that raised the center of gravity height lowered the vehicle's SSF and TTR, while increasing the tire width raised the TTR but left the SSF essentially unchanged.

Winkler, Bogard, and Campbell [55] examined the influence of twelve variables on the tilt-table testing of a light truck-like vehicle. This vehicle, a Ford Aerostar van, was tested in 113 individual tests to evaluate the repeatability of the tilt-table method. The five general areas investigated were vehicle lateral constraint, facility and vehicle placement geometry, facility rigidity, hysteresis of the vehicle tire and

suspension system, and dynamics of the tilt-table. (The specifics and detailed results are reported in Reference [56].) In general, the tilt-table method was found to be quite robust in that measurement results appeared to be insensitive to most of the variables considered. Surface friction under the low-side tires and trip rail geometry were the primary exceptions to this rule. With this in mind, it was suggested that a high friction surface and a low trip rail be used to enhance the accuracy of the TTR.

Winkler, Campbell, and Mink [51] performed a round-robin study of the center of gravity height measurement of light truck-type vehicles. The study was supervised by the University of Michigan Transportation Research Institite (UMTRI) with measurements being taken in the laboratories of Chrysler Corporation, Ford Motor Company, General Motors Corporation, and the National Highway Traffic Safety Administration. The primary objectives of the study were (i) to determine how experimental procedures in the participating laboratories resulted in significant differences in the measured vertical position of the center of gravity, and (ii) to gain insight into the physical causes of such differences.

Three vehicles - a Chrysler mini-van, a full-sized Ford pickup truck, and a GM sport/utility vehicle - were used as measurement subjects, as well as a reference, or calibration, "buck". The center of gravity position of the buck had been determined by calculation and was used as a reference sample of known quantity.

Prior to the start of this study and after each laboratory made their measurements, UMTRI made reference measurements to check for changes in properties of the vehicles over the period of the study. The test vehicles were tested in similar configurations, including all fluid levels full, tire inflation pressures, seat positions, etc., at each lab. Each laboratory measured the cg height as well as wheelbase, in-

dividual wheel loads, spindle heights, and the height of four sprung mass reference points marked on the fender of each vehicle above each wheel.

Results of the study found that repeatability of results within each of the individual laboratories was generally good. However, there were significant differences in the center of gravity measurement results - greater than 1 inch (25 mm) - between the different laboratories. The reference measurements made by UMTRI indicated that the properties of the subject vehicles did not change over the period of the measurement program, so that the cg height differences were due to the specific procedures performed at each of the laboratories. The authors then examined the procedures performed at each laboratory and made recommendations which could account for the cg height measurement variability.

Clover et al. [57] assessed the repeatability of the tilt table measurement method in determining the tilt table ratio for a set of sixteen unloaded vehicles. They used the Ford Motor Company tilt table located at Diversified Service Technologies (DST) in Romulus, MI, which has a 1 inch trip rail. They tested vans, passenger cars, light trucks, utility vehicles, and a control vehicle. The control vehicle was the 1991 Ford Aerostar used in Reference [56]. This control vehicle was tested four times prior to and four times after the testing of the sixteen vehicles in order to provide a check on the test procedure. The 16 test vehicles were split into four groups of four with the test order being shuffled during each round of measurement to eliminate bias in the order of testing.

The authors found their test results to be very repeatable. Seventeen of the tests - the twice-measured control vehicle and fifteen of the test vehicles - led to statistical information about measured tilt table angle. One of the test vehicles, a Corvette,

did not tip up even when the table reached its limit of travel, and so its results were not included in the statistical analysis. For the 17 tests, they found "the standard deviation of the tilt table angle characteristic of test results for a single vehicle taken over a period of two or three days to be about 0.0017 radians, or about 0.1 degrees".

The authors also used data from the R. L. Polk database of registered vehicles and from the FARS database to attempt to determine the relationship between the Tilt Table Ratio (TTR) for the sixteen vehicles and fatal rollover accidents. They analyzed rates of rollover for single and multi-vehicle fatal accidents per million registered vehicle as a function of TTR. The data indicated that the total fatal rollovers per million registered vehicles increased with tilt table ratio, with an R^2 value of 0.52. They also analyzed rates of rollover as a function of the rate of rollovers per single vehicle accident. The data indicated that the first event rollovers per fatal single vehicle accident decreased with tilt table ratio, with an R^2 value of 0.49.

Bernard and Clover [58] examined the validation process used to check computer simulation output results. The authors stated that validation of a simulation is an ongoing analytical exercise. They pointed out that the validity of a computer simulation is made by verifying steady state checks with the mathematical models. This in effect checks for user input errors in vehicle geometry and mass, suspension parameters, steering compliance, etc. They also believed that the complexity of the model required for vehicle simulation varies with the vehicle and with the maneuver, and that the model choice can usually be made without vehicle or component testing.

Nalecz and Lu [59] performed full-scale vehicle testing for tripped vehicle rollover. They tested 8 vehicles - 1986 Chevrolet Chevette, 1985 Ford Thunderbird, 1988 Toyota Pickup, 1985 Ford F-150 Pickup, 1984 Ford Bronco II, 1985 Ford Bronco,

1988 Dodge Caravan, and 1987 Mitsubishi Van. Rollovers were measured at pre-trip lateral velocities as low as 3.6 m/s (8 mph). Scatter in the measurements made it impossible to draw conclusions regarding the effects of vehicle design parameters on rollover. They suggested adding directional stability-improvement technologies such as anti-lock braking systems and traction-control systems to reduce vehicle skid and spin out leading to rollover.

CHAPTER 3. BACKGROUND

Rollover is a complex event which has been the subject of repeated investigations. The literature indicates that experimental work with full-scale vehicles is helpful but repeatability of the experiments is a formidible technical challenge. A possible solution are mathematical models which can be used for vehicle simulation. However the literature indicates that the level of complexity of computer simulations varies from simple one dimensional models to models of great complexity. Thus an initial challenge is to determine what level of complexity is sufficient to study rollover events. Secondly, and just as important, is the issue of validation, namely, how do we view calculated results when experimental results are notoriously nonrepeatable?

Computer Simulation for Rollover

There are various levels of computer simulation software on the market. For the simulations presented here, we used the commercially available software VDANL, a fairly complex PC-based program with a wide user community.

The Vehicle Dynamics Analysis, Non-Linear (VDANL) simulation software analyzes vehicle lateral and directional control and stability. This software was designed to study vehicle handling and braking capabilities throughout the maneuvering range of light vehicles. The VDANL simulation utilizes 15 degrees of freedom - six degrees

of freedom for sprung mass motions, four degrees of freedom for unsprung mass motions, four degrees of freedom for wheel rotations, and one degree of freedom for the steering system.

Allen et al. [46] measured mass and weight distribution, vehicle geometry (which includes track width and wheelbase), center of gravity location, spring rates, roll stiffness, suspension geometry, steering ratio and compliance, and some tire parameters, for forty-one vehicles. Based on available data, rules of thumb and experience, they estimated the moments of inertia, heave damping, steering system natural frequency and damping.

They tested 12 vehicles and then used VDANL [48, 45, 49] to simulate the maneuvers performed on the full-scale vehicles for comparison, with a view toward predicting rollover behavior.

The full-scale testing of the twelve vehicles was broken down into (a) low level lateral acceleration maneuvers and then into (b) limit lateral acceleration maneuvers. The vehicles were fully instrumented and the steering time profiles from the test vehicles were used as input to the computer simulations. Vehicle measures saved for comparison to computer output include yaw rate, slip angle, lateral acceleration, roll rate, and roll angle.

After completion of the full-scale testing, the authors simulated computer models of these vehicles in equivalent maneuvers. They found good correspondence between calculations and field test results for low lateral acceleration dynamic conditions, maneuvers less than 0.3 g's, where the tire side forces are in their linear range. These maneuvers included a steady state turn circle and sinusoidal steer inputs.

The full-scale field tests were then compared with the computer simulation of

the limit lateral acceleration maneuvers. These maneuvers included conditions of up to 0.8 g's of lateral acceleration. For the 12 vehicles, the authors stated that the measurements and the computer simulation results were almost identical. However, in two of the vehicles where spinout was predicted in the full-scale test, the computer simulation results did not match.

Vehicle 8 (Honda Civic, 4-door sedan) and Vehicle 23 (Toyota Pickup, 4x4 Long Bed) were both predicted to spinout with the given steer input. However, neither vehicle did. In order to match the computer simulation with the field test results, the authors modified the measured tire data used in the simulation. They stated that the tire data was adequate for the low lateral acceleration maneuvers but was not able to predict the reduction in the rear tire/road coefficient of friction due to the lightly loaded rear axle.

At this point, a discussion of Reference [46] tire modeling is in order. Lateral forces were limited by a friction coefficient μ_y where

$$\mu_y = \frac{SN}{SN_t}\left(B_1\ F_z + B_3 + B_4\ F_z^2\right) \tag{3.1}$$

The coefficients B_1, B_3 and B_4 were obtained from data measured on a tire test machine. SN_t is the so-called skid number of the test machine, and SN is a parameter intended to scale the test machine results up or down to reflect differences between the surface of the test machine and the test track where vehicle tests were performed. To get the desired drop in μ_y at light loads, the authors modified the constant Calspan parameter, B_3, associated with normal load, F_z, in Equation 3.1. They found that by lowering B_3 for the rear tires 15 percent and lowering the throttle at the end of the reversal steer, that they could make the calculated results for the small four door sedan (Vehicle 8) directionally unstable and spinout.

For Vehicle 23, the Toyota Pickup, a 15 percent reduction in B_3 as with Vehicle 8 was used in the computer simulation. However, combining this change with the drop in throttle does not result in a spinout. They found that changing the Calspan coefficient, and keeping a constant throttle setting, was sufficient to cause the desired spinout.

The authors also noted that this Toyota Pickup was highly sensitive in the simulations to maneuver speed and to the timing of the steer input. For example, the authors stated that the pickup spins out under a reversal steer profile at a speed of 60 ft/s (41 mph) but does not at 50 ft/s (34 mph). They also stated that the spinout can be averted by modifying the steer maneuver conditions.

These calculations illustrate that, in the region of limit performance, computed results are extremely sensitive to small changes in input parameters, including vehicle speed and steer angle amplitude and timing.

The following section presents a series of computer simulations using VDANL to illustrate the complexity of the rollover maneuver and the sensitivity of the simulations to subtle changes in the following maneuvers: a J-turn steer input, a reverse steer input, and a split μ surface. The light truck used in this section (Vehicle 23) is being used in all of the following examples. Appendix A presents vehicle parameters and Table 3.1 gives some particularly important vehicle parameters.

J-Turn Simulation

The maneuver in the following simulations is a simple J-turn. The input road-wheel steer angle profile is trapezoidal with the magnitude of the input increasing from zero to a given magnitude in 0.5 seconds. Figure 3.1 illustrates a trapezoidal

Table 3.1: VDANL Simulation Vehicle Parameters

a	1.23 m	(4.05 ft)	b	1.58 m	(5.18 ft)
M	1649 kg	(113 $lb_m \cdot s^2/ft$)	h	0.646 m	(2.12 ft)
I_{cg}	339 $kg \cdot m^2$	(250 $ft \cdot lb_f \cdot s^2$)	T	1.41 m	(4.62 ft)
M_u	263 kg	(18 $lb_m \cdot s^2/ft$)	M_s	1386 kg	(95 $lb_m \cdot s^2/ft$)

steer with a maximum magnitude of 6 degrees. The vehicle has an initial forward velocity of 88 ft/s (60 mph). An output path for the 6 degree input steer is shown in Figure 3.2. The coefficient of friction, μ_y, characterizing the tire surface is 1.0.

Figures 3.3 and 3.4 show the roll angle and lateral acceleration of the sprung mass for a 6 degree and a 7 degree input steer. In the 6 degree steer maneuver, the vehicle reaches a maximum lateral acceleration of 26.5 ft/s^2 (0.82 g's) and a maximum roll angle of -4.2 degrees. In the 7 degree maneuver, the vehicle rolls over. These are very severe maneuvers which illustrate that, near the limit, very small changes can be important.

Reverse Steer Simulation

In this maneuver, the vehicle is subjected to a +/- step steer input of 5 and 6 degrees as shown in Figure 3.5. Again the tire surface coefficient of friction, μ_y, is 1.0. The period and amplitude of the steer pattern, 1.5 seconds, pushes human ergonomic limits.

Figure 3.6 shows the lateral acceleration of the sprung mass for the input steer angle time histories of Figure 3.5. The peak lateral acceleration is about 26.6 ft/s^2 (0.83 g's) for the 5 degree maneuver. Figure 3.7 shows the roll angle of the sprung

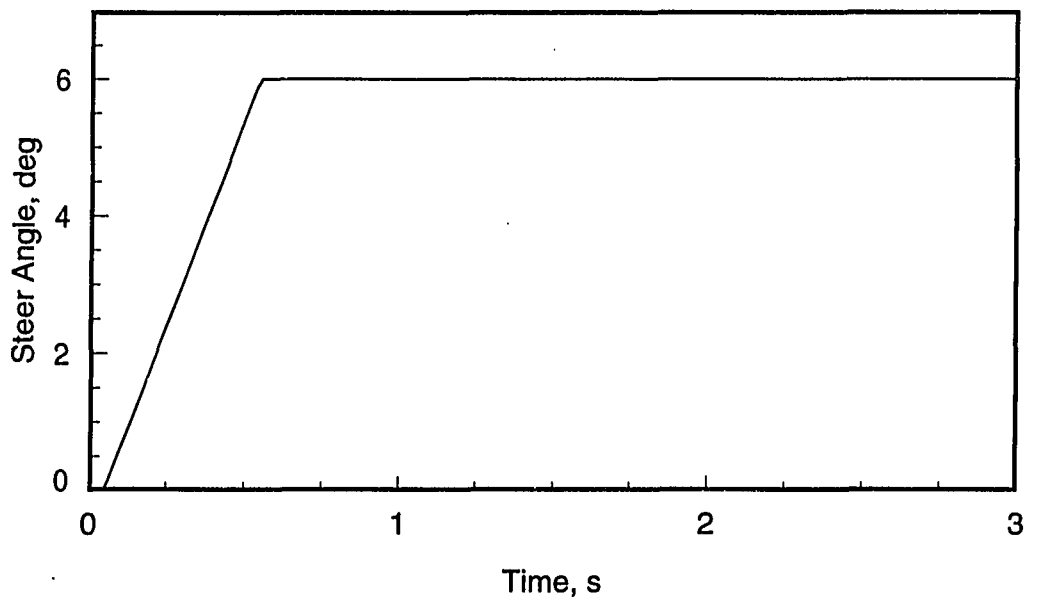

Figure 3.1: Input Steer for Computer Simulation

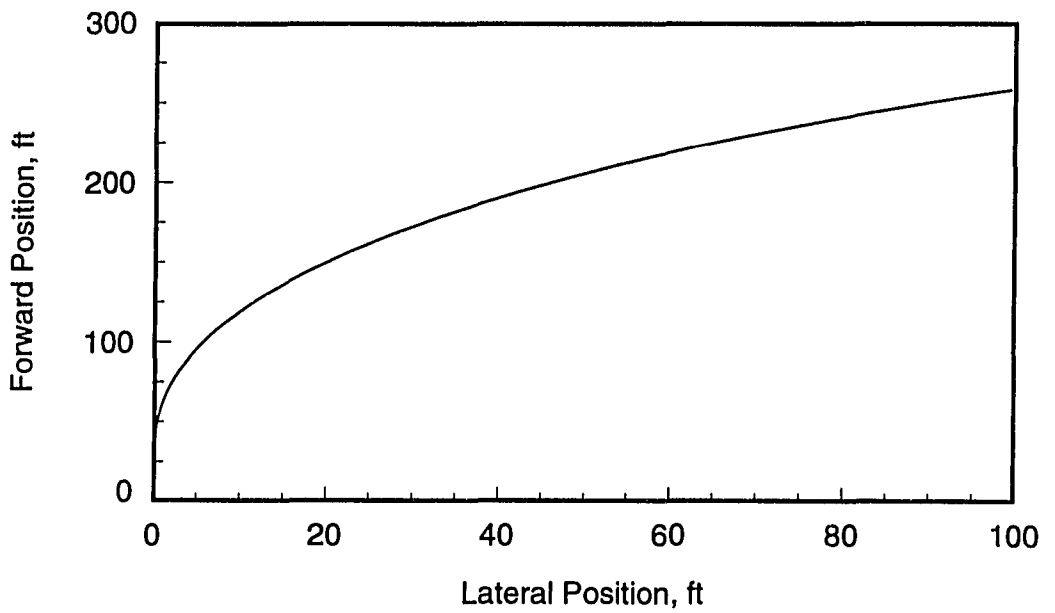

Figure 3.2: Typical J-Turn Path

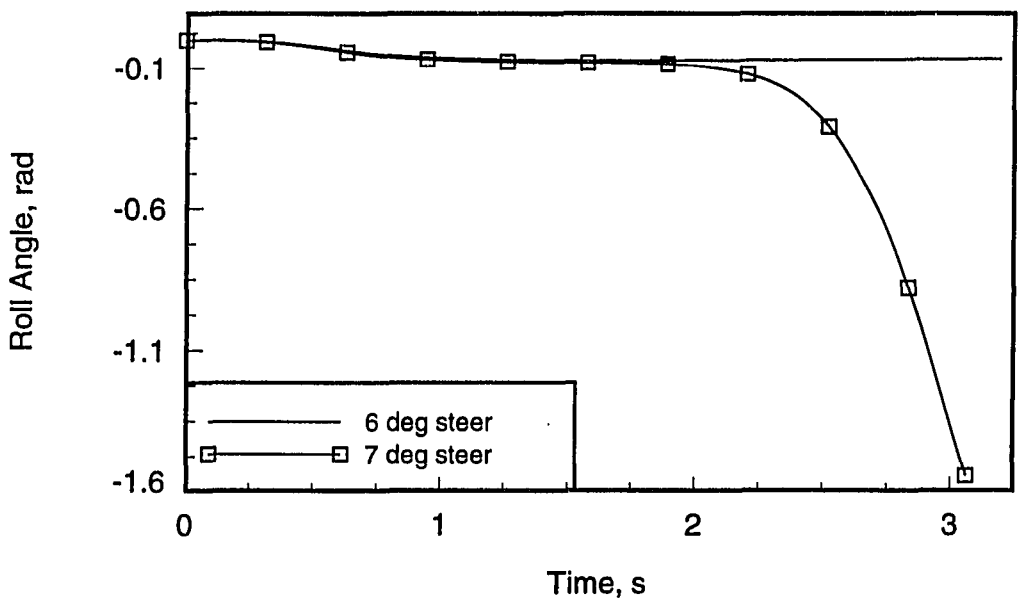

Figure 3.3: J-Turn Roll Angle Comparison

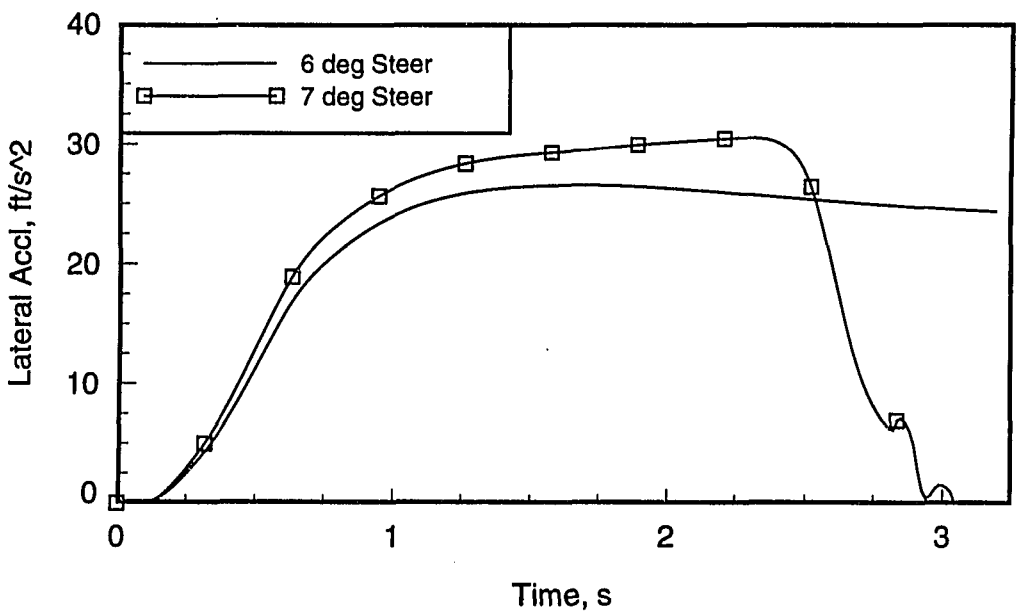

Figure 3.4: J-Turn Lateral Acceleration (ft/s^2) Comparison

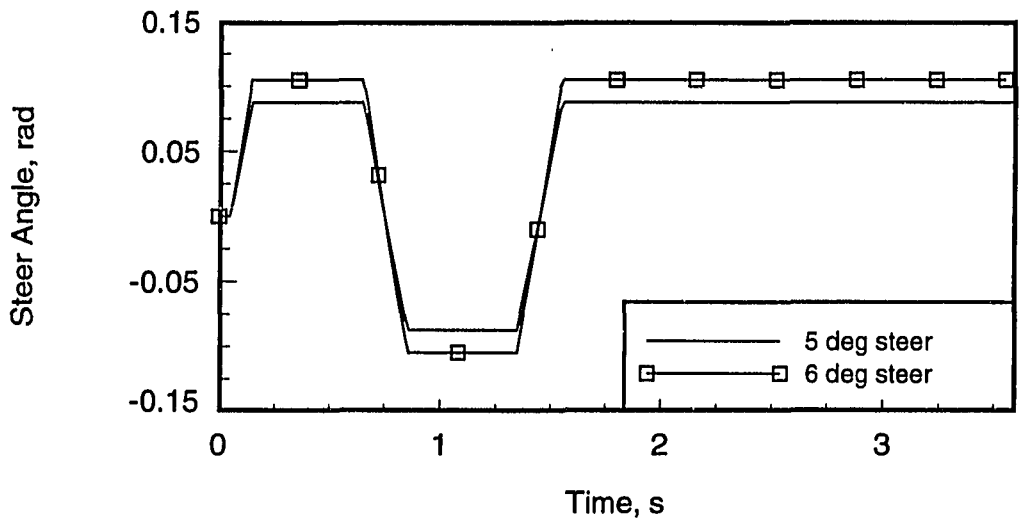

Figure 3.5: Input Steer Angle for 5 and 6 degree Reverse Steer Maneuver

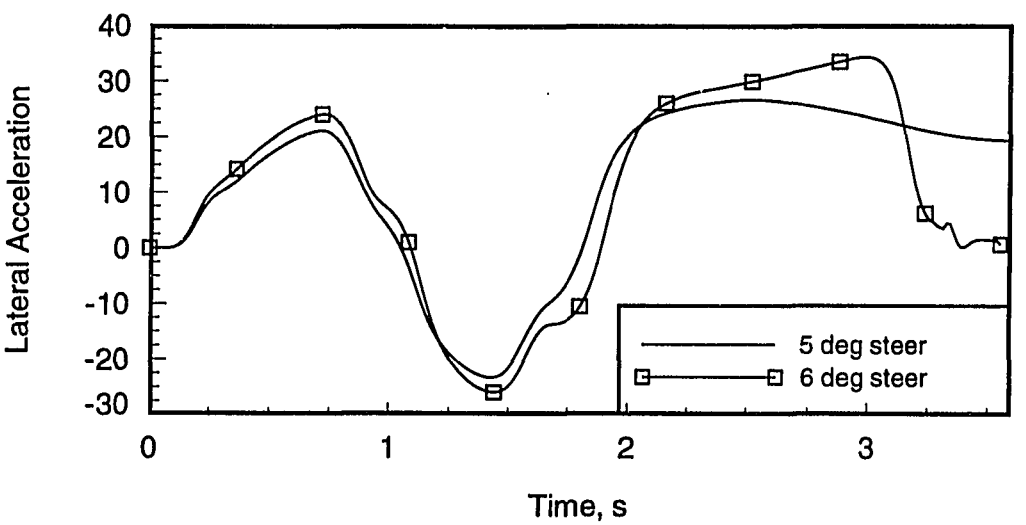

Figure 3.6: Reverse Steer Lateral Acceleration Comparison

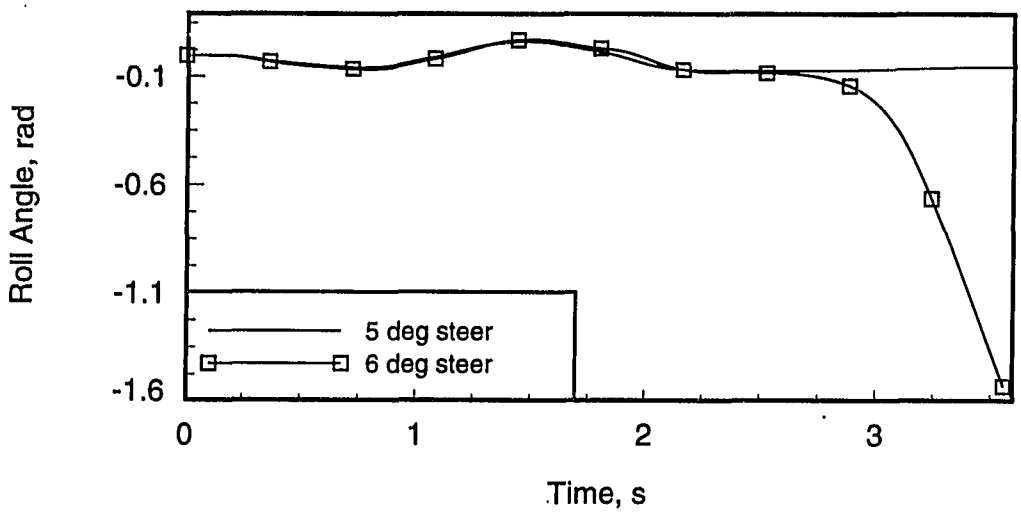

Figure 3.7: Reverse Steer Roll Angle Comparison

mass for this maneuver. The peak roll angle is about -0.073 radians or -4.2 degrees for the 5 degree maneuver. The 6 degree maneuver rolls over.

Clearly the reverse steer maneuver led to rollover at lower steer angles than the J-turn, not a surprising result given the transient overshoot of lateral acceleration.

Split μ

The J-turn and the reverse steer yield rollover under very high amplitude steering conditions at high vehicle velocity. The next two examples yield rollover in the one case at low velocity, in the other with no steer at all.

Consider two tripped scenarios - a sudden μ increase as in an ice/pavement discontinuity and a split-μ surface with braking in a shoulder/pavement discontinuity. Table 3.2 gives values for the surface coefficients in the simulations.

Table 3.2: VDANL Simulation μ_y Parameters

Ice/Pavement	μ_{ice}	0.10	$\mu_{pavement}$	1.00
Shoulder/Pavement	$\mu_{shoulder}$	0.40	$\mu_{pavement}$	1.00

Ice/Pavement Split μ In the ice/pavement discontinuity scenario (Figure 3.8), the vehicle has a constant steer input. The steer input is 5 degrees and the forward velocity is 35 mph (15.65 m/s). The vehicle develops a substantial yaw rate on the initial section of dry pavement. As the vehicle leaves the first section of pavement and drives onto the low μ surface, it continues to yaw in a clockwise direction, developing an increasing sideslip angle, β. When the vehicle again encounters the high μ dry pavement surface, it has a very large sideslip angle, yielding a sudden large lateral force at the outside tires.

Figures 3.9, 3.10, and 3.11 present VDANL results for the ice/pavement maneuver as described in Figure 3.8. The sideslip angle approaches 60 degrees during the on-ice portion of the maneuver. The roll angle plot indicates that rollover results when the vehicle model encounters the high μ surface.

It is interesting to compare the time trace from Figure 3.10 with the simple model of Reference [31] which calls for this vehicle to lift wheels under sudden sustained lateral acceleration of about 23.13 ft/s^2 (0.72 g's).

Shoulder/Pavement Split μ In the shoulder/pavement discontinuity(Figure 3.12), there is a split coefficient of friction between the left and right sides of the vehicle. (Consider the situation when two right side tires are on the shoulder, two

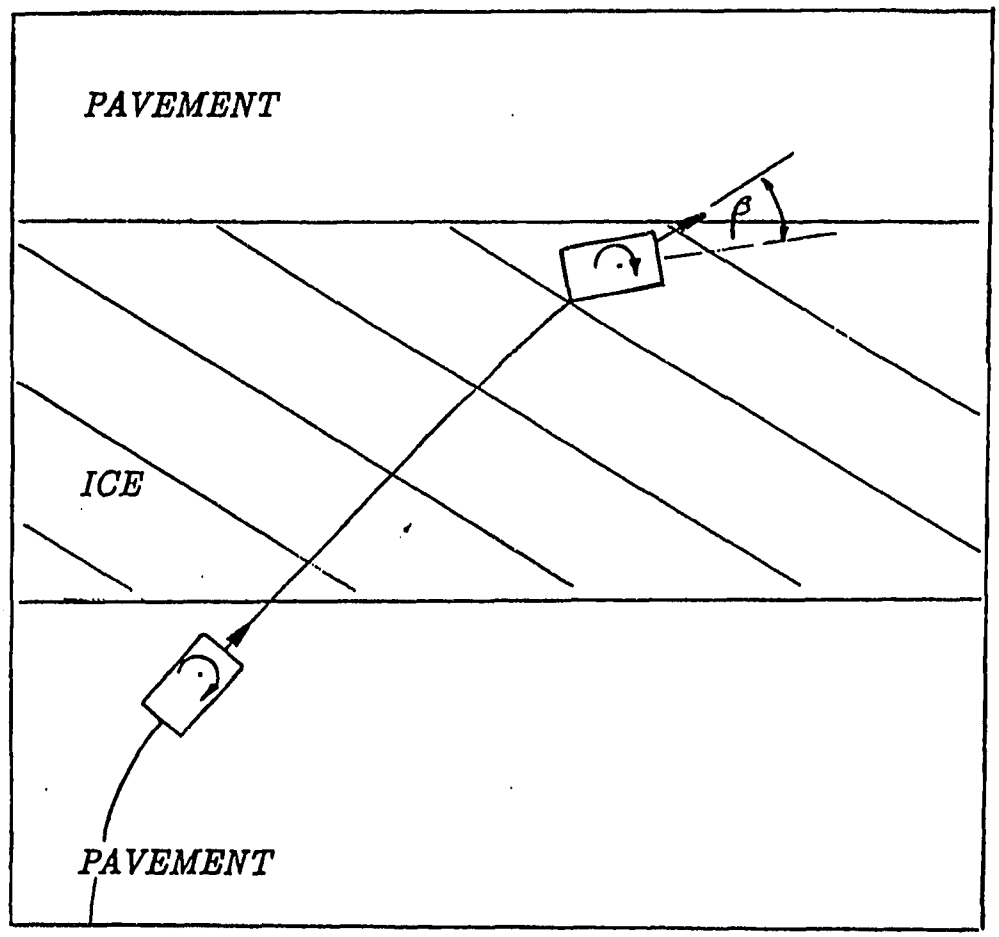

Figure 3.8: Sketch of Ice/Pavement Split μ Maneuver

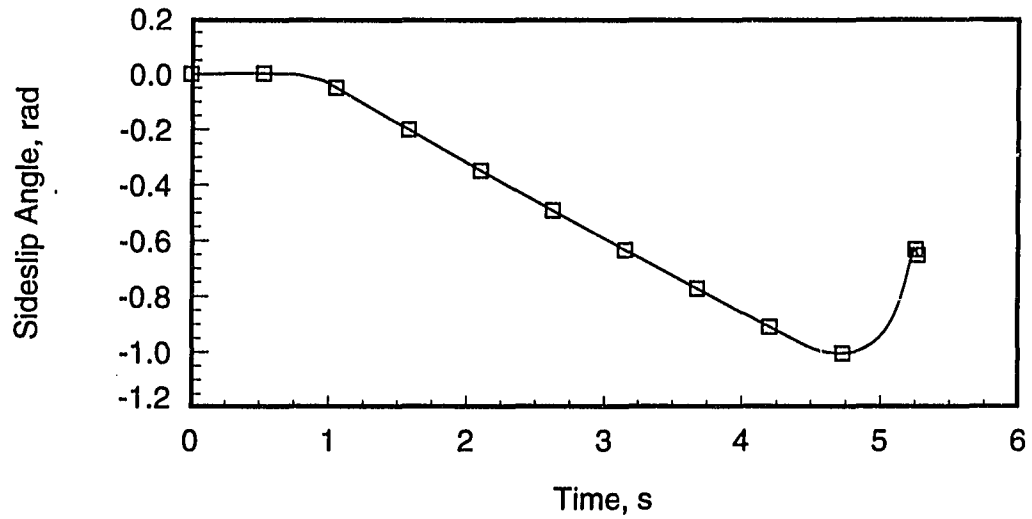

Figure 3.9: Plot of Sideslip Angle, β, for Ice/Pavement Maneuver

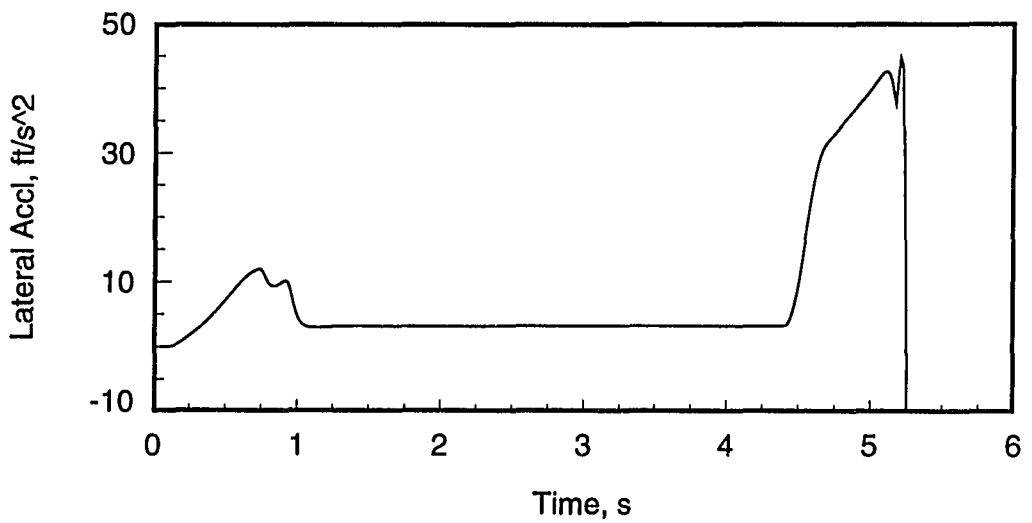

Figure 3.10: Plot of Sprung Mass Lateral Acceleration (ft/s^2) for Ice/Pavement Maneuver

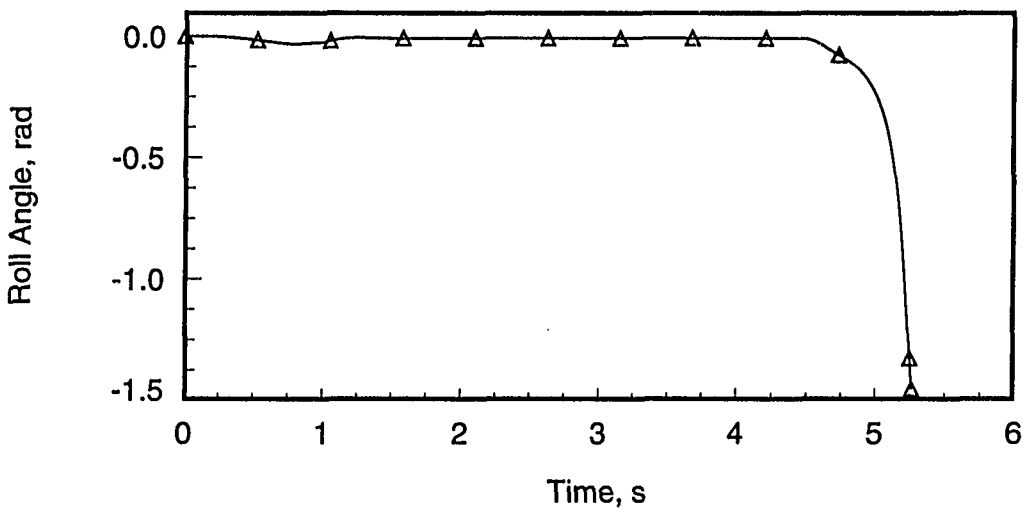

Figure 3.11: Plot of Sprung Mass Roll Angle for Ice/Pavement Maneuver

left side tires are on the roadway). The vehicle is going straight ahead at 29.1 m/s (65 mph) at the beginning of the simulation, and no steer is applied at any time. When severe braking is applied, unequal side-to-side brake forces cause a yaw moment. The yaw moment yields a yaw angle and subsequent lateral motion. When the brakes are released, the suddenly increased lateral forces and velocities are sufficient to cause the vehicle to rollover.

Figure 3.13 gives a time history of the braking force. Results for the shoulder/pavement follow in Figures 3.14, 3.15 and 3.16 for sideslip angle, lateral acceleration, and roll angle, respectively.

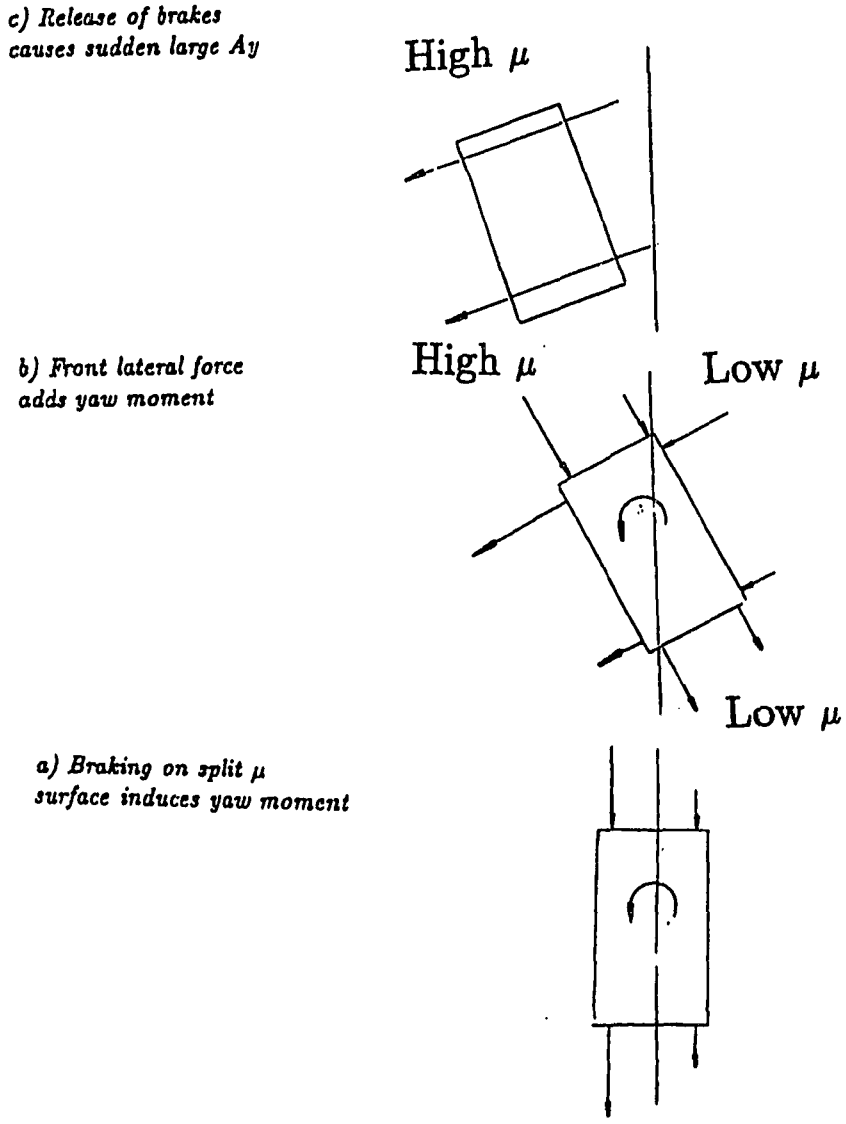

Figure 3.12: Sketch of Shoulder/Pavement Split μ Maneuver

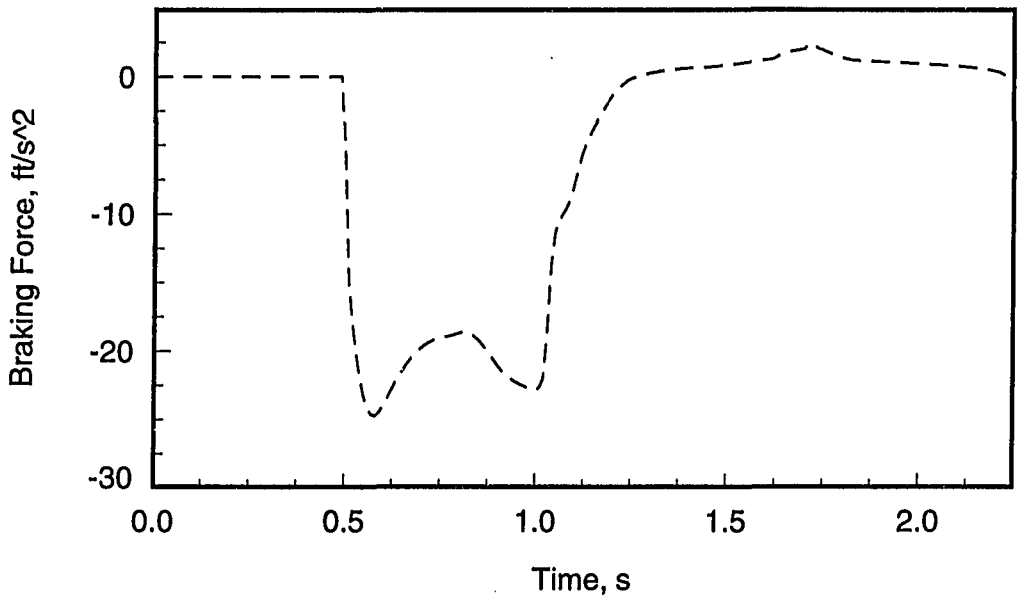

Figure 3.13: Plot of Braking Force for Shoulder/Pavement Split μ Maneuver

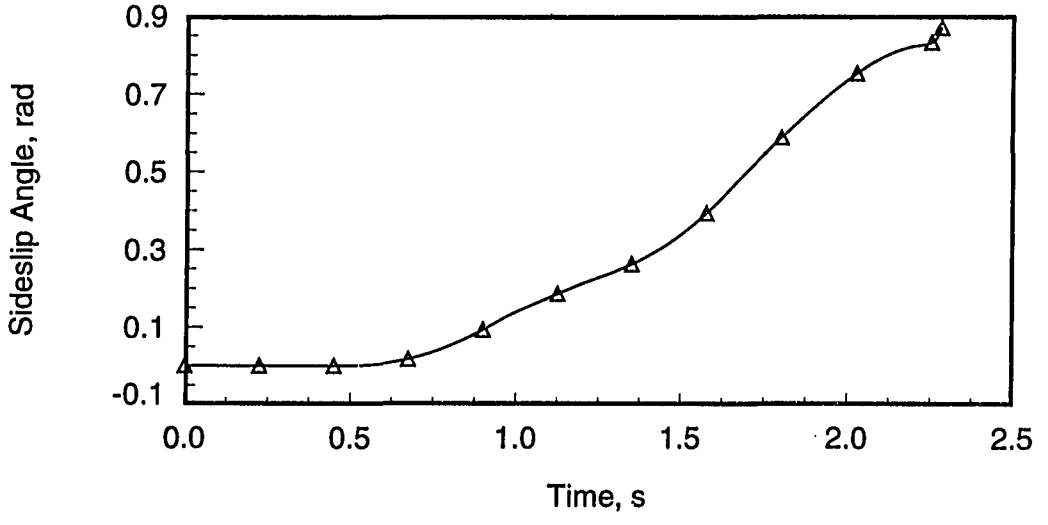

Figure 3.14: Plot of Sideslip Angle, β, for Shoulder/Pavement Split μ Maneuver

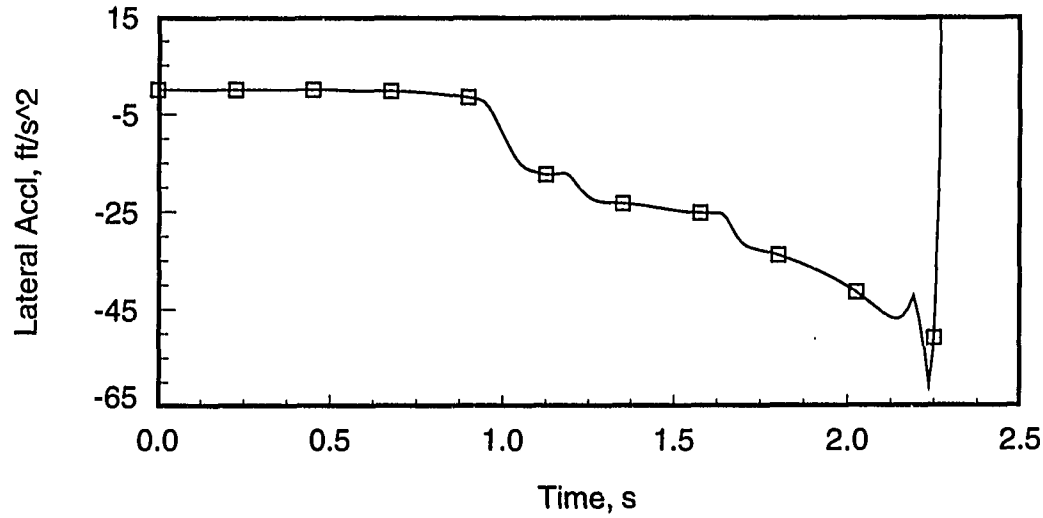

Figure 3.15: Plot of Lateral Acceleration for Shoulder/Pavement Split μ Maneuver

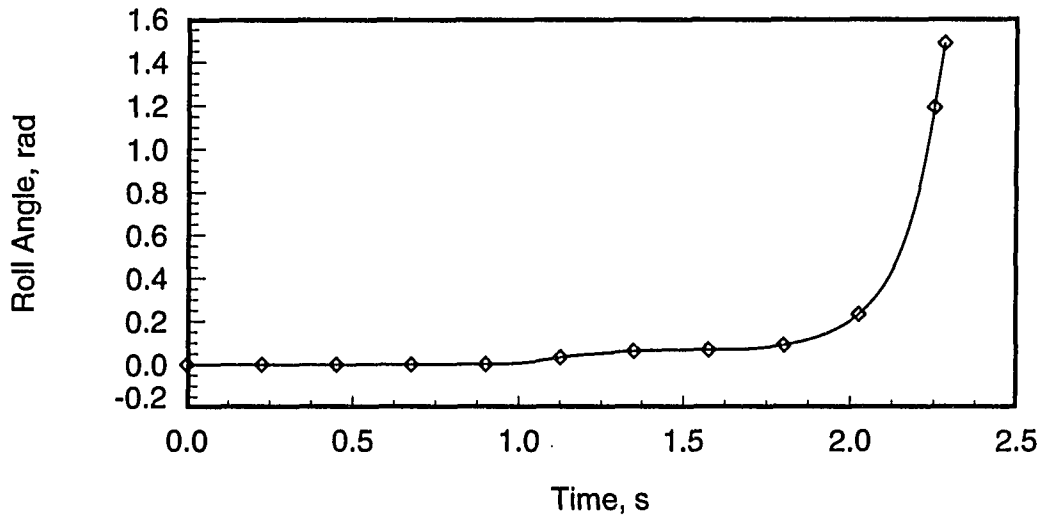

Figure 3.16: Plot of Sprung Mass Roll Angle for Shoulder/Pavement Split μ Maneuver

Summary

These simulations present a vehicle model that is quite roll-resistant on a high-μ surface, requiring a combination of high speed and very-high-amplitude steering to elicit rollover. Yet simulations indicate the same vehicle model can be tripped to rollover at low speeds or with, in the case of the side-to-side split-μ surface, no steer at all. This leads to an interest in tripped rollover which will frequently recur in this thesis.

Testing for Rollover

Since vehicle tests which intentionally culminate in rollover are difficult, expensive, and potentially dangerous, it is not surprising that such tests are rare. The literature review has already discussed work on this topic. This section presents additional details of the most recent of these experiments.

Nalecz [59] presented the results of experimental full-scale testing of eight vehicles in a variety of maneuvers. These eight vehicles ranged from a small passenger car to pickups and utility vehicles and vans. These included a 1986 Chevrolet Chevette, 1985 Ford Thunderbird, 1988 Toyota Pickup, 1985 Ford F-150 Pickup, 1984 Ford Bronco, 1985 Ford Bronco II, 1988 Dodge Caravan, and a 1987 Mitsubishi Van. The maneuvers included tripped rollover with an immovable curb and with soil/pavement discontinuities.

The authors performed a total of 77 experiments including the following number of test runs (in parenthesis) for each vehicle listed: Ford Thunderbird (4), Ford Bronco II (12), Ford Bronco (12), Mitsubishi Van (13), Toyota Pickup (13), Dodge Caravan (8), Ford F-150 (11), and Chevrolet Chevette (4). The authors stated that the

passenger cars (Chevette and Thunderbird) could not be rolled over in the attempted maneuvers, the Thunderbird because of reaching the maximum test speed of 45 mph without rollover and the Chevette because the vehicle's braking system could not be made to lock-up in order to produce the desired skidding motion.

Table 3.3 summarizes some of their test results for the vehicles which rolled over. Note, the maneuvers include WSS (Wet Skid into Soil), WSC (Wet Skid into Curb), DSS (Dry Skid into Soil), and DSC (Dry Skid into Curb). The vehicles include BRII (Ford Bronco II), BR (Ford Bronco), MITV (Mitsubishi Van), TOPK (Toyota Pickup), DOGC (Dodge Caravan), and F-150 (Ford F-150). The "Load" was used by the authors to determine the influence of payload on vehicle rollover velocities.

An interesting feature of the data, which will be an important issue in subsequent sections of this thesis, is the impact lateral velocity needed to initiate rollover. Note there are values as low as 3.6 m/s or about 8 mph.

The authors experienced no rollovers from non-impact maneuvers, maneuvers which included a curved path across a discontinuity or which were skidded on pavement. A maneuver was classified as a rollover when the outriggers touched the ground. Rollovers occurred only during the pavement-soil or pavement-curb impact maneuvers. And in these maneuvers, the vehicles had to be skidding prior to the curb or pavement-soil discontinuity before rolling over.

The authors initially believed that they would be able to perform repeatable and uniform vehicle-impact test conditions. They found that this was not possible. They stated that although the vehicles negotiated essentially the same curved path, that each test encountered the terrain discontinuity or curb under different conditions, making comparison between test runs difficult.

The authors stated that although their primary emphasis during the project was to analyze the influence of vehicle parameters and the velocity at rollover, no useful relationships with consistently high correlations were found. They stated that the full-scale test runs did not provide sufficient information to perform a definitive analysis on the influences of vehicle design characteristics on the tripped-rollover behavior of light vehicles.

Reference [59] verifies the notion that (a) rollover is a complex event, (b) it is hard to measure and hard to simulate with confidence because hard-to-measure details are important, and (c) tripped-rollover could be initiated at low lateral velocities.

The subsequent chapters of this thesis deal with the details of rollover. Chapter 4 discusses smooth surface rollover with attention to the analytical theory behind static rollover measures - the static stability factor, the tilt-table ratio, and the cable side pull test. Chapter 5 discusses tripped rollover, with attention to both interactions with a rigid barrier and so-called furrow tripping in which the vehicle slides some distance on a highly-resistive surface. Chapter 6 provides sensitivity analyses which give a measure of importance to sometimes hard to measure vehicle parameters.

Table 3.3: Rollover Test Results (Reference [59])

No.	Vehicle	Man-euver	Initial Forward Velocity	Load	Impact Lateral Velocity	Impact Lateral Accel'n	h	T
			mph	lbf	m/s (mph)	g's	m	m
4	BRII	WSS	40	0	-3.55 (-7.9)	0.11	0.74	1.428
6	BRII	WSS	40	442	-3.92 (-8.8)	0.34	0.65	1.428
10	BRII	WSC	35	0	-8.44 (-18.9)	0.63	0.74	1.428
12	BRII	WSC	35	442	-5.99 (-13.4)	0.46	0.65	1.428
14	BR	WSS	40	0	-8.37 (-18.7)	0.56	0.77	1.630
16	BR	WSS	42	422	-7.34 (-16.4)	0.60	0.81	1.630
20	BR	WSC	35	0	-6.07 (-13.6)	0.62	0.77	1.630
22	BR	WSC	30	422	-4.55 (-10.2)	0.55	0.81	1.630
24	MITV	WSS	35	0	-5.16 (-11.5)	0.68	0.71	1.402
26	MITV	WSS	35	422	-4.15 (-9.3)	0.65	0.75	1.402
31	MITV	WSC	30	0	-3.69 (-8.3)	0.47	0.71	1.402
33	MITV	WSC	30	422	-4.21 (-9.4)	0.60	0.75	1.402
35	TOPK	DSS	35	0	-3.72 (-8.3)	0.10	0.59	1.357
37	TOPK	WSS	35	422	-6.72 (-15.0)	0.62	0.65	1.357
41	TOPK	WSC	35	0	-6.02 (-13.5)	0.22	0.59	1.357
43	TOPK	WSC	30	422	-4.94 (-11.1)	0.48	0.65	1.357
47	DOGC	WSC	35	0	-6.50 (-14.5)	0.72	0.66	1.552
49	DOGC	WSC	35	422	-5.91 (-13.2)	0.52	0.71	1.552
51	F150	DSS	35	0	-6.18 (-13.8)	0.62	0.72	1.638
53	F150	DSS	35	422	-6.19 (-13.8)	0.63	0.75	1.638
56	F150	DSC	40	0	-5.33 (-11.9)	0.57	0.72	1.638

CHAPTER 4. UNTRIPPED ROLLOVER

This chapter presents an overview of untripped rollover from an analytical and an empirical point of view. By definition here, smooth surface rollover occurs on a surface with coefficient of friction, μ, limiting the shear forces generated at the tire-road interface. The coefficient μ may depend on the normal load. By our definition of smooth surface, μ is not dependent on the position on the surface.

Simulation of smooth surface rollover can be accomplished with a variety of models from simple one degree of freedom models through complex multibody models. Bernard et al. [31] considered very simple models to show that the simple formula for limit acceleration in a steady turn,

$$\frac{A_y}{g} = \frac{T}{2h} \tag{4.1}$$

can be extended to include the effects of overturning moment and sprung mass roll about the roll axis

$$\frac{A_y}{g} = \frac{\frac{T}{2}}{(h + \bar{a} + \bar{b})} \tag{4.2}$$

where $\bar{a}$ and $\bar{b}$ are lateral deflections per g due to overturning moment and sprung mass roll. This can be shown to lead to predicted roll in a steady turn in the range of about 0.9 T/2h for cars and utility vehicles. Reference [31] went on to call for the use of more sophisticated models for transient maneuvers wherein timing of the lateral forces between axles is important.

The following sections consider smooth surface rollover and tests for measuring the limits of a vehicle's propensity to roll over.

Smooth Surface Rollover

In 1967, during straight line braking experiments, a car traveling at 60 mph on a dry, flat surface overturned. The car apparently became unstable and spun when its rear wheels, but not front wheels, locked up during braking. In an effort to understand this event, Kemp and Neilson [3] derived equations for the vertical motion and for the angular momentum and numerically solved for the rates of roll for overturning on a smooth road.

McHenry [12] approximated the minimum speed for rollover on a uniform surface without obstacle contact. He assumed that the resistive force is approximately constant and equal to the minimum value that will produce rollover. With this assumption, the minimum initial kinetic energy must be equal to the energy lost during the lateral sliding and in lifting the center of gravity.

$$\frac{1}{2}mV^2 = \mu\, m\, g\, y_o' + m\, g\, (R - h) \tag{4.3}$$

where y_o' is the sliding distance of the contact point O during the rollover motion, μ is the coefficient of friction of the uniform surface, and R is the distance of the center of gravity from point O, namely

$$R = \sqrt{h^2 + \left(\frac{T}{2}\right)^2} \tag{4.4}$$

so that

$$\frac{1}{2}mV^2 = \mu\, m\, g\, y_o' + m\, g \left[\sqrt{h^2 + \left(\frac{T}{2}\right)^2} - h\right]$$

$$= \mu\, m\, g\, y_o' + m\, g\, h \left[\sqrt{1 + \left(\frac{T}{2h}\right)^2} - 1 \right] \tag{4.5}$$

The minimum initial value of the effective friction coefficient occurs when

$$\mu_{min} = \frac{T}{2h} \tag{4.6}$$

Substituting into Equation 4.3 from Equations 4.4 and 4.6 and solving for V yields

$$V = \sqrt{2\, g \left[\frac{T}{2h} y_o' + h \left(\sqrt{1 + \left(\frac{T}{2h}\right)^2} - 1 \right) \right]} \tag{4.7}$$

where V is the minimum lateral speed on a smooth surface without obstacle contact.

Bickerstaff [13] discussed rollover as a function of lateral acceleration which occurs when the roll stiffness of the vehicle is saturated and the vehicle becomes a rigid body. At this point no additional roll occurs between the sprung mass and the suspension. In normal suspension deflection, roll is stable since removal of the acceleration will restore the vehicle to it's original position. However once the maximum lateral acceleration has been achieved, the vehicle becomes unstable since roll may continue even with decreasing lateral acceleration. He then goes on to describe the cable pull test.

Rice et al. [14, 15] evaluated untripped flat-surface vehicle maneuvers using both simulation and full-scale experiments. The authors studied the effects of a variety of configurational and operational factors on rollover response. These factors included initial speed, steering input patterns, braking techniques, suspension damping, loading, and tire characteristics. They concluded that vehicle rollover response is dominated by the vehicle's rigid body geometry but with contributions from suspension effects. They noted that untripped rollover is difficult to predict and accomplish even on high μ surfaces.

Bernard et al. [31] addressed smooth surface rollover in steady turn tests, a suddenly applied lateral force, transients without braking such as a lane change or slalom, and a drastic brake and steer maneuver.

The following sections discuss three commonly used metrics used to represent static roll stability - the static stability factor, tilt-table ratio, and side-pull ratio. All three measures are approximations of the maximum lateral acceleration, in g's, which a particular vehicle can sustain in a steady turn, on a constant μ surface, without rolling over.

Static Stability Factor, SSF

The static stability factor is the ratio of the vehicle's half-track to its center of gravity height - the well known T/2h. This comes from the simple formula for limit acceleration in a steady turn, namely

$$\frac{A_y}{g} = \frac{T}{2h} \tag{4.8}$$

The measurement of the track width is the average of the front and rear track widths.

This metric assumes the vehicle to be a rigid body with no tire or suspension deflections or motions. It is therefore calculated based on the static center of gravity height and the track width, discounting any change in the center of gravity's position due to the vehicle's suspension and tires, as would be seen in a real cornering situation. Winkler [51] noted that measuring the center of gravity height is a difficult task and can be a source of fairly large errors. He found differences greater than 1 inch (25 mm) in a round robin study of the center of gravity height measurement at various laboratories.

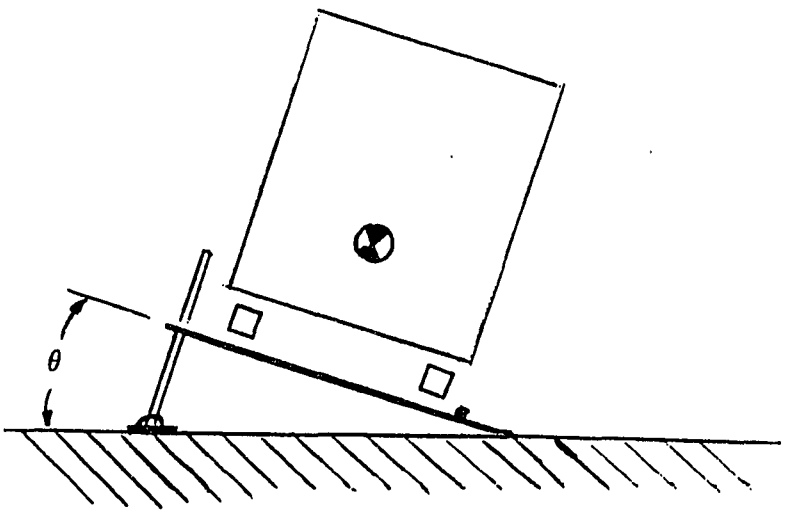

Figure 4.1: Rigid Block on Tilt Table

Tilt Table Ratio, TTR

Tilt table testing has the goal of measuring the minimum angle at which a vehicle on an inclined table will tip over. The tangent of this minimum angle is called the tilt table ratio, TTR. The utility of TTR hinges on an analogy between TTR and the minimum lateral acceleration required to tip over a vehicle which is traversing a steady turn. Since the analogous lateral acceleration is the minimum required to upset the vehicle, TTR is associated, through the analogy, with tipping the vehicle exactly one-quarter-turn.

Figure 4.1 shows a rigid block on a tilt table. The position of the table to elicit tip over of the block has the center of gravity of the block over the lower corner of the block. This occurs when $\tan\theta = T/2h$.

In practice it is expected that the test vehicles will tip at an angle whose tangent

is less than T/2h. There are several phenomena at work that, summed together, lead to this lessening of the measured angle.

There is one artifact of the testing which tends toward a higher measured angle. In particular, the test is commonly done with a one-inch-high stop at the downhill side of the vehicle. This has the effect of lowering the effective value of h, which has the tendency to increase TTR.

On the other side are several effects which wash out the effect of the downhill stop and ensure that the TTR will be less than T/2h.

First of all, consider that the overturning moment is caused by the downhill tires flexing inboard. As the test approaches lift of the uphill tires, the total shear load on the downhill tires is W $\sin\theta$. For typical tilt table angles, this shear load is less than the analogous load in steady turn on a flat surface by a factor of (1 - $\sin\theta$), about thirty percent. Nevertheless, the inboard tire flexure can lead to significant lowering of TTR.

Similar arguments hold for rolling toward the downhill side of the vehicle. In particular, for typical tilt table angles the apparent roll gain of the vehicle becomes $\overline{\phi}$ $\sin\theta$, where $\overline{\phi}$ is the roll gain under flat surface conditions. The motion of the sprung mass center toward the downhill side shortens the effective track dimension.

Another tendency to decrease TTR derives from lateral compliance of the suspension-inboard motion of the wheel hubs due to suspension compliance. Finally consider that the sum of the normal loads must be W $\cos\theta$. This unloads the suspensions by a factor of (1- $\cos\theta$) and the vehicle must go up (in the sense perpendicular to the tilt table). For typical tilt table angles and typical suspensions, the suspension loads will drop by about thirty percent, yielding a significant increase of center of

gravity height. This increase, which is typically more than the distance lost to the downhill stop, is artificial in the sense that it is not analogous to on-road conditions. Furthermore, the change in TTR due to the unloading of the suspensions penalizes most severely those vehicles with soft ride rates, a trend that would not be reflected in over-the-road vehicle operation or static pull testing.

NHTSA test results [60] support the expectation that TTR will be less than T/2h. From over 400 vehicle data sets included in the NHTSA test results, 111 include TTR and T/2h values. Appendix B presents TTR and T/2h measurements from these 111 vehicles. The data shows that the measurements yield TTR between 73% and 97% of T/2h. Calculations of the mean ratio of TTR/(T/2h) values presented by NHTSA is 0.86, with a standard deviation of 0.05.

Cable Pull Test or Side Pull Ratio, SPR

The cable pull test or side pull ratio simulates a steady turn. The line of action of the cable is through the vehicle's center of gravity, parallel to the horizontal plane and normal to the vehicle's longitudinal axis. See Figure 4.2. The side pull force required for rollover can be expressed as an equivalent lateral acceleration. This equivalent lateral acceleration is a measure of the effective track width to center of gravity height ratio for the vehicle to tip over exactly a one-quarter-turn. The side pull force is sensitive to several other factors such as the the roll gradient and the vertical and lateral center of gravity shift.

As the vehicle sprung mass rotates about the roll axis, the sprung mass center of gravity moves closer to the outside wheel rollover axis. Furthermore, due to tire and suspension compliance, the outside wheel rollover axis and the center of gravity

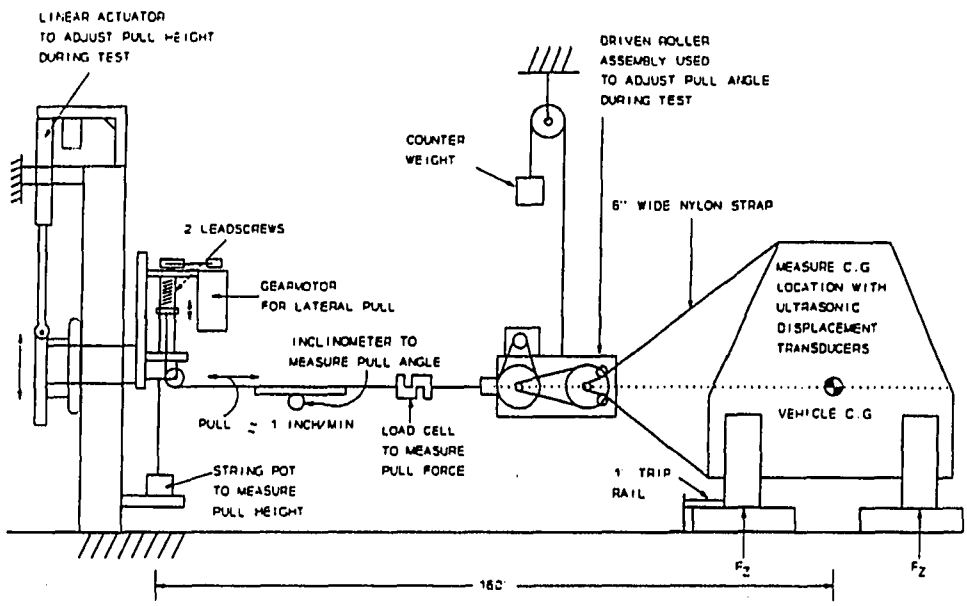

Figure 4.2: Cable Pull Test. (References [1,50])

are brought closer together, so that the resulting effective track width at rollover is significantly narrower than the basic static level. The sprung mass center of gravity can also translate vertically because of the suspension response to the side forces and suspension kinematics. Vehicle squat and jacking either improve or reduce rollover resistance, respectively.

Chrstos and Guenther [50] stated that the side pull test may be time consuming and that the belts applying the side force may damage the vehicle. Furthermore the side pull test requires knowledge of the center of gravity height and any errors in the cg height measurement will be carried over to the side pull test. They also emphasized

that the side pull test does not give an absolute steady state lateral acceleration level at which a vehicle will rollover. For example, this test applies a body force to the sprung mass at the total vehicle center of gravity height when in reality each "rigid body" of the vehicle (e.g. frame/body, front and rear suspension, engine) are acted upon by a horizontal force equal to its mass times the lateral acceleration level. Thus there is an increased lateral suspension deflection, approximately 15 percent for passenger cars and slightly higher for light trucks and utility vehicles.

Bickerstaff [13] and Bernard et al. [31] give the following steady state lateral acceleration required to produce rollover

$$\frac{a_{ro}}{g} = \left(\frac{T}{2h}\right)\left(\frac{1}{(1+\frac{H'}{h_{roll}}\frac{K_\phi}{57.3})}\right) \tag{4.9}$$

where H' is the distance of the center of gravity above the roll axis at the longitudinal cg location, h_{roll} is the location of the roll axis above the ground at the longitudinal cg location, and K_ϕ is the sprung mass roll flexibility gradient, e.g. the degree of body roll per g of lateral acceleration.

This expression shows that the minimum acceleration required for rollover is reduced when the roll gradient K_ϕ is increased, the track width T is reduced, or the center of gravity height h is increased. This expression ignores the effects of the tires or jacking effects due to swing axle suspensions.

Allen et al. [46] studied the effects of the roll gradient (which leads to the lateral shift of the sprung mass due to roll angle), the change in center of gravity vertical location at rollover (which accounts for suspension squat/lift effects), and the change in track width (which accounts for tire and suspension compliance effects) on side

pull test results. They found that the most important explanatory variable is the roll gradient, followed by the cg height and track change, with the majority of the effect explained by the combination of roll gradient and cg height change. The authors also state that there are additional factors which are not readily explainable by the studied variables.

CHAPTER 5. TRIPPED ROLLOVER

This chapter presents an overview of tripped rollover from an analytical and an empirical point of view. Tripped rollover occurs because of sudden increases in lateral force due to obstacles or by changing surface characteristics.

Analyses of tripped rollover includes the well–known simple curb trip model offered as early as 1959 by Meriam [61] and later presented in a vehicle context by Jones [9, 10], and discussed by McHenry [12] and Bickerstaff [13]. In this scenario, a one degree of freedom vehicle model has lateral sliding motion and impacts an immovable obstacle such as a rigid curb. An equation [61, 9, 10] commonly associated with the minimum lateral velocity for a curb trip resulting in rollover is

$$v_{ro} > \sqrt{\frac{2g}{mh} I_o \left(\sqrt{1 + \left(\frac{T}{2h}\right)^2} - 1 \right)} \tag{5.1}$$

where v_{ro} is the minimum lateral velocity for rollover, g is the gravitational constant, m is the mass of the vehicle, I_o is the roll moment of inertia about the impact point, h is the distance of the center of gravity above the curb, and T is the track width. For vehicle parameters normally associated with cars and utility vehicles, the trip velocity falls within a narrow range of ten miles per hour.

Bernard et al. [31] also analyzed tripped rollover using a simple model. In particular, they used a two degree of freedom model subject to sudden lateral force

at the tires. The model predicted wheel lift for a suddenly applied lateral acceleration for a typical passenger car to be about 0.60 T/2h and for a utility vehicle to be about 0.66 T/2h.

More complex models offer the potential for the consideration of more complex scenarios. Chapter 3 addressed two tripped scenarios. The first of these concerned a dry pavement to ice to dry pavement trajectory wherein the vehicle attained a fairly large yaw rate on the dry pavement, spun out on the ice, then rolled over because of high forces deriving from sliding off the ice back on to a dry surface. The second concerned braking on a split μ surface, e.g., gravel on one side and pavement on the other, which led to rapid spin out and rollover on the pavement. Both these scenarios were simulated using a fairly complex multi-degree of freedom nonlinear simulation, and both rollovers resulted from a very sudden increase in lateral force on the tires.

This chapter addresses the potential for rollover due to a sudden increase in lateral force. The initial phase of the motion, that is the motion up to the sudden increase in lateral force, is not considered here. Thus the models are simple - typically a block is the model for the vehicle, and the applied forces, rather than deriving from normal loads and sideslip angles as in the ice/pavement or split μ scenario, are applied by rigid stops or very simple analytical representations of tire/road or tire/ground interactions.

The following sections address tripped rollover due to curb impact and due to furrow tripping. These sections address the mechanics of the vehicle rolling a one-quarter-turn onto its leading side and then address the mechanics of the vehicle which has enough energy to leave the ground and land on its roof in a two-quarter turn.

Curb Trip - One-Quarter-Turn

In deriving the minimum lateral speed for rollover as a result of impact with a curb or obstacle, Baker [62] used conservation of energy, assuming that the total kinetic energy of the vehicle at the time of obstacle contact is converted into potential energy as the height of the center of gravity is increased. The minimum velocity is then derived when the kinetic energy, $\frac{1}{2}\ m\ v^2$, is equal to the increase in potential energy, $m\ g\ \Delta h$, where Δh is the maximum height of the center of gravity during rollover minus its original height from the ground.

$$\begin{aligned} v_e^2 &= 2\ g\ \Delta h \\ &= 2g\left(\sqrt{h^2+\left(\frac{T}{2}\right)^2}-h\right) \end{aligned} \tag{5.2}$$

where h is the height of the cg from the ground, T is the track width, and v_e is the minimum velocity using the conservation of energy analysis. So that

$$v_e = \sqrt{2gh\left(\sqrt{1+\left(\frac{T}{2h}\right)^2}-1\right)} \tag{5.3}$$

Equation 5.3 underestimates the minimum velocity since energy loss during the collision is not taken into account.

In Figure 5.1, a uniform block is assumed to approach a rigid stop of negligible height at velocity v. When it hits the stop, it takes on a rotational constraint wherein it swings about a hinge, initially with angular velocity $\dot{\theta}_O$. The relationship between v and $\dot{\theta}_O$ can be derived based on momentum considerations. In particular, conservation of angular momentum about the contact point O requires

$$I_O\ \dot{\theta}_O = m\ v\ \frac{b}{2} \tag{5.4}$$

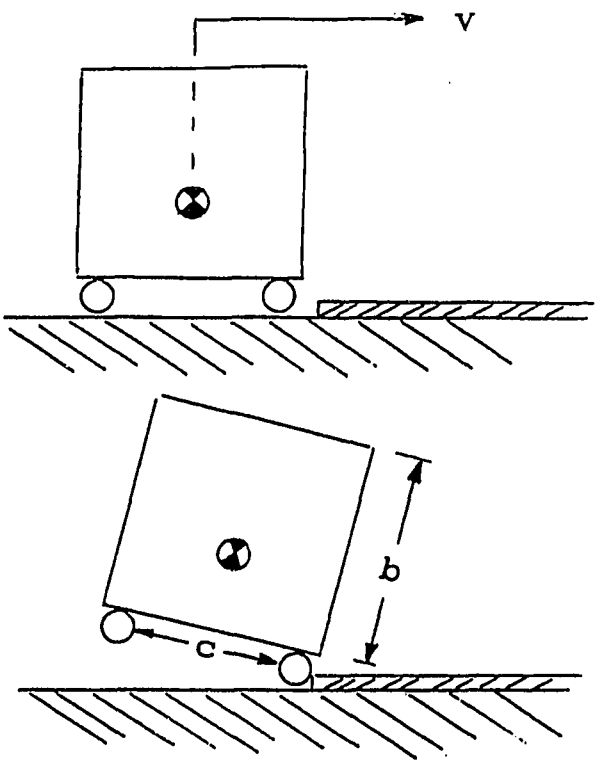

Figure 5.1: One Degree of Freedom Model for Curb Impact

where I_O is the moment of inertia of the mass about the contact point.

In order for the block to rotate exactly one-quarter turn after impact, the center of gravity must rise vertically through a distance above the hinge, Δh. The kinetic energy of rotation must be large enough to lift the mass center through this distance.

Thus the conditions for overturning are given by:

$$\frac{1}{2}I_o\dot{\theta}^2 \geq \frac{mg}{2}\left(\sqrt{b^2+c^2}-b\right) \tag{5.5}$$

Substituting from Equation 5.4 for $\dot{\theta}$ and solving for v gives

$$v^2 \geq \frac{4g}{mb}I_o\left(\sqrt{1+\frac{c^2}{b^2}}-1\right) \tag{5.6}$$

This derivation was presented by Meriam in 1959 [61].

In 1973, Jones [9] made the assumption that tripping of a car sliding sideways could be modeled by the block of Figure 5.1 using

$$\mathrm{b} = 2\ \mathrm{h}$$

and

$$\mathrm{c} = \mathrm{T}$$

where h is the vehicle's center of gravity height and T is its track width. Making these substitutions in Equation 5.6 yields

$$v^2 \geq \frac{2g}{mh}I_o\left(\sqrt{1+\left(\frac{T}{2h}\right)^2}-1\right) \tag{5.7}$$

where v is the critical sliding velocity, CSV. (McHenry [12] and Ford and Thompson [4] also made this assumption.)

This CSV formulation can be more clearly understood by considering in detail the roll moment of inertia which can be written

$$I_o = I_{cg} + m\left(\left(\frac{T}{2}\right)^2 + h^2\right) \tag{5.8}$$

A very useful approximation for I_{cg} in Equation 5.8 is

$$I_{cg} = a\ m\ \left(\left(\frac{T}{2}\right)^2 + h^2\right) \tag{5.9}$$

where a is a dimensionless constant. In this case, the critical sliding velocity from Equation 5.7 becomes

$$\text{CSV(a)} = \sqrt{2g(a+1)h\left(1+\left(\frac{T}{2h}\right)^2\right)\left(\sqrt{1+\left(\frac{T}{2h}\right)^2}-1\right)} \tag{5.10}$$

Bickerstaff [13] in 1976 used

$$\text{a} = 0$$

This led to

$$\text{CSV(0)} = \sqrt{2gh\left(1+\left(\frac{T}{2h}\right)^2\right)\left(\sqrt{1+\left(\frac{T}{2h}\right)^2}-1\right)} \tag{5.11}$$

Meriam [61] in 1959 and Jones [9] in 1973 used a better value

$$\text{a} = 1/3$$

which means

$$I_{cg} = \frac{m}{3}\left(\left(\frac{T}{2}\right)^2 + h^2\right) \tag{5.12}$$

This approximates I_{cg} based on the assumption that the block has mass uniformly distributed about a rectangle of dimensions T by 2h. This approximation leads to

$$\text{CSV(.33)} = \sqrt{\frac{8gh}{3}\left(1+\left(\frac{T}{2h}\right)^2\right)\left(\sqrt{1+\left(\frac{T}{2h}\right)^2}-1\right)} \tag{5.13}$$

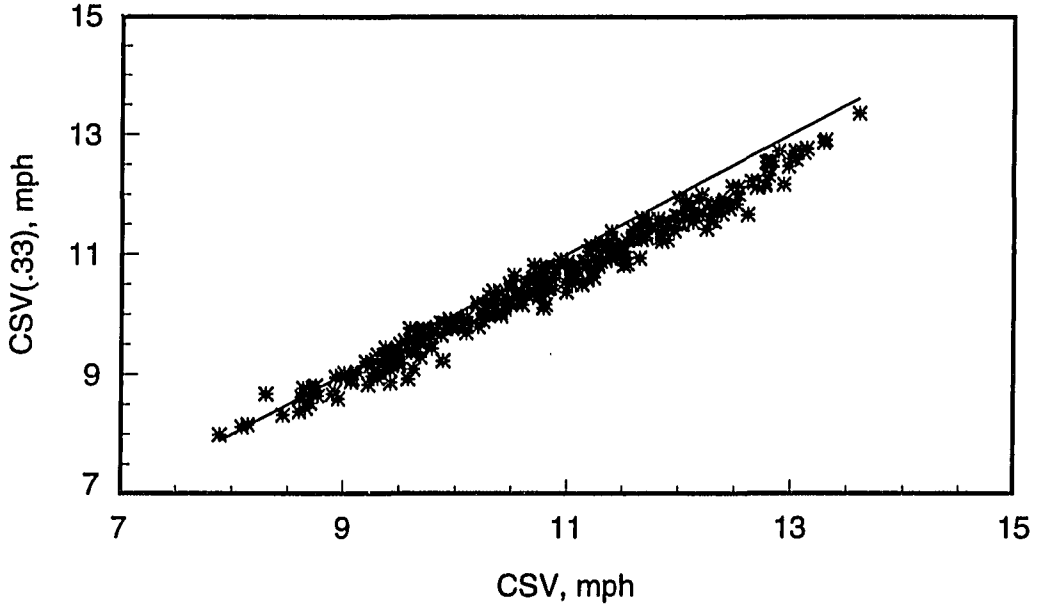

Figure 5.2: CSV(.33) versus CSV.

In the context of Reference [9], which concerns vehicles rather than blocks, the question of whether it is reasonable to approximate I_{cg} based on a uniform rectangular block needs to be addressed. We tested this assumption using a data set presented by Garrott [60]. Figure 5.2 presents results.

The 329 points in the figure were calculated from data in Garrott [60]. (There are over 400 vehicles in the data base. Only 329 data sets include all of the parameters needed for these calculations.) In each case, the vehicle data from Reference [60] is used to calculate CSV using both Equation 5.7, which is plotted on the horizontal axis, and Equation 5.13, which is plotted on the vertical axis. If the data fell directly on the line, the data would indicate that the roll moment of the vehicles about their center of gravity is given by Equation 5.12. The mismatch between the points and

the line derives from the mismatch between the measured roll moment of the vehicles about their own cg and the uniform rectangular block approximation.

A visual examination of the figure indicates that the match, while not perfect, is still quite good. An improved match can be obtained by setting

$$a = 0.404$$

which is to say

$$I_{cg} = \frac{1.21 \text{ m}}{3}\left(\left(\frac{T}{2}\right)^2 + h^2\right) \tag{5.14}$$

Using this formulation for the moment of inertia about the mass center in Equation 5.8 into Equation 5.7 yields

$$\text{CSV}(.404) = \sqrt{\frac{8.43\, gh}{3}\left(1 + \left(\frac{T}{2h}\right)^2\right)\left(\sqrt{1 + \left(\frac{T}{2h}\right)^2} - 1\right)} \tag{5.15}$$

Figure 5.3 replots results from the 329 vehicles of Reference [60], with results from Equation 5.15 on the vertical axis, and again with results from Equation 5.7 on the horizontal axis. Detailed analysis of these results show that for 99% of the vehicles in the data set, the results from Equation 5.15 are within 5% of the results of Equation 5.7.

The point is this: The approximation of Equation 5.9, which has been applied from time to time by researchers considering rollover, is reasonable. Furthermore, the calculations given above indicate that a = .404 provides a very good fit to NHTSA data.

A consequence of this point is that, as indicated by Equation 5.15, CSV depends on T and h.

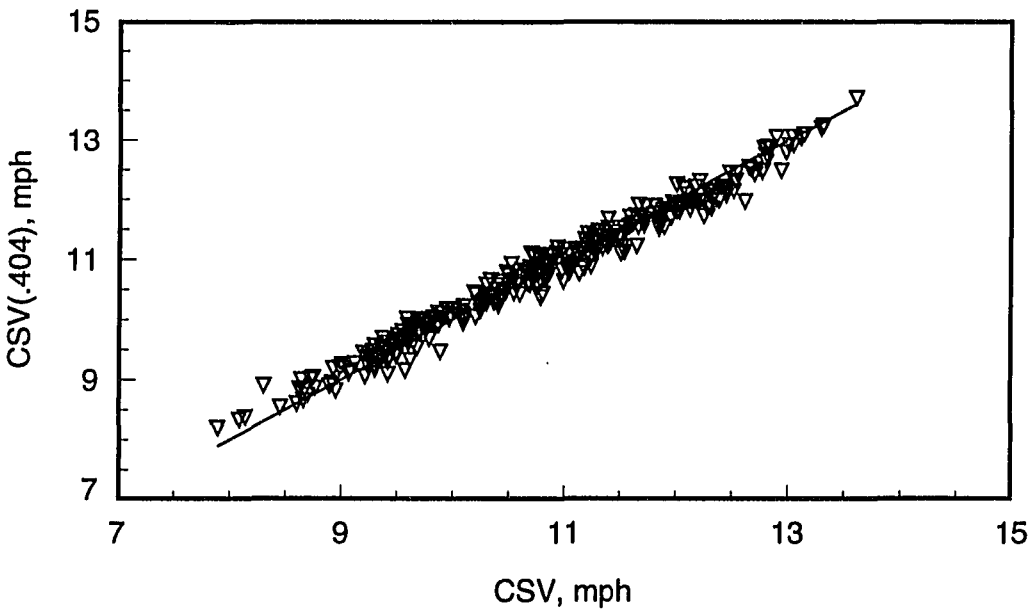

Figure 5.3: CSV(.404) versus CSV.

The so-called static stability factor T/2h gives the steady state lateral acceleration for tip over of a block, and its inverse tangent yields the TTR for a rigid block. Thus it is not surprising to have it appear prominently in the CSV formulation.

The appearance in Equations 5.10, 5.13 and 5.15 of h alone, however, is not a repetition of previous simple measures. Its appearance in the CSV formulation has interesting consequences.

Consider Figure 5.4, which presents a family of plots of CSV(.404) versus T/2h at various values of h. The plot, which is based on Equation 5.15, clearly indicates the increase in CSV with h at constant T/2h. The figure indicates that the trip velocity is low, within a narrow range of 4.5 m/s (10 mph), for vehicle parameters normally associated with cars and utility vehicles. The figure makes it clear that,

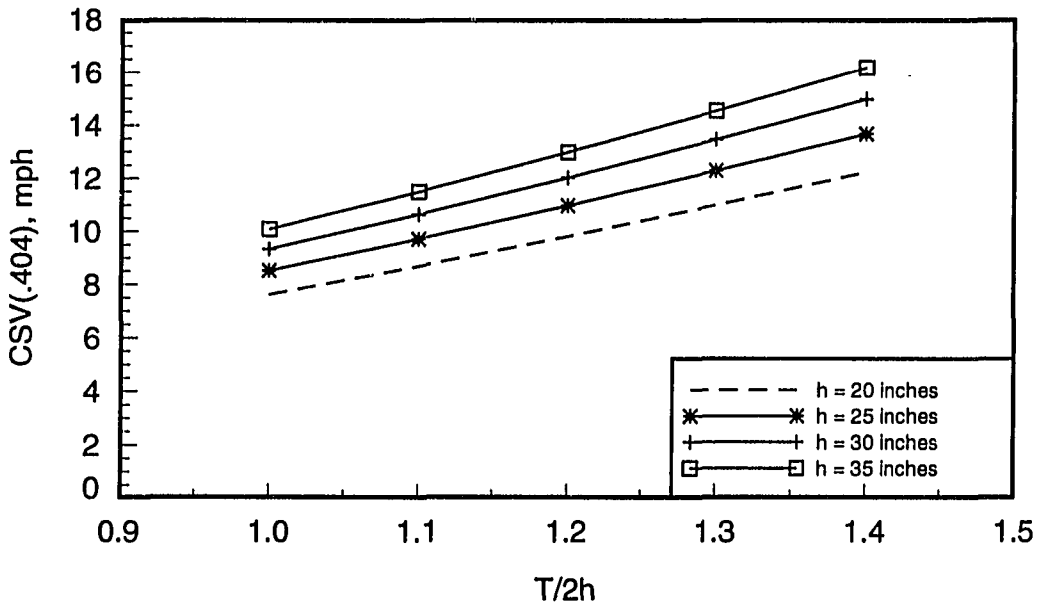

Figure 5.4: CSV(.404) Model. Varying cg height.

given the same T/2h, increasing h calls for higher CSV. To put it in terms of individual calculations, a rigid block with T/2h = 1.2 and h = 0.508 m (20 inches) has about the same CSV as a rigid block with T/2h = 1.0 and h = 0.838 m (33 inches).

Figure 5.5 gives CSV values for a family of plots of CSV(.404) versus T/2h at various values of track width, T. This plot clearly indicates the increase in CSV with T at constant T/2h. However, a comparison of Figures 5.4 and 5.5 indicates that track width does not affect the magnitude of the CSV as much as the center of gravity height, at a constant T/2h value.

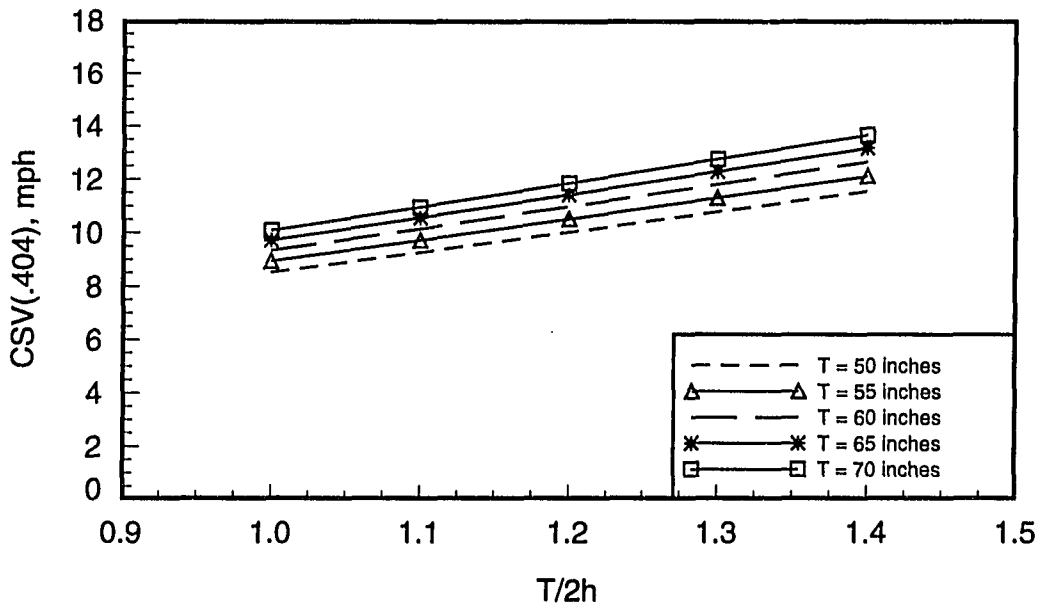

Figure 5.5: CSV(.404) Model. Varying track width.

Trip On a Sideslope

Malliaris et al. [18] and Harwin and Emery [35] stated that NCSS and CARS data, respectively, showed that between 60 and 80 percent of rollover accidents were initiated off the road through ditch, drop-off, or embankments. Thus sideslope appears to be an important factor in the occurrence of vehicle rollover and in accident statistics. The effect of sideslope can be examined in the context of a simple trip model as follows.

In Figure 5.6 a vehicle encounters a sideslope while sliding laterally. The critical sliding velocity analysis may be modified to include the effects of the sideslope when the vehicle impacts an immovable obstacle such as a curb. In this case, the distance

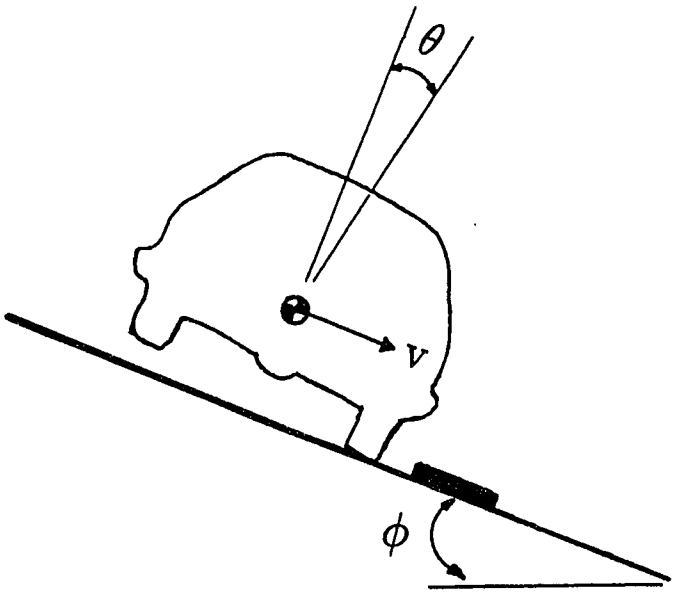

Figure 5.6: Roll on a Sideslope

through which the center of gravity must be raised is

$$\Delta h = (1 - sin\phi) \sqrt{\left(\frac{T}{2}\right)^2 + h^2} \tag{5.16}$$

where ϕ is the angle of the sideslope. Then the CSV formulation yields

$$CSV = \sqrt{\frac{2gI_o}{mh}\left[\sqrt{\left(1 + (\frac{T}{2h})^2\right)} - cos\phi - \frac{T}{2h}sin\phi\right]} \tag{5.17}$$

Substituting for I_o as in Equations 5.8 and 5.9 where

$$I_{cg} = a\ m\ \left(\left(\frac{T}{2}\right)^2 + h^2\right) \tag{5.18}$$

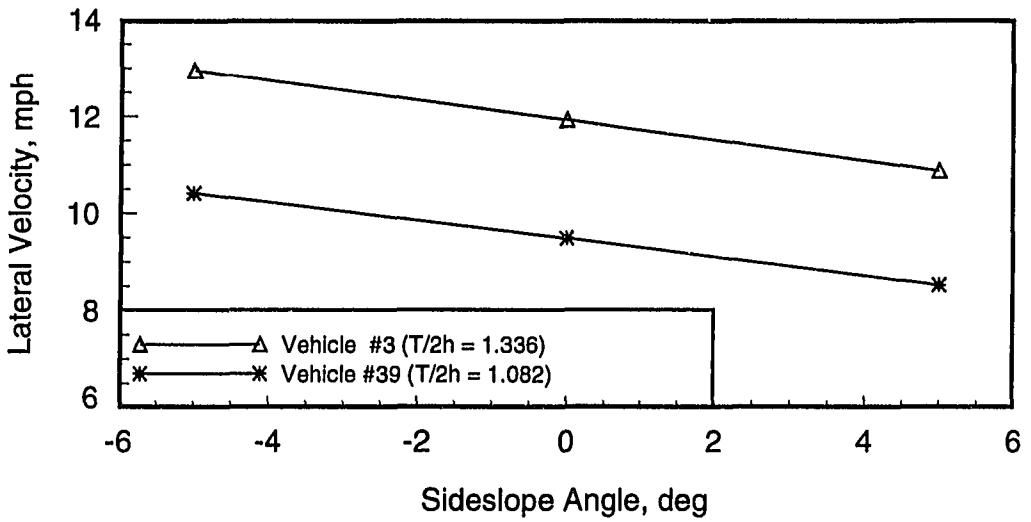

Figure 5.7: Comparison of Vehicles #3 and #39. Minimum Lateral Velocities for Curb Trip on Sideslope.

yields

$$CSV = \sqrt{2gh(a+1)\left(1+(\frac{T}{2h})^2\right)\left[\sqrt{\left(1+(\frac{T}{2h})^2\right)} - cos\phi - \frac{T}{2h}sin\phi\right]} \qquad (5.19)$$

Figure 5.7 compares CSV from Equation 5.19 for Vehicles #3 and #39 in Appendix C on a 5 degree uphill and a 5 degree downhill sideslope. The calculations for a level ground curb trip are also shown for comparison and are 12.01 and 9.90 mph for Vehicles #3 and #39, respectively. Changing the sideslope by 5 degrees increases (or decreases) the minimum lateral velocity for Vehicle #3 by 8 percent and for Vehicle #39 by 10 percent.

In summary, at a given T/2h, high cg vehicles have the highest minimum lateral velocities, and clearly sideslope has a substantial impact on these velocities.

Curb Trip - Two-Quarter-Turn

The CSV calculation yields a metric which is intended to indicate tipping over and rotating exactly one quarter-turn. Experience, anecdotal evidence, and the literature [34, 42] indicate that serious rollover accidents frequently involve multiple quarter-turns. Thus it seems reasonable to examine the simple metrics under consideration here for their relationship to multiple-quarter-turn events.

It is convenient to address this topic in the context of CSV. In particular, the derivation and calculations presented here extend the CSV analysis to the next quarter-turn.

Consider again Figure 5.1. The following addresses the question: What is the minimum initial velocity V2 to cause the rigid block to roll a total of two one-quarter turns?

Consider a rigid block with width T, center of gravity height h, and center of gravity to top-of-block distance $\overline{H}$. Figure 5.8 illustrates the scenario. The block starts at velocity V2. It hits the stop with its lower right corner and, just as in the calculation leading to CSV in Equation 5.7, loses energy while taking on a rotational velocity, here called $\dot{\theta}_2$.

$$I_o \, \dot{\theta}_2 = m \;\; \mathrm{V2} \;\; h \tag{5.20}$$

The equations of motion as the block rotates about the point of impact are

$$m(R\dot{\theta}^2 cos\theta + R\ddot{\theta} sin\theta) = -F_y \tag{5.21}$$

$$m(R\dot{\theta}^2 sin\theta - R\ddot{\theta} cos\theta) = W - F_z \tag{5.22}$$

and

$$I_o\ddot{\theta} = -WRcos\theta \tag{5.23}$$

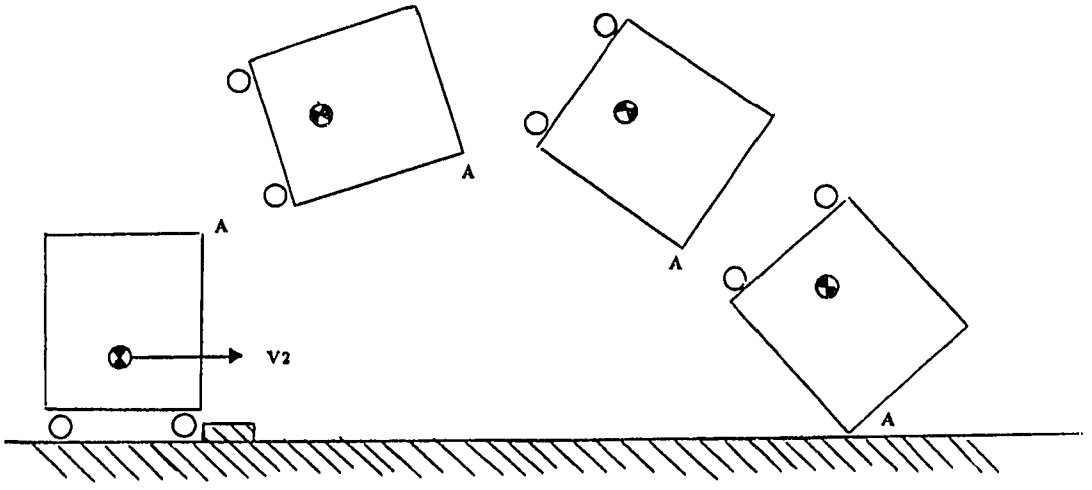

Figure 5.8: Two Quarter-Turn Model

where

$$R = \sqrt{(T/2)^2 + h^2} \tag{5.24}$$

Assuming conservation of energy after impact, the total kinetic and potential energy remains constant.

$$\frac{1}{2} I_o \dot{\theta}^2 + m\ g\ R\ sin\theta = \overline{C} \tag{5.25}$$

The constant, $\overline{C}$, may be computed from the initial conditions θ_o and $\dot{\theta}_2$. Recall that $\theta_o = \tan^{-1}((2h)/T)$.

The post impact forces F_y and F_z can be calculated from the hinge on the block from Equations 5.21 and 5.22. If $\dot{\theta}_2$ is high enough, at some angle $\overline{\theta}$ F_z will become negative. (If V2 is high enough, $\overline{\theta} = \theta_0$.) This implies, in the context of analogy to a vehicle scenario, tensile force between the impact point and the vehicle, clearly an impossible situation. At this point, the block can move freely vertically and

horizontally. Assume its rotation rate at release is $\dot{\theta}_3$, which can be calculated based on energy considerations in Equation 5.25.

Its vertical velocity at the point of release will be R*$\dot{\theta}_3$*sin$\overline{\theta}$. The equations of motion now become

$$\ddot{y}_{cg} = 0 \tag{5.26}$$

$$\ddot{z}_{cg} = g \tag{5.27}$$

$$\ddot{\theta} = 0 \tag{5.28}$$

The block now has constant rotation rate, constant horizontal velocity, and constant downward vertical acceleration due to gravity. Tracking the upper right hand corner, labeled A in Figure 5.8, allows calculation of the position and orientation of the block at impact as shown in the figure.

Now comes an important question - what are the boundary conditions at impact of corner A? To span the range of possibilities, the analysis considers so-called ice impact, illustrated in Figure 5.9 by the roller connection, and so-called hinge impact, which is identical in form to the first impact of this and the CSV scenario. (The ice impact, though not under that name, has been considered in the rollover literature [36].)

The main thrust of both boundary conditions is to determine whether or not there is sufficient energy for the block to complete a second quarter-turn. This occurs when sufficient kinetic energy is available to raise the center of gravity high enough to tip the next quarter-turn. The center of mass rotates about a radius $\overline{R}$ which is a function of T and $\overline{H}$.

$$\overline{R} = \sqrt{(T/2)^2 + \overline{H}^2} \tag{5.29}$$

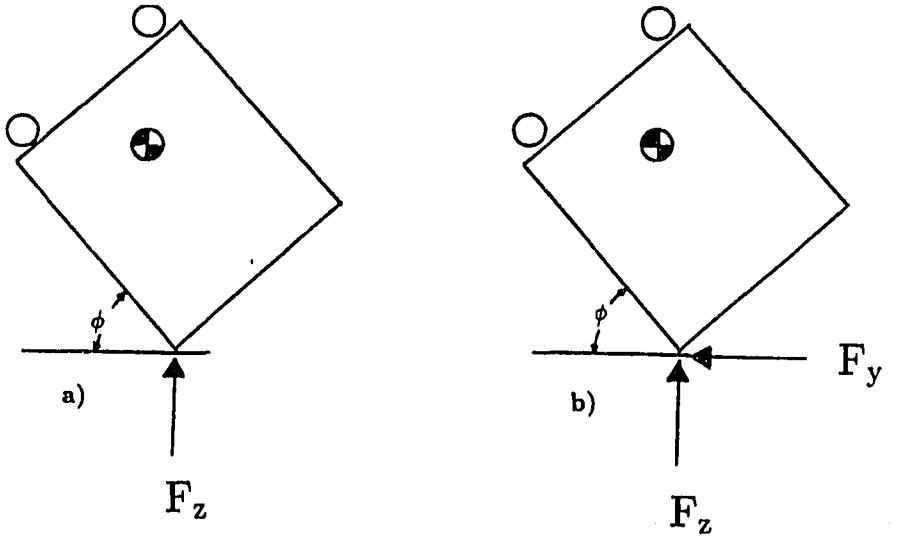

Figure 5.9: Impact Models. a) Ice Impact. b) Hinge Impact

where $\overline{H}$ is the vertical distance from the center of gravity to the top of the vehicle.

In the ice-hit scenario, there are no lateral forces, so the lateral velocity remains unchanged. Vertically, conservation of linear momentum yields

$$m\ \dot{z}_1 - \int F_z\ dt = m\ \dot{z}_2 \tag{5.30}$$

and from angular momentum:

$$I_{cg}(\dot{\phi}_1 - \dot{\phi}_2) = \overline{R}cos\phi \int F_z dt \tag{5.31}$$

Substituting from Equation 5.30 into Equation 5.31 results in equations which may be used to solve for the new angular velocity $\dot{\phi}_2$:

$$I_{cg}\dot{\phi}_2 = I_{cg}\dot{\phi}_1 + m(\dot{z}_2 - \dot{z}_1)\ \overline{R}cos\phi \tag{5.32}$$

where

$$\dot{z}_2 = -\overline{R}\ \dot{\phi}_2\ cos\phi \tag{5.33}$$

At this point, if the $\dot{\phi}_2$ value is negative, the block falls back on its side. If the value is positive, the available kinetic energy may be compared with the potential energy needed to roll the block the next quarter turn. Since for the ice-hit the velocity in the y-direction remains constant, a second quarter-turn requires

$$\frac{1}{2} I_{cg}\ \dot{\phi}_2^2 + \frac{1}{2}\ m\ \dot{z}_2^2 \geq\ m\ g\ \overline{R}\ (1 - sin\phi) \tag{5.34}$$

In the hinge-hit scenario, there are both vertical and horizontal impulses at the point of impact. Thus,

$$m\ \dot{y}_1 - \int F_y\ dt = m\ \dot{y}_2 \tag{5.35}$$

$$m\ \dot{z}_1 - \int F_z\ dt = m\ \dot{z}_2 \tag{5.36}$$

and

$$I_{cg}\dot{\phi}_1 - (\int Fz\ dt)\ \overline{R}cos\phi + (\int F_y dt)\ \overline{R}sin\phi = I_{cg}\dot{\phi}_2 \tag{5.37}$$

where

$$\dot{y}_2 = \overline{R}\ \dot{\phi}_2\ sin\phi \tag{5.38}$$

$$\dot{z}_2 = -\overline{R}\ \dot{\phi}_2\ cos\phi \tag{5.39}$$

As before, if $\dot{\phi}_2$ is greater than zero, the kinetic and potential energies are compared to see whether or not there is enough kinetic energy to lead to another quarter-turn. This calls for

$$\frac{1}{2}\ I_{cg}\ \dot{\phi}_2^2 + \frac{1}{2}\ m\ \dot{y}_2^2 + \frac{1}{2}\ m\ \dot{z}_2^2 \geq\ m\ g\ \overline{R}\ (1 - sin\phi) \tag{5.40}$$

which can be written

$$\frac{1}{2}\ \left(I_{cg} + m\overline{R}^2\right)\ \dot{\phi}_2^2 \geq\ m\ g\ \overline{R}\ (1 - sin\phi) \tag{5.41}$$

Table 5.1: Some Characteristics of V2 and CSV Values

		Range	Maximum	Minimum	Mean	Standard Deviation
CSV	m/s	2.56	6.08	3.53	4.81	0.53
	mph	5.72	13.61	7.89	10.75	1.18
V2I	m/s	3.07	11.09	8.02	9.54	0.51
	mph	6.87	24.81	17.94	21.35	1.15
V2H	m/s	2.89	9.99	7.10	8.62	0.52
	mph	6.47	22.35	15.88	19.29	1.16

Two-Quarter-Turn Calculations Appendix C presents calculations of the initial velocity V2 for 329 vehicle parameter sets given by Garrott [60]. (Of the 421 data sets, only 329 had T, h, Roof Height, mass, and I_{cg} information.) Appendix C also includes values of T/2h and critical sliding velocity (CSV) calculations. Appendix D presents an identification key for the vehicles in Appendix C. V2I refers to the minimum initial lateral velocity to yield two quarter turns under ice-impact conditions, and V2H indicates the minimum initial lateral velocity to yield two quarter turns under hinge-impact conditions. In each case, the values for V2I and V2H were found by incrementing initial lateral velocities until a high enough velocity was found to yield the second quarter turn.

Table 5.1 gives some characteristics of the data presented in Appendix C. The V2 values are much higher than the corresponding CSV values. In particular, if the analogy between rigid block dynamics and vehicle dynamics holds for two-quarter-turns, it is necessary to associate lateral velocities close to 9 m/s (20 mph) with vehicles involved in multiple-quarter-turn events.

Note also that the spread in the data, as seen both in the range and the standard

Table 5.2: Comparison of Vehicles #3 and #39

Vehicle Number	T (m)	h (m)	T/2h (-)	I_{cg} (kg-m^2)	Mass (kg)	RoofHt (m)
3	1.480	0.554	1.336	551.	1518.6	1.38
39	1.372	0.634	1.082	646.	1392.1	1.61
				CSV	V2I	V2H
3				5.37 m/s	8.81 m/s	9.62 m/s
				12.01 mph	19.70 mph	21.53 mph
39				4.43 m/s	8.71 m/s	9.65 m/s
				9.90 mph	19.48 mph	21.58 mph

deviation, is about the same for CSV as for V2. In particular, the standard deviation for CSV is about 10 percent of the mean CSV, and the standard deviation for V2 is about 5 percent of the mean V2. Thus V2 is less sensitive than CSV to variation in vehicle characteristics.

Finally, consider the data presented in Table 5.2 comparing two vehicles from Appendix C. Note the wide range of CSV values and the virtually identical V2 values. This is a recurring feature of the data in Appendix C - vehicles associated with wide-ranging CSV values can map to similar V2 values. This indicates that, for some vehicles, the one-quarter-turn measure CSV gives a qualitatively different result than the two-quarter-turn measure V2.

Figure 5.10 presents a plot of some of the data, namely, V2H versus CSV from Equation 5.7. (These data yield less scatter than V2I versus CSV.) The plot gives an idea of the scatter in the data. The linear fit through these data yields

$$\text{V2H} = 0.80\ \text{CSV} + 10.7 \tag{5.42}$$

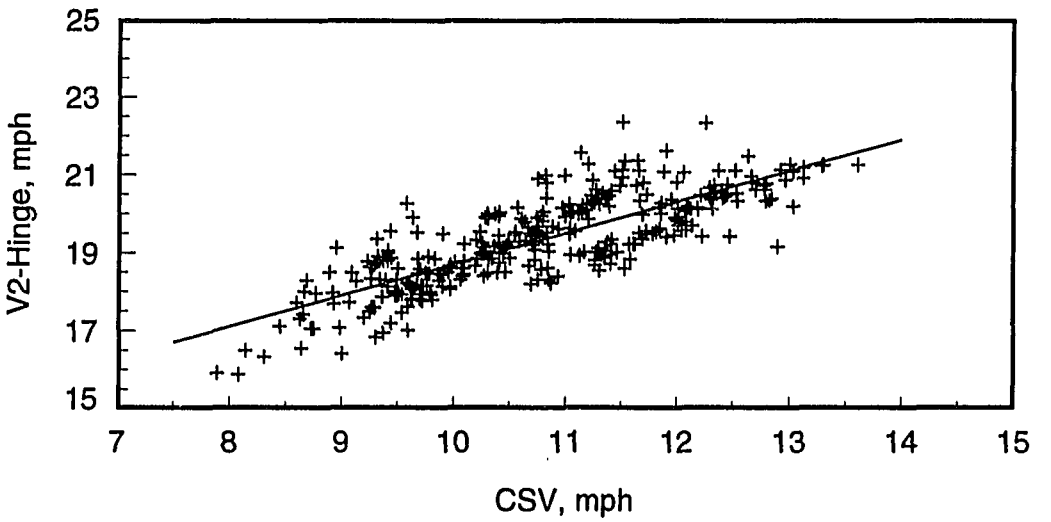

Figure 5.10: Relationship of V2H to CSV

which has $R^2 = 0.66$.

It is reasonable to ask if there are new factors coming into play in the V2 formulation, factors which are not accounted for in the CSV formulation. Since the calculation of V2, the minimum velocity for a two-quarter-turn event, depends on numerical work to determine the orientation of the block at impact, it is impossible to determine analytically which new parameters or groups of parameters are important.

A purely intuitive assessment of the relationship between CSV and V2 leads to consideration of the roof height as an important parameter. This might help explain, for example, the relationship between calculations for Vehicle #3, which has relatively high CSV and low roof height, and Vehicle #39, which has relatively low CSV and high roof height.

Preliminary work with these data indicates a good correlation between the ratios

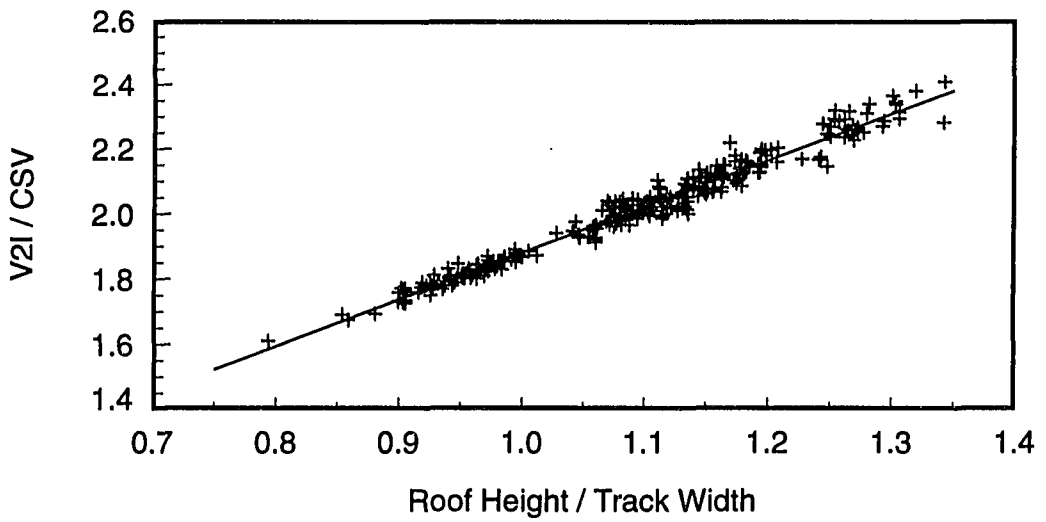

Figure 5.11: Relationship of $\frac{V2I}{CSV}$ to $\frac{Roof\ Height}{Track\ Width}$.

V2/CSV and Roof Height/Track Width. In particular, for the results from Appendix C, the relationship for ice impact is

$$\frac{\text{V2I}}{\text{CSV}} = 0.45 + 1.43\ \frac{\text{Roof Height}}{\text{Track Width}} \tag{5.43}$$

with $R^2 = 0.97$, and for hinge impact

$$\frac{\text{V2H}}{\text{CSV}} = 0.59 + 1.12\ \frac{\text{Roof Height}}{\text{Track Width}} \tag{5.44}$$

with $R^2 = 0.97$. Figures 5.11 and 5.12 present the data underlying these equations.

Curb Trip - Experimental Results

In 1984, Brown et al [19] performed full-scale curb vehicle tests with a 1977 Chevrolet Chevette. The vehicle was pulled with four wheels in contact with the "road" surface angled at 15 degrees into the curb. The vehicle was released 4 feet

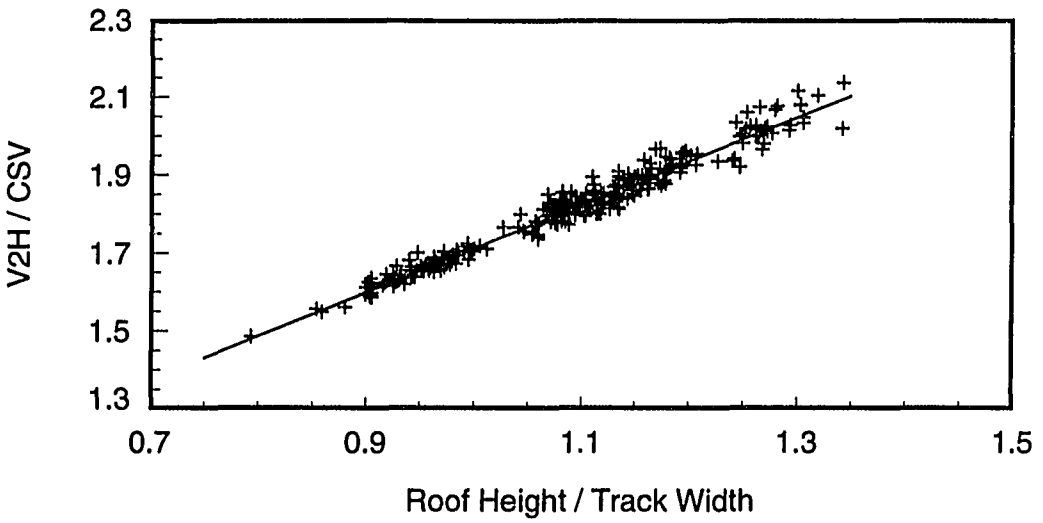

Figure 5.12: Relationship of $\frac{V2H}{CSV}$ to $\frac{Roof\ Height}{Track\ Width}$.

from the curb with enough lateral velocity so that the vehicle struck the curb at 25 mph, at which time the vehicle rolled over. The authors did not run the full-scale test at velocities less than 25 mph to find the minimum trip velocity of the 1977 Chevrolet Chevette.

In 1989, Thomas et al. [33] performed five curb tests with measured lateral velocities of 29.3 to 30.2 mph. The curb trip vehicles each had a 2.5 degree pre-impact roll angle, were released from the tow device, and impacted a 6 inch square curb. Two of the five curb trip test vehicles rolled over, yielding 1 and 1-1/2 revolutions over an average distance of 47 feet.

In 1990, Cooperrider, Thomas, and Hammoud [36] performed full-scale vehicle rollover tests including curb and soil trip tests and dolly rollover. The authors claim that the 1981 Dodge Challenger (T/2h = 1.335) had average decelerations of 12.4 g's with lateral velocities of 29.6 mph for the curb trip test. The 1979 Datsun B210

(T/2h = 1.288) had average decelerations of 13.2 g's with lateral velocities of 29.3 mph.

In 1994, Nalecz and Lu [59] performed full-scale testing of vehicles in a variety of maneuvers including curb and soil tripping. Rollovers were measured at pre-trip lateral velocities as low as 3.6 m/s (8 mph). The results of these tests were summarized and discussed in Chapter 3.

Furrow Trip

For a vehicle sliding sideways and impacting an immovable obstacle such as a curb, Meriam [61] and later Jones [9, 10, 63] derived an equation for the minimum lateral velocity for a one-quarter-turn roll. In many off-road accidents, however, the vehicle slides through soil and creates a furrow. See Figure 5.13. For example, Malliaris et al. [18] stated that NCSS data files showed that over 80 percent of the rollovers were initiated off the road through ditch, drop-off, or embankment characterizations, and that only about 10 percent of the accidents were classified as curb tripped. Deleys and Brinkman [21] stated that the vast majority of rollovers occur within 30 ft (9.1 m) of the roadway and that relatively few occur or are initiated on the shoulder. Orlowski et al. [26] stated that approximately twice as many vehicles roll over on dirt or sod as roll over on pavement. Harwin and Emery [35] stated that their CARS database showed that 61.7% of their accident data in rollover was generated off-road, specifically, in the ditch (23.3%), on flat soil (24.0%), or on an embankment or slope down (14.4%).

In the furrow trip analysis presented here, the motion has similar stages to the curb trip analysis. The furrow trip motion entails (a) the vehicle sliding sideways

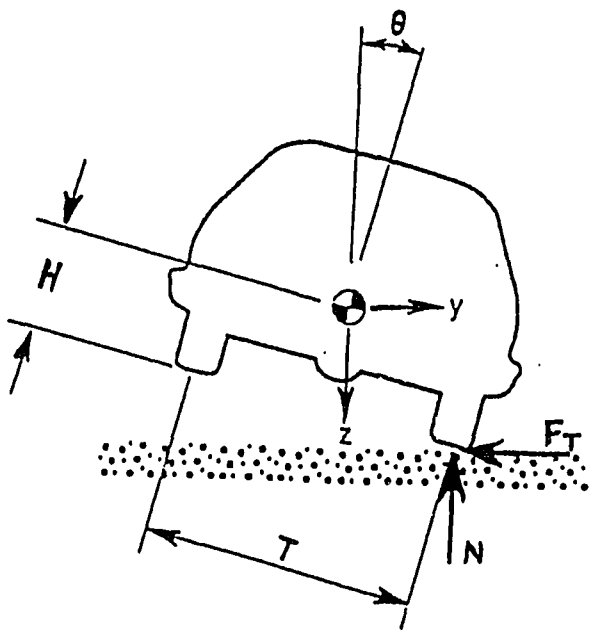

Figure 5.13: Laterally Sliding Vehicle in Soil

with all wheels in contact with the ground, (b) wheel lift and continuing translation of the vehicle on the leading tires, and (c) vehicle completing a one-quarter-turn with leading tires in ground contact, or (d) vehicle losing all wheel contact and becoming airborne and impacting the ground in either a one- or two-quarter-turn event.

One of the first questions which needs to be addressed is how to model the opposing soil trip force. This thesis considers three simple options, increasing the force with the lateral distance traveled due to increased furrow depth, $F_t = K\ y$, assuming a constant force, $F_t = F_o$, or a velocity dependency, $F_t = C\ \dot{y}$.

In any case, the vehicle is subject to a short duration force $F_t = F(y, \dot{y})$. The

equations of motion as the vehicle progresses through the stages numerically solve for the minimum velocity to cause a one-quarter turn rollover of the block for the variety of formulations for F_t given. Output from the numerical calculations is the distance the block travels laterally to the right before tipping one-quarter turn, the so-called furrow length.

During translation, the tripping force opposes the vehicle's motion. Before the vehicle tips up, the equations of motion are

$$M\ddot{y}_{cg} = -F_t \tag{5.45}$$

$$M\ddot{z}_{cg} = 0 = W - N_r - N_l \tag{5.46}$$

and

$$I_{cg}\ddot{\theta} = 0 = \frac{N_l\, T}{2} - \frac{N_r\, T}{2} + F_t\, h \tag{5.47}$$

where M is the total mass of the vehicle, F_t is the tripping force, W is the total weight of the vehicle, and N_l and N_r are the forces at the left and right tires, respectively.

As the vehicle slides laterally to the right, the forces at the left tire will decrease and the forces at the right tire, N_r, will increase. The force at the right tire may be found from equations 5.46 and 5.47.

$$N_r = \frac{W}{2} + \frac{F_t h}{T} \tag{5.48}$$

As the vehicle's left tire lifts off, the force N_l becomes zero and $\ddot{z}_{cg}$, $\ddot{\theta}$, and $\dot{\theta}$ become nonzero. The vehicle tips up as it continues to translate, pivoting about this moving point of contact. The equations of motion now become

$$M\ddot{y}_{cg} = -F_t \tag{5.49}$$

$$M\ddot{z}_{cg} = W - N_r \tag{5.50}$$

and

$$I_{cg}\ddot{\theta} = F_t R \sin\theta - N_r R \cos\theta \tag{5.51}$$

where R is the distance from the contact point to the center of gravity.

The lateral acceleration at the contact point may be calculated knowing the acceleration of the center of gravity, the roll angle, θ, the roll velocity and the roll acceleration.

$$\ddot{y}_{Contact\ Point} = \ddot{y}_{cg} - R\ddot{\theta}\sin\theta - R\dot{\theta}^2\cos\theta \tag{5.52}$$

Note that

$$\ddot{z}_{Contact\ Point} = 0.0 \tag{5.53}$$

since the pivot point stays in contact with the ground. N_r may be calculated from equation 5.50 as follows

$$N_r = W - M\ddot{z}_{cg} \tag{5.54}$$

At low lateral velocity values the vehicle will tip back down and come to rest. With sufficient lateral velocity, the vehicle tips so that the center of gravity passes over the right tire contact point ($\theta > 90$ degrees) and the vehicle does a one-quarter turn, not losing contact with the ground. At high lateral velocities, the vehicle may leave the ground, becoming airborne.

In this case, the vehicle is no longer touching the ground so that $F_t = 0$ and $N_r = 0$ and the equations of motion become

$$\ddot{y}_{cg} = 0 \tag{5.55}$$

$$\ddot{z}_{cg} = g \tag{5.56}$$

and

$$\ddot{\theta} = 0 \tag{5.57}$$

One final note in the furrow trip analysis: In the transition between pure translation and translation with rotation about the contact point, mathematically the contact point may stop its motion to the right and slide back to the left. In order to prevent this analytically, we latch the contact point at the right side at the point where the right side contact point reaches maximum displacement to the right. Then the equations of motion become

$$I_{Contact\ Point}\ddot{\theta} = -WR\cos\theta \tag{5.58}$$

Since the contact point is latched, the velocities and accelerations at the contact point are

$$\ddot{y}_{Contact\ Point} = \ddot{z}_{Contact\ Point} = 0 \tag{5.59}$$

$$\dot{y}_{Contact\ Point} = \dot{z}_{Contact\ Point} = 0 \tag{5.60}$$

and the acceleration at the center of gravity may be calculated from

$$\ddot{y}_{cg} = R\dot{\theta}^2\cos\theta + R\ddot{\theta}\sin\theta \tag{5.61}$$

and

$$\ddot{z}_{cg} = R\dot{\theta}^2\sin\theta - R\ddot{\theta}\cos\theta \tag{5.62}$$

Once the accelerations are known, the F_t and N_r values may be calculated from the remaining equations of motion:

$$M\ddot{y}_{cg} = -F_t \tag{5.63}$$

and

$$M\ddot{z}_{cg} = W - N_r \tag{5.64}$$

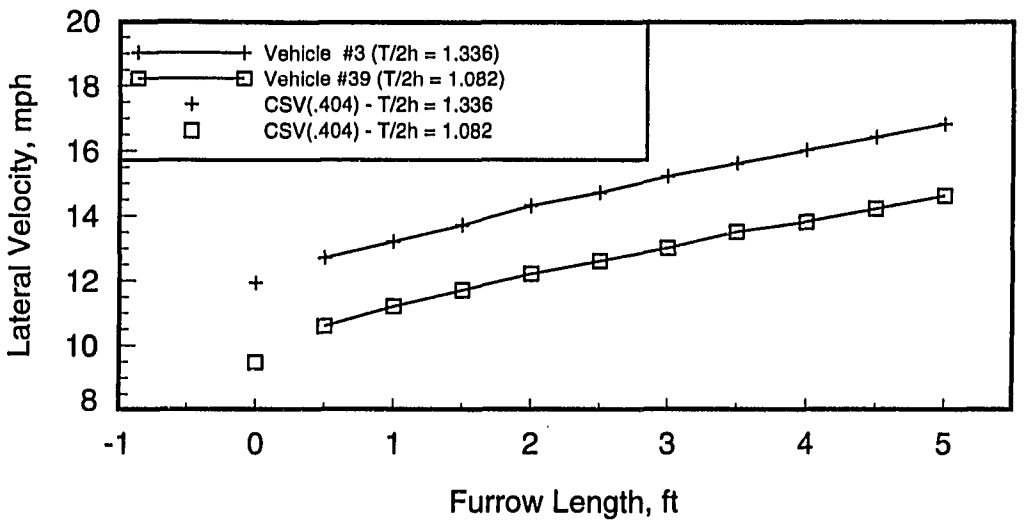

Figure 5.14: Trip Force, F_t = K y. Minimum Lateral Velocities for One-Quarter-Turn Rollover.

One-Quarter-Turn

In an iterative procedure, the preceding equations can be used to determine the minimum lateral velocity to lead to a one-quarter-turn rollover as a function of furrow length.

Figure 5.14 presents results of one-quarter-turn rollover for the soil trip force, F_t = K y, for Vehicles #3 and #39 in Appendix C. The figure includes the critical sliding velocity, CSV(.404) from Equation 5.15, for the vehicles impacting a curb and results of the calculations for the furrow trip lateral velocities at furrow lengths of 0.5 ft to 5.0 ft. The calculations indicate that as the furrow length gets very small, the minimum velocity to cause a one-quarter-turn tip over approaches the CSV as given by Equation 5.15. For longer furrow lengths, the minimum tip velocity increases.

Figure 5.15 presents calculations for Vehicle #3 showing the effects of modeling

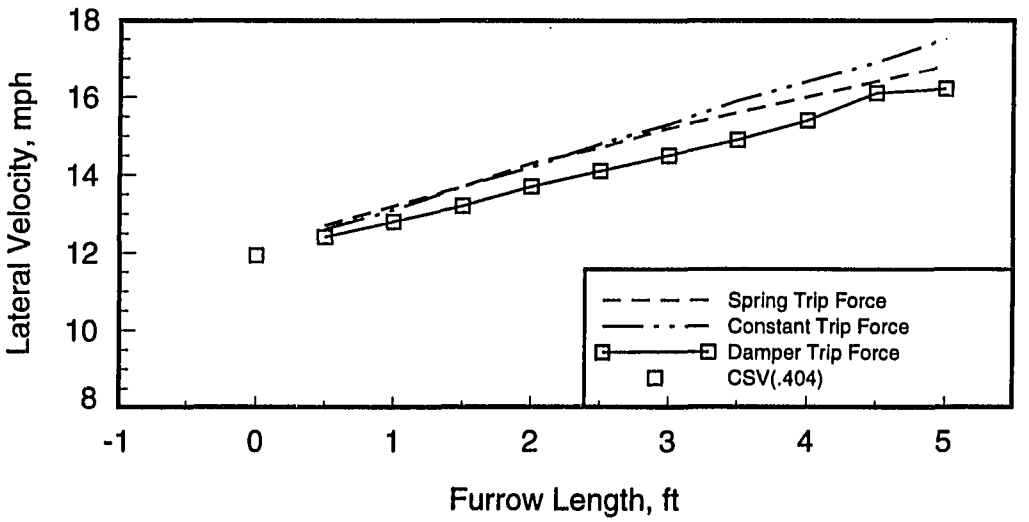

Figure 5.15: Comparison of Trip Forces for One-Quarter Tip Over. Vehicle #3, T/2h = 1.336.

the soil trip force as a spring force, $F_t = K\,y$, a constant tripping force, $F_t = F_o$, and a velocity dependent tripping force, $F_t = C\,\dot{y}$. Each result is for a one-quarter-turn roll at the given furrow length. A remarkable feature of the numerical calculations is that the tip velocity is not particularly sensitive to the characteristics of the soil trip force, F_t. Thus this simple model supports the view that, for short furrow lengths of a meter or so, the length of the furrow alone is a good indicator of minimum velocity to initiate rollover. Figure 5.16 provides similar results for Vehicle #39. (Calculations from Figure 5.15 give lateral velocities in the range of 12 to 18 mph for Vehicle #3 and lateral velocities in the range of 10 to 15.5 mph for Vehicle #39.)

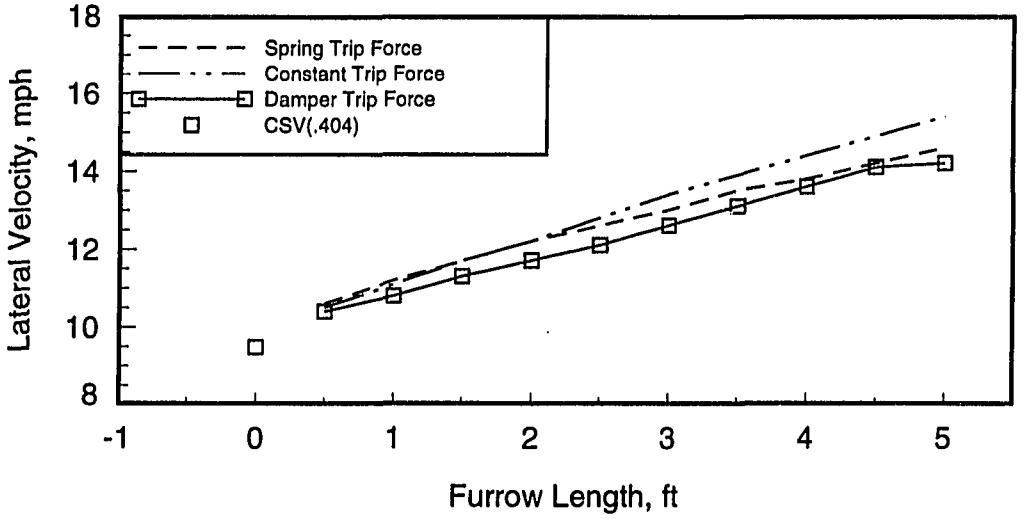

Figure 5.16: Comparison of Trip Forces for One-Quarter Tip Over. Vehicle #39, T/2h = 1.082.

Two-Quarter-Turn

We now apply the criteria for a two-quarter-turn, derived earlier in this section, to the furrow trip scenario. The vehicle is allowed to become airborne after traversing a given furrow distance. The rotational, lateral, and vertical velocities and the center of gravity height are used to determine the kinetic and potential energies for the two-quarter-turn when the vehicle impacts the leading edge corner of the roof. Equation 5.34 for the ice-hit and Equation 5.41 for the hinge-hit are used in the analysis to determine whether or not the vehicle rolls onto its roof or whether it falls back onto its side.

Figure 5.17 presents calculations for the ice- and hinge-hit impact conditions for Vehicle #3 (T/2h = 1.336) and Figure 5.18 presents calculations for the ice- and hinge-hit impact conditions for Vehicle #39 (T/2h = 1.082). The figures show that

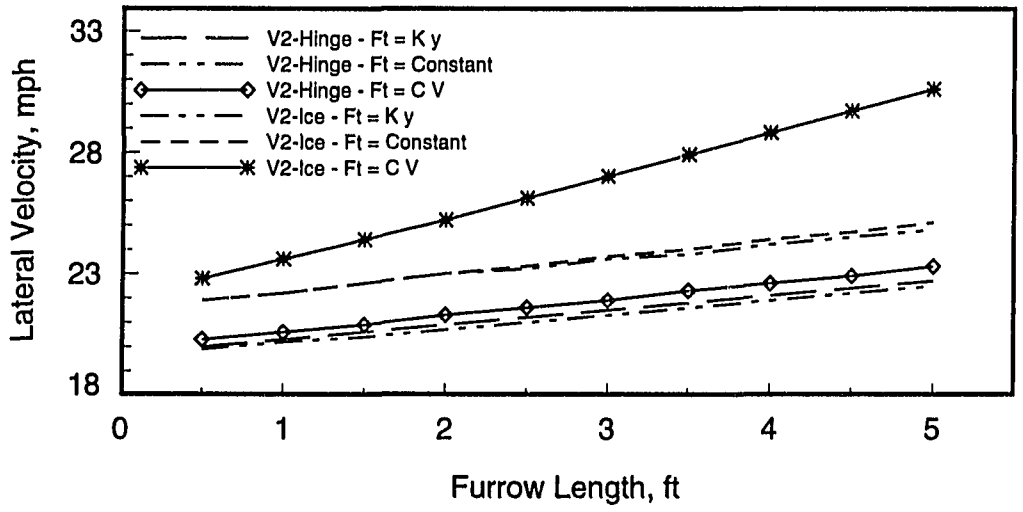

Figure 5.17: Comparison of Trip Forces for Two-Quarter-Turn Maneuvers. Vehicle #3, T/2h = 1.336.

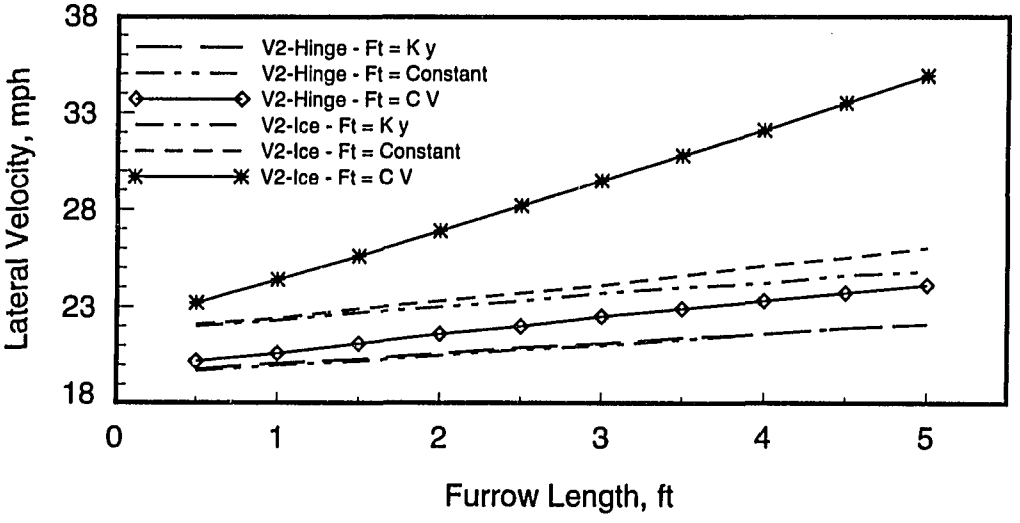

Figure 5.18: Comparison of Trip Forces for Two-Quarter-Turn Maneuvers. Vehicle #39, T/2h = 1.082.

the V2I lateral velocities are consistently higher than the V2H lateral velocities for all furrow lengths and for both vehicles. The V2I velocities range from 2 mph to 11 mph higher than the V2H calculations. These figures also show that, for the most part, that the furrow trip forces give similar results except for the velocity dependent force, $F_t = C\,\dot{y}$. These differences are relatively small for the hinge-hit calculations, especially at low furrow distances. However, these differences are remarkable for the ice-hit calculations above 1 foot furrow distances.

Figure 5.19 compares the passenger car (T/2h = 1.336) and the utility vehicle (T/2h = 1.082) in both the one- and two-quarter-turn furrow trip maneuver. The soil tripping force is modeled as $F_t = K\,y$. The figure indicates that T/2h is important in the one-quarter-turn analysis. Furthermore, the two-quarter-turn analysis leads to initial velocity values about twice as high as the CSV values. It also appears that the two-quarter-turn values for the $F_t = K\,y$ model are not very sensitive to either furrow length or to vehicle configuration. This is a remarkable finding in that if one views the simple model presented here as representative of a vehicle in an accident scenario, the inevitable conclusion must be that for the two-quarter-turn analysis, vehicle parameters are not important.

Figure 5.20 again compares the passenger car and utility vehicle, this time for the ice boundary condition at the second impact. Again the two-quarter-turn calculations are insensitive to furrow length and vehicle configuration.

Table 5.3 summarizes the two-quarter-turn results for Vehicle #3. Results from the two-quarter-turn calculations in the curb trip scenario are summarized in Table 5.2. The minimum curb trip lateral velocity for a roof hit in the hinge-hit was 19.7 mph (8.81 m/s) and in the ice-hit was 21.5 mph (9.62 m/s).

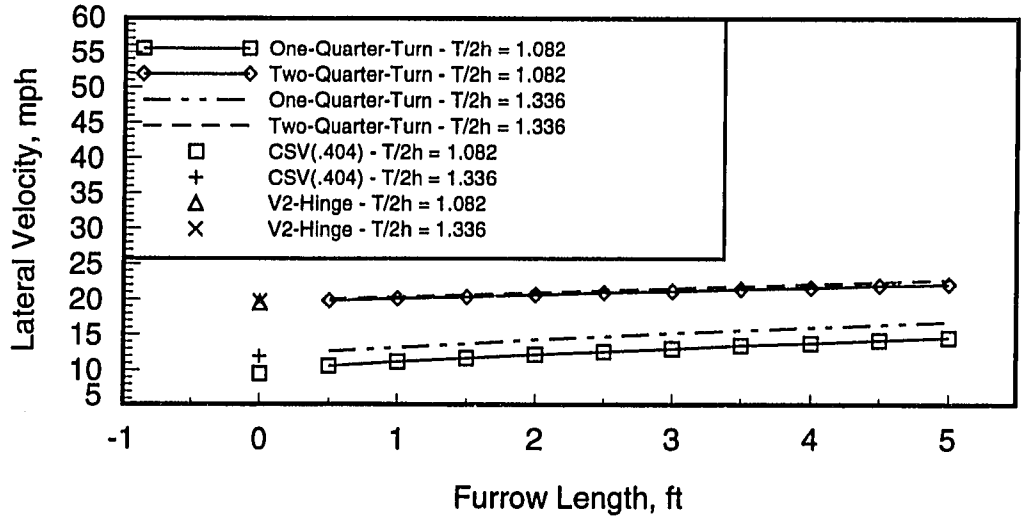

Figure 5.19: Comparison of Lateral Velocities for One- and Two-Quarter-Turn Maneuvers. Hinge-Hit. T/2h = 1.082 and 1.336.

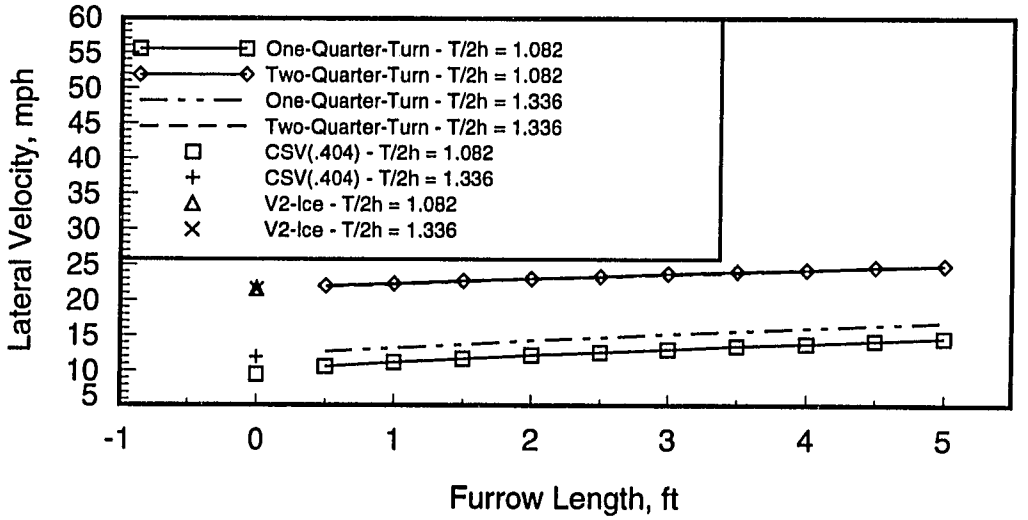

Figure 5.20: Comparison of Lateral Velocities for One- and Two-Quarter-Turn Maneuvers. Ice-Hit. T/2h = 1.082 and 1.336.

Table 5.4 summarizes the two-quarter-turn results for Vehicle #39. Results from the two-quarter-turn calculations in the curb trip scenario are also summarized in Table 5.2. The minimum curb trip lateral velocity for a roof hit in the hinge-hit was 19.5 mph (8.71 m/s) and in the ice-hit was 21.6 mph (9.65 m/s).

Table 5.3: Furrow Trip Lateral Velocities of Vehicle #3, in mph

Vehicle Number	T (m)	h (m)	T/2h (-)
3	1.480	0.554	1.336
Furrow	$F_t = K\ y$	F_t = Constant	$F_t = C\ \dot{y}$
Distance (ft)	Hinge-hit/Ice-hit	Hinge-hit/Ice-hit	Hinge-hit/Ice-hit
0.5	20.0/21.9	19.9/21.9	20.3/22.8
1.0	20.3/22.2	20.2/22.2	20.6/23.6
1.5	20.6/22.6	20.4/22.6	20.9/24.4
2.0	20.9/23.0	20.7/23.0	21.3/25.2
2.5	21.2/23.2	21.0/23.3	21.6/26.1
3.0	21.5/23.6	21.3/23.7	21.9/27.0
3.5	21.8/23.8	21.6/24.0	22.3/27.8
4.0	22.1/24.2	21.9/24.4	22.6/28.7
4.5	22.4/24.5	22.2/24.7	22.9/29.7
5.0	22.7/24.8	22.5/25.1	23.2/30.6

Table 5.4: Furrow Trip Lateral Velocities of Vehicle #39, in mph

Vehicle Number	T (m)	h (m)	T/2h (-)
3	1.372	0.634	1.082
Furrow	$F_t = K\ y$	F_t = Constant	$F_t = C\ \dot{y}$
Distance (ft)	Hinge-Hit/Ice-Hit	Hinge-hit/Ice-hit	Hinge-hit/Ice-hit
0.5	19.8/22.0	19.7/22.1	20.2/23.2
1.0	20.1/22.3	20.0/22.4	20.6/24.4
1.5	20.3/22.7	20.2/22.9	21.1/25.6
2.0	20.6/23.0	20.5/23.3	21.6/26.9
2.5	20.9/23.3	20.8/23.7	22.0/28.2
3.0	21.1/23.7	21.0/24.1	22.5/29.5
3.5	21.4/24.0	21.3/24.6	22.9/30.8
4.0	21.6/24.2	21.6/25.1	23.3/32.1
4.5	21.9/24.6	21.9/25.5	23.7/33.5
5.0	22.1/24.8	22.1/26.0	24.1/34.9

CHAPTER 6. SENSITIVITY ANALYSIS

Sensitivity analysis is used by designers to show how a change in a parameter will change the performance of the model. In meeting a specific design criteria, performing a sensitivity analysis gives the designer a feel for which parameters are most helpful to change. This is especially helpful in very complex models where the influence of changes in design variables on the final model output is not intuitive.

Sensitivity analysis can be applied to a mathematical model through Taylor series expansion. For example, the following is an investigation of the effects of changing the track width and center of gravity height in a simple wheel lift-off model in a steady turn.

Let $\overline{A}_y$ be the steady state lateral acceleration yielding wheel lift in a simple model. Then

$$\frac{\overline{A}_y}{g} = \frac{T}{2h} \tag{6.1}$$

To find the rate of change of this limit acceleration with changes in the track width, we write the first order expansion of the steady state lateral acceleration with respect to T.

$$\begin{aligned} \frac{A_y}{g} &= \frac{\overline{A}_y}{g} + \frac{d(\overline{A}_y/g)}{dT}\Delta T \\ &= \frac{\overline{A}_y}{g} + \frac{1}{2h}\Delta T \end{aligned}$$

$$= \frac{\overline{A}_y}{g}\left(1+\frac{\Delta T}{T}\right) \tag{6.2}$$

In the same way, considering the center of gravity height, h, yields

$$\begin{aligned}\frac{A_y}{g} &= \frac{\overline{A}_y}{g} + \frac{d(\overline{A}_y/g)}{dh}\Delta h \\ &= \frac{\overline{A}_y}{g} - \frac{T}{2h^2}\Delta h \\ &= \frac{\overline{A}_y}{g}\left(1-\frac{\Delta h}{h}\right)\end{aligned} \tag{6.3}$$

Equations 6.2 and 6.3 indicate that small percentage changes in T have the same magnitude effect as small percentage changes in h.

The remainder of this section is devoted to sensitivity analysis in this same spirit, namely, we look for the effect of small percentage changes in parameters in various models. We will consider sensitivity of both straightforward measures of limit acceleration and of two proposed measures of roll resistance, the tilt table ratio and critical sliding velocity.

Steady Turn

Bernard et al. [31] presented several mathematical models for rollover in a steady turn. The simplest of those models, which has been presented often in the literature for wheel liftoff in a steady turn, is

$$\frac{\overline{A}_y}{g} = \frac{T}{2h} + \phi \tag{6.4}$$

where ϕ is the superelevation of the road. This model is a single degree of freedom quasi-static model of a vehicle in a steady turn. This model requires knowledge of

only two measured vehicle parameters, assumes that transients are not important, and that the sum of the lateral forces is constant.

Reference [31] presented a two degree of freedom model which included the effects of the sprung mass rolling to the outside of the turn and of the tire-road contact patch deflecting under the vehicle due to the lateral forces.

$$\frac{\overline{A}y}{g} = \frac{\frac{T}{2} + h\phi}{h + \overline{a} + \overline{b}} \tag{6.5}$$

where length $\overline{a}$ is the distance that the outside tire force deflects under the vehicle for each g of lateral acceleration and length $\overline{b}$ is the roll gain, the distance the mass center moves to the outside of the turn for each g of lateral acceleration. This equation is a crude measure for the highest lateral acceleration that can be sustained in a steady turn with superelevation ϕ, including the effects of tire deflection and the rolling of the mass center to the outside of the turn.

To again examine how changes in track width and center of gravity height affect the lateral acceleration, a first order Taylor series expansion may be performed with respect to T, h, $\overline{a}$, and $\overline{b}$. With respect to track width, T, we have

$$\frac{Ay}{g} = \frac{\overline{A}y}{g} + \frac{d(\overline{A}y/g)}{dT}\Delta T \tag{6.6}$$

Differentiating and rearranging yields

$$\frac{Ay}{g} = \frac{\frac{T}{2}}{h + \overline{a} + \overline{b}}\left(1 + \frac{\Delta T}{T}\right) + \frac{h\phi}{h + \overline{a} + \overline{b}} \tag{6.7}$$

Thus, for no superelevation, a small percent change in track width yields the same percent change in the limit lateral acceleration.

With respect to center of gravity height, h, we have

$$\frac{Ay}{g} = \frac{\overline{A}y}{g} + \frac{d(\overline{A}y/g)}{dh}\Delta h$$

Table 6.1: Typical Vehicle Values (Reference [31])

	Passenger Car	Utility Vehicle
T	1.49 m	1.35 m
h	0.55 m	0.61 m
h_1	0.29 m	0.29 m
h_2	-0.15 m	0.0 m
h_3	0.44 m	0.36 m
W_s	11 605.23 N	11 605.23 N
W_u	1 648.08 N	1 648.08 N
$\bar{b}$	0.05 m/g	0.031 m/g
ζ	0.2	0.2
$\bar{a}$	0.025 m/g	0.025 m/g
$\frac{T}{2h}$	1.355	1.107

$$= \frac{\frac{T}{2}+h\phi}{h+\bar{a}+\bar{b}} + \frac{\phi(h+\bar{a}+\bar{b}) - (\frac{T}{2}+h\phi)}{(h+\bar{a}+\bar{b})^2}\Delta h$$

$$= \frac{\overline{A}_y}{g}\left(1 + \frac{h\phi(h+\bar{a}+\bar{b}) - h(\frac{T}{2}+h\phi)}{(\frac{T}{2}+h\phi)(h+\bar{a}+\bar{b})}\ \frac{\Delta h}{h}\right) \tag{6.8}$$

For no superelevation, this expression becomes

$$\frac{A_y}{g} = \frac{\overline{A}_y}{g}\left(1 - \frac{h}{(h+\bar{a}+\bar{b})}\ \frac{\Delta h}{h}\right) \tag{6.9}$$

This indicates that changing h by a small percent lowers the lateral acceleration a smaller percentage. Using parameters from Table 6.1 for typical values of h, $\bar{a}$, and $\bar{b}$ for a passenger car (T/2h = 1.355) and a utility vehicle (T/2h = 1.107), Equation 6.9 will yield sensitivities of about -0.88 and -0.92, respectively, i.e., for these vehicle parameters, a one percent increase in h will yield a 0.88 percent decrease in limit acceleration for the car, and a 0.92 percent decrease for the utility vehicle.

With respect to the effective overturning moment, $\bar{a}$, we have

$$\frac{A_y}{g} = \frac{\overline{A}_y}{g} + \frac{d(\overline{A}_y/g)}{d\bar{a}}\Delta\bar{a}$$

Table 6.2: Sensitivity Coefficients of Limit Lateral Acceleration in a Steady Turn

Equation Number	Passenger Car (T/2h = 1.355)	Utility Vehicle (T/2h = 1.107)
6.7 (Track)	1.00	1.00
6.9 (h)	-0.88	-0.92
6.10 ($\overline{a}$)	-0.038	-0.040
6.11 ($\overline{b}$)	-0.047	-0.080

$$\begin{aligned} &= \frac{\frac{T}{2}+h\phi}{h+\overline{a}+\overline{b}} - \frac{\frac{T}{2}+h\phi}{(h+\overline{a}+b)^2}\Delta\overline{a} \\ &= \frac{\overline{A}_y}{g}\left(1-\frac{\overline{a}}{(h+\overline{a}+\overline{b})}\ \frac{\Delta\overline{a}}{\overline{a}}\right) \end{aligned} \tag{6.10}$$

Increasing the effective overturning moment, $\overline{a}$, by 1 percent lowers the limit lateral acceleration by much less than 1 percent. Specifically, for the passenger car and utility vehicle of Table 6.1, this yields sensitivities of -0.038 and -0.040, respectively.

With respect to the roll gain, $\overline{b}$, the results are similar to the results given by Equation 6.10

$$\begin{aligned} \frac{A_y}{g} &= \frac{\overline{A}_y}{g} + \frac{d(\overline{A}_y/g)}{d\overline{b}}\Delta\overline{b} \\ &= \frac{\overline{A}_y}{g}\left(1-\frac{\overline{b}}{(h+\overline{a}+\overline{b})}\ \frac{\Delta\overline{b}}{\overline{b}}\right) \end{aligned} \tag{6.11}$$

Thus, increasing the roll gain, $\overline{b}$, by 1 percent lowers the limit lateral acceleration by much less than 1 percent. Again, for the passenger car and utility vehicle of Table 6.1, the sensitivities are -0.047 and -0.080, respectively.

Table 6.2 summarizes sensitivity coefficients for the typical parameters of the passenger car and the utility vehicle.

In summary, sensitivity analysis of a simple equation modeling wheel lift off in a steady turn indicates that changes in track width and/or center of gravity height

are very important. Changes in roll gain and/or overturning moment are an order of magnitude less important.

These simple metrics model steady turns. Reference [31] also presented metrics useful for transient maneuvers. These are discussed in the next section.

Suddenly Applied Lateral Force

Bernard et al. [31] also developed a simple two degree of freedom model to include roll transients. In this analysis, there are two coupled masses. The two degrees of freedom are the roll of the sprung mass about the roll center and the lateral motion of the entire vehicle. In a steady turn, this model yields

$$\frac{\overline{A}_y}{g} = \frac{\frac{T}{2}}{h + \overline{a} + \frac{W_s \overline{b}}{W_s + W_u}} \tag{6.12}$$

where W_s is the sprung mass weight and W_u is the unsprung mass weight. See Figure 6.1.

Again, taking a first order Taylor series expansion of equation 6.12 with respect to track width yields

$$\begin{aligned} \frac{A_y}{g} &= \frac{\overline{A}_y}{g} + \frac{d(\overline{A}_y/g)}{dT}\Delta T \\ &= \frac{\frac{T}{2}}{h + \overline{a} + \frac{W_s \overline{b}}{W_s + W_u}} \left(1 + \frac{\Delta T}{T}\right) \\ &= \frac{\overline{A}_y}{g}\left(1 + \frac{\Delta T}{T}\right) \end{aligned} \tag{6.13}$$

Taking a first order Taylor series expansion of equation 6.12 with respect to center of gravity height, h

$$\frac{A_y}{g} = \frac{\overline{A}_y}{g} + \frac{d(\overline{A}_y/g)}{dh}\Delta h$$

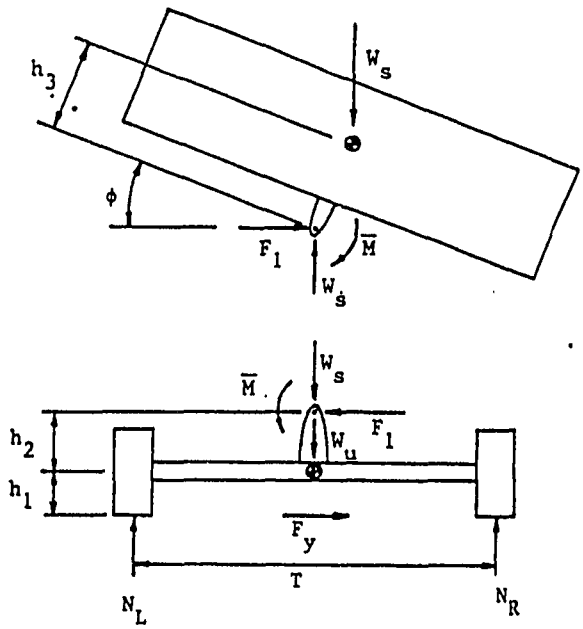

Figure 6.1: Diagram of Two Degree of Freedom Model (Reference [31]).

$$= \frac{\frac{T}{2}}{h + \bar{a} + \frac{W_s \bar{b}}{W_s + W_u}} \left(1 - \frac{\Delta h}{h + \bar{a} + \frac{W_s \bar{b}}{W_s + W_u}} \right)$$

$$= \frac{\overline{A}_y}{g} \left(1 - \frac{h}{h + \bar{a} + \frac{W_s \bar{b}}{W_s + W_u}} \frac{\Delta h}{h} \right) \tag{6.14}$$

From Equation 6.13, an increase of 1 percent in track width changes the lateral acceleration by 1 percent as was seen before in the steady turn analysis, Equation 6.7. However, the sensitivity of h in Equation 6.14 is slightly higher than in Equation 6.9, namely, for the parameters of Table 6.1, a one percent increase in h yields a 0.89

Table 6.3: Sensitivity Coefficients of Limit Lateral Acceleration for a Suddenly Applied Lateral Force

Equation No.	Passenger Car	Utility Vehicle
6.13 (Track)	1.00	1.00
6.14 (h)	-0.89	-0.92
6.15 ($\overline{a}$)	-0.040	-0.038
6.16 ($\overline{b}$)	-0.071	-0.041

percent decrease in limit lateral acceleration for the passenger car and a 0.92 percent decrease for the utility vehicle.

Taking a first order Taylor series expansion of equation 6.12 with respect to the overturning moment due to tire deflection, $\overline{a}$, yields

$$\begin{aligned} \frac{A_y}{g} &= \frac{\overline{A}_y}{g} + \frac{d(\overline{A}_y/g)}{d\overline{a}}\Delta\overline{a} \\ &= \frac{\overline{A}_y}{g}\left(1 - \frac{\overline{a}}{h + \overline{a} + \frac{W_s\overline{b}}{W_s+W_u}}\ \frac{\Delta\overline{a}}{\overline{a}}\right) \end{aligned} \tag{6.15}$$

and, taking a first order Taylor series expansion of equation 6.12 with respect to the roll gain, $\overline{b}$, yields

$$\begin{aligned} \frac{A_y}{g} &= \frac{\overline{A}_y}{g} + \frac{d(\overline{A}_y/g)}{d\overline{b}}\Delta\overline{b} \\ &= \frac{\overline{A}_y}{g}\left(1 - \frac{\frac{W_s}{W_s+W_u}\ \overline{b}}{h + \overline{a} + \frac{W_s\overline{b}}{W_s+W_u}}\ \frac{\Delta\overline{b}}{\overline{b}}\right) \end{aligned} \tag{6.16}$$

Table 6.3 summarizes the sensitivities of these parameters to the passenger car and utility vehicle of Table 6.1.

In determining the role of damping in roll stability Bernard et al. [31] derived equations which include suspension effects such as the roll natural frequency ω_n, the roll damping ratio ζ, and the roll gain $\overline{\phi}$. Again they considered the two degree of

freedom model and addressed the transient results from a suddenly applied lateral force. They found

$$\frac{\overline{A}_y}{g} = \frac{\frac{T}{2}}{h_1 + h_2 + \bar{a} + (1 + e^{-\zeta\pi})(h_3 + \bar{b})} \tag{6.17}$$

where h_1, h_2, and h_3 are the distance from the ground to the unsprung mass center, the distance from the unsprung mass center to the roll center, and the distance from the roll center to the sprung mass center, respectively.

Taking a first order Taylor series expansion of equation 6.17 with respect to track width, T, yields

$$\frac{A_y}{g} = \frac{\overline{A}_y}{g}\left(1 + \frac{\Delta T}{T}\right) \tag{6.18}$$

Taking a first order Taylor series expansion of equation 6.17 with respect to the distance from the ground to the unsprung mass center, h_1, yields

$$\frac{A_y}{g} = \frac{\overline{A}_y}{g}\left(1 - \frac{h_1}{(h_1 + h_2 + \bar{a} + (1 + e^{-\zeta\pi})(h_3 + \bar{b}))}\,\frac{\Delta h_1}{h_1}\right) \tag{6.19}$$

and with respect to the distance from the unsprung mass center to the roll center, h_2,

$$\frac{A_y}{g} = \frac{\overline{A}_y}{g}\left(1 - \frac{h_2}{(h_1 + h_2 + \bar{a} + (1 + e^{-\zeta\pi})(h_3 + \bar{b}))}\,\frac{\Delta h_2}{h_2}\right) \tag{6.20}$$

and with respect to the tire deflection, $\bar{a}$,

$$\frac{A_y}{g} = \frac{\overline{A}_y}{g}\left(1 - \frac{\bar{a}}{(h_1 + h_2 + \bar{a} + (1 + e^{-\zeta\pi})(h_3 + \bar{b}))}\,\frac{\Delta \bar{a}}{\bar{a}}\right) \tag{6.21}$$

and with respect to the distance of the roll center to the sprung mass center, h_3,

$$\frac{A_y}{g} = \frac{\overline{A}_y}{g}\left(1 - \frac{h_3(1 + e^{-\zeta\pi})}{(h_1 + h_2 + \bar{a} + (1 + e^{-\zeta\pi})(h_3 + \bar{b}))}\,\frac{\Delta h_3}{h_3}\right) \tag{6.22}$$

Table 6.4: Sensitivity Coefficients of Limit Lateral Acceleration for a Suddenly Applied Lateral Force

Equation No.	Passenger Car	Utility Vehicle
6.18 (Track)	1.00	1.00
6.19 (h_1)	-0.316	-0.317
6.20 (h_2)	0.164	0.0
6.22 (h_3)	-0.736	-0.604
6.21 ($\overline{a}$)	-0.0273	-0.0273
6.23 ($\overline{b}$)	-0.0837	-0.0520
6.24 (ζ)	0.179	0.143

and with respect to the roll gain, $\overline{b}$,

$$\frac{A_y}{g} = \frac{\overline{A}_y}{g}\left(1 - \frac{\overline{b}(1+e^{-\zeta\pi})}{(h_1+h_2+\overline{a}+(1+e^{-\zeta\pi})(h_3+\overline{b}))}\frac{\Delta\overline{b}}{\overline{b}}\right) \tag{6.23}$$

and, last, with respect to damping, ζ, yields

$$\frac{A_y}{g} = \frac{\overline{A}_y}{g}\left(1 + \frac{\zeta\pi e^{-\zeta\pi}(h_3+b)}{(h_1+h_2+\overline{a}+(1+e^{-\zeta\pi})(h_3+b))}\frac{\Delta\zeta}{\zeta}\right) \tag{6.24}$$

Table 6.4 summarizes how a 1 percent change in the particular parameter (such as track width in Equation 6.18) affects the percent change in the limit lateral acceleration. These parameters are taken from Table 6.1 for a typical passenger car (T/2h = 1.355) and utility vehicle (T/2h = 1.107). It can be seen that track width affects the limit lateral acceleration at one to one. The smallest effects are seen by changing the distance that the outside tire deflects under the vehicle, $\overline{a}$.

Using parameters from Table 6.1 for the utility vehicle and passenger car, changes in the damping coefficient, ζ, with respect to lateral acceleration from Equation 6.24 are shown in Figure 6.2. It can be seen that the largest changes in lateral acceleration occur when ζ is about 0.4 with increasing benefits from ζ of 0 to 0.4. Typical values of ζ for road vehicles are between 0.1 and 0.2.

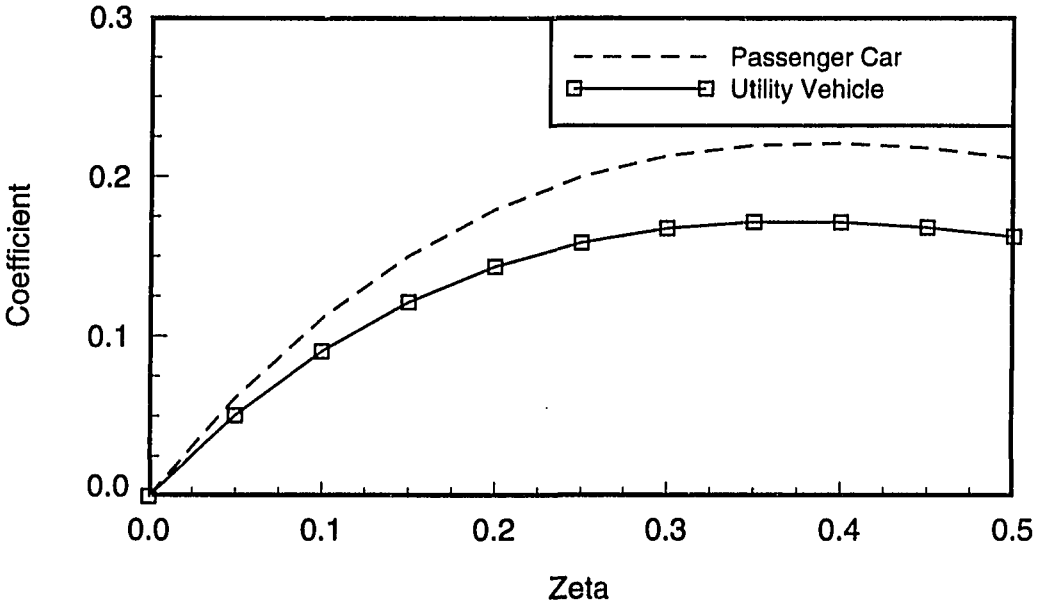

Figure 6.2: Sensitivity of ζ with respect to A_y/g.

In summary, these analyses, which are based on simple models and valid under very special situations, indicate that track and overall center of gravity height are very important, and that roll damping, ζ, can be important in transient situations involving suddenly applied lateral force. Roll gain and overturning moment are far less important than track width and center of gravity height measures, and, in sudden transients, less important than damping. However, these simple models indicate that, from a vehicle simulation point of view, errors in modeling either roll gain or overturning moment could make a significant difference under conditions when the vehicle model is near rollover.

Critical Sliding Velocity

The Critical Sliding Velocity, derived in Chapter 4, is a function of only track width, T, and center of gravity height, h. Chapter 5 showed that, given constant T/2h, CSV increased rapidly with h. This is to say that CSV will be higher for bigger vehicles. Here we examine CSV in the context of sensitivity, namely, we examine the sensitivity of CSV with respect to T and h.

From Equation 5.19 the general equation for Critical Sliding Velocity (CSV) is

$$\text{CSV(a)} = \sqrt{2gh(a+1)\left(1+(\frac{T}{2h})^2\right)\left[\sqrt{\left(1+(\frac{T}{2h})^2\right)} - cos\phi - \frac{T}{2h}sin\phi\right]} \qquad (6.25)$$

where ϕ is the angle of the sideslope.

This equation may be differentiated with respect to the track and center of gravity height parameters, with respect to the dimensionless constant a, and with respect to the sideslope angle. The results are given in the following equations.

Differentiating Equation 6.25 with respect to track width, T:

$$\frac{dCSV}{dT} = \frac{T}{4}\sqrt{\frac{2g(a+1)}{h^3}\frac{\left(\sqrt{\left(1+(\frac{T}{2h})^2\right)} - cos\phi - \frac{T}{2h}sin\phi\right)}{\left((\frac{T}{2h})^2+1\right)}}$$
$$+\frac{1}{2}\left[\frac{T}{4h^2\sqrt{(\frac{T}{2h})^2+1}} - \frac{sin\phi}{2h}\right]\sqrt{\frac{2gh(a+1)\left((\frac{T}{2h})^2+1\right)}{\left(\sqrt{\left(1+(\frac{T}{2h})^2\right)} - cos\phi - \frac{T}{2h}sin\phi\right)}} \qquad (6.26)$$

For a sensitivity analysis, Equation 6.26 may be simplified in terms of Equation 6.25 as follows:

$$\frac{dCSV}{CSV} = \frac{\left(\frac{T}{2h}\right)^2}{\left((\frac{T}{2h})^2+1\right)}\frac{dT}{T} - \frac{\left(\frac{T}{2h}\right)^2\left(\frac{h}{T}\right)sin\phi}{\left(\sqrt{\left(1+(\frac{T}{2h})^2\right)} - cos\phi - \frac{T}{2h}sin\phi\right)}\frac{dT}{T}$$

$$+\frac{\frac{1}{2}\left(\frac{T}{2h}\right)^2}{\left(\sqrt{\left(1+(\frac{T}{2h})^2\right)}-cos\phi-\frac{T}{2h}sin\phi\right)\sqrt{\left((\frac{T}{2h})^2+1\right)}}\frac{dT}{T} \qquad (6.27)$$

Equation 6.25 may also be differentiated with respect to center of gravity height, h to get:

$$\frac{dCSV}{dh}=\frac{1}{2}\sqrt{\frac{2g(a+1)}{h}\left(1+(\frac{T}{2h})^2\right)\left(\sqrt{\left(1+(\frac{T}{2h})^2\right)}-cos\phi-\frac{T}{2h}sin\phi\right)}$$

$$-\frac{T^2}{4}\sqrt{\frac{2g(a+1)}{h^5}\frac{\left(\sqrt{\left(1+(\frac{T}{2h})^2\right)}-cos\phi-\frac{T}{2h}sin\phi\right)}{\left(1+(\frac{T}{2h})^2\right)}}$$

$$+\frac{1}{4}\left[\frac{Tsin\phi}{h^2}-\frac{T^2}{2h^3\sqrt{\left((\frac{T}{2h})^2+1\right)}}\right]\sqrt{\frac{2gh(a+1)\left((\frac{T}{2h})^2+1\right)}{\left(\sqrt{\left(1+(\frac{T}{2h})^2\right)}-cos\phi-\frac{T}{2h}sin\phi\right)}} \qquad (6.28)$$

For a sensitivity analysis, Equation 6.28 may also be simplified in terms of Equation 6.25.

$$\frac{dCSV}{CSV}=\frac{1}{2}\frac{dh}{h}-\frac{\left(\frac{T}{2h}\right)^2}{\left((\frac{T}{2h})^2+1\right)}\frac{dh}{h}$$

$$+\frac{\left(\frac{T}{2h}\right)^2}{\left(\sqrt{\left(1+(\frac{T}{2h})^2\right)}-cos\phi-\frac{T}{2h}sin\phi\right)}\left(\frac{hsin\phi}{T}-\frac{\frac{1}{2}}{\sqrt{\left((\frac{T}{2h})^2+1\right)}}\right)\frac{dh}{h} \qquad (6.29)$$

Equation 6.29 may be rearranged to be

$$\frac{dCSV}{CSV} = \left[\frac{1}{2}-\frac{\left(\frac{T}{2h}\right)^2}{\left(1+(\frac{T}{2h})^2\right)}-\frac{\frac{1}{2}\left(\frac{T}{2h}\right)^2}{\left(\sqrt{\left(1+(\frac{T}{2h})^2\right)}-cos\phi-\frac{T}{2h}sin\phi\right)\sqrt{\left(1+(\frac{T}{2h})^2\right)}}\right]\frac{dh}{h}$$

$$+ \frac{Tsin\phi}{4h\left(\sqrt{\left(1+(\frac{T}{2h})^2\right)}-cos\phi-\frac{T}{2h}sin\phi\right)}\frac{dh}{h} \qquad (6.30)$$

Note that the sensitivity coefficients in Equations 6.27 and 6.29 differ by a factor of 0.5. In other words, the sensitivity coefficient of Equation 6.27 is subtracted from 0.5 to get the coefficient as given in Equation 6.29.

Taking the derivative of Equation 6.25 with respect to the dimensionless constant, a, gives

$$\frac{dCSV}{da} = \frac{1}{2}\sqrt{\frac{2gh}{(a+1)}\left((1+(\frac{T}{2h})^2\right)\left(\sqrt{\left(1+(\frac{T}{2h})^2\right)} - cos\phi - \frac{T}{2h}sin\phi\right)} \quad (6.31)$$

Equation 6.31 may be manipulated and simplified in terms of Equation 6.25 as follows:

$$\frac{dCSV}{CSV} = \frac{\frac{1}{2}\,a}{(a+1)}\;\frac{da}{a} \quad (6.32)$$

For the value a = 0.404, which fit data very well in Chapter 5, then

$$\frac{dCSV}{CSV} = 0.144\;\frac{da}{a} \quad (6.33)$$

The 0.404 value was based on a best fit through vehicle test data. Equation 6.33 indicates that if a particular vehicle has an a value ten percent different from a = 0.404, the calculated CSV would be 1.4 percent different from the "correct" value.

With respect to sideslope angle, ϕ:

$$\frac{dCSV}{d\phi} = \frac{1}{3}\left(sin\phi - \frac{Tcos\phi}{2h}\right)\sqrt{6gh\frac{\left(1+(\frac{T}{2h})^2\right)}{\left(\sqrt{\left(1+(\frac{T}{2h})^2\right)} - cos\phi - \frac{T}{2h}sin\phi\right)}} \quad (6.34)$$

And, for a sensitivity analysis, Equation 6.34 may also be simplified in terms of Equation 6.25 to get:

$$\frac{dCSV}{CSV} = \frac{\phi\left(sin\phi - \frac{Tcos\phi}{2h}\right)}{2\left(\sqrt{\left(1+(\frac{T}{2h})^2\right)} - cos\phi - \frac{T}{2h}sin\phi\right)}\frac{d\phi}{\phi} \quad (6.35)$$

The effects of changing the sideslope between -5 degrees, zero degrees (equivalent to level ground CSV), and +5 degrees are given in Figure 6.3. The results for zero degrees are given as a check since there is zero sensitivity to ϕ at $\phi = 0$. Note that a positive ϕ is analogous to a maneuver where a vehicle slides downhill and impacts an immovable object. As can be seen in Figure 6.3, for a given vehicle at a fixed T/2h ratio, the effects of the increasing "downslope" decreases the CSV, and increasing "upslope" increases CSV.

Figures 6.4 and 6.5 compare sensitivity from the level ground and the sideslope analyses with respect to the track width and to the center of gravity height. Figure 6.4 addresses the sensitivity with respect to the track width. Increasing track width on a positive sideslope (downhill) changes CSV the most while the negative sideslope (uphill) changes CSV less than on level ground. The effects are more pronounced at lower T/2h values than at higher T/2h values by a factor of 2. Increasing track width on all sideslope angles increases the change in CSV.

Figure 6.5 addresses sensitivity with respect to the center the gravity height. As before, the effects are more pronounced on the downhill sideslope as compared to the level ground and uphill sideslope. Also the extreme sensitivity in CSV with respect to h for the utility vehicle (T/2h = 1.107) differ by about a factor of 2 as compared to the passenger car (T/2h = 1.355).

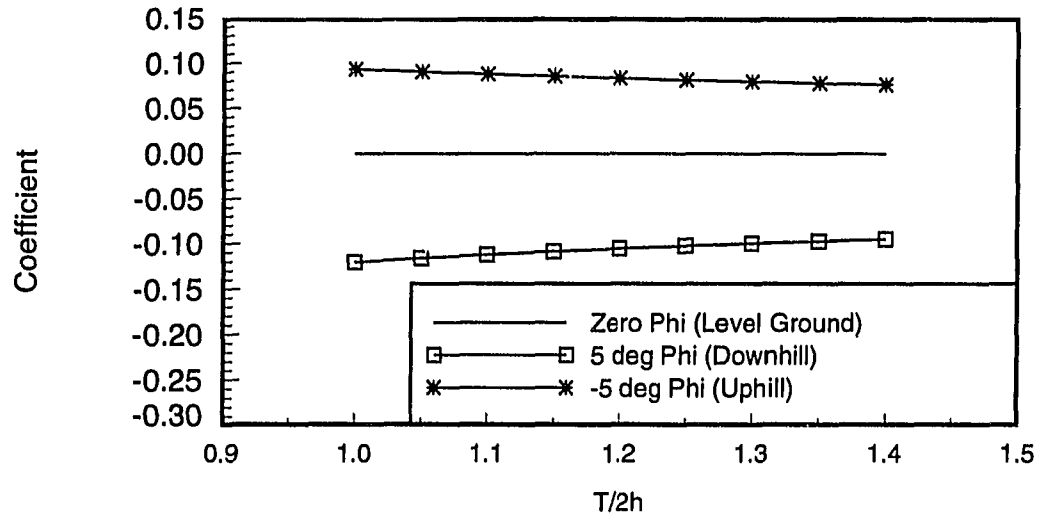

Figure 6.3: Minimum Lateral Velocities on a Sideslope. Comparison of $d\phi/\phi$ Coefficients.

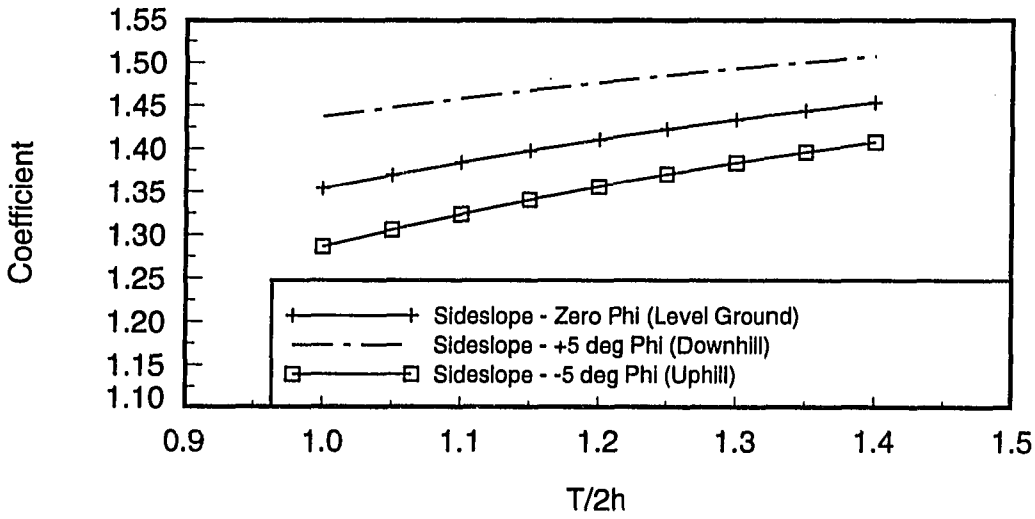

Figure 6.4: CSV on a Sideslope and Level Ground. Comparison of dT/T Coefficients.

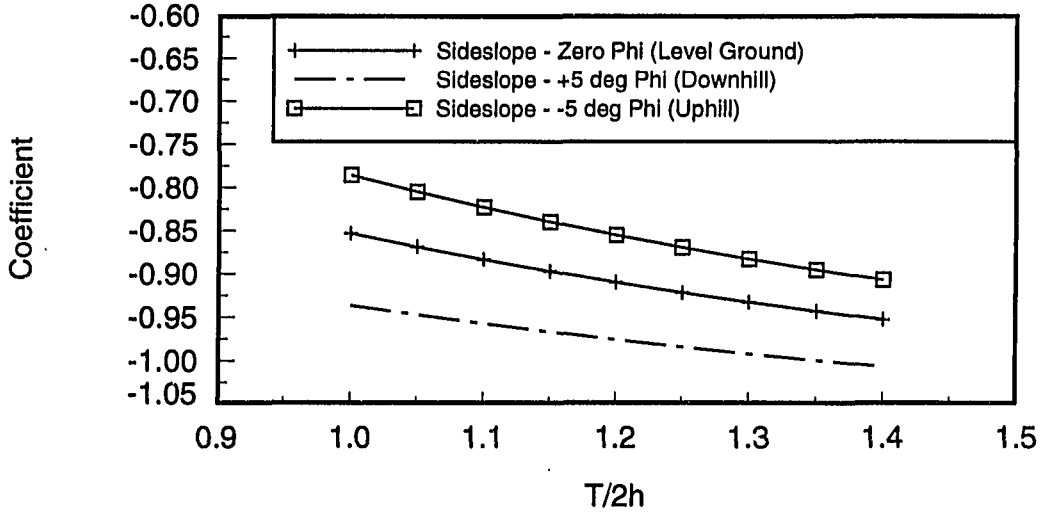

Figure 6.5: CSV on a Sideslope and Level Ground. Comparison of dh/h Coefficients.

Tilt Table Ratio

It is theoretically possible to find the sensitivities of tilt table tests through finite difference analysis of test results. In practice, we expect errors in measuring h to make this impossible. We can get a feel for the sensitivity by assuming that the Tilt Table Ratio (TTR) tests a rigid block. In this case,

$$\mathrm{TTR} = \frac{\mathrm{T}}{2\mathrm{h}} \tag{6.36}$$

Differentiating with respect to track, T, yields

$$\frac{\mathrm{d(TTR)}}{\mathrm{dT}} = \frac{1}{2\mathrm{h}} \tag{6.37}$$

so that

$$\frac{\mathrm{d(TTR)}}{\mathrm{TTR}} = \frac{\mathrm{dT}}{\mathrm{T}} \tag{6.38}$$

Thus a one percent change in Track, T, will yield a one percent change in TTR.

Differentiating TTR of a rigid block with respect to center of gravity height, h, yields

$$\frac{d(TTR)}{dh} = -\frac{T}{2h^2} \tag{6.39}$$

so that

$$\frac{d(TTR)}{TTR} = -\frac{dh}{h} \tag{6.40}$$

Thus a one percent change in cg Height, h, will yield a negative one percent change in TTR.

These results indicate that, for a rigid vehicle, a small percentage change in T alone or h alone would yield the same change in tilt angle.

CHAPTER 7. SUMMARY AND CONCLUSIONS

Rollover of cars and light trucks is of great interest to vehicle designers in the automotive industry and to regulators in government agencies. This interest derives in large part from the consequences of rollover accidents. For example, the Fatal Accident Reporting System (FARS) data indicates that, in 1990, about 15,900 people died in the United States in single vehicle crashes. Of these, 8100 people (51%) were fatalities in accidents which included rollover [1].

The literature indicates that many rollovers occur in single vehicle accidents. Experiments have been run from time to time to try to understand these events. Scatter in the experimental results inevitably limits the researchers ability to come to decisive conclusions. Simulation, on the other hand, yields repeatable results, but enough important parametric data, particularly data about the limits of adhesion of the tire/road interface, again make limited the potential for definitive conclusions.

Motivation for the analysis to be presented by this thesis was provided by several simulations. Various rollover scenarios were simulated to reenact rollover in a J-turn, in a reverse steer maneuver, and in a split μ surface. It was again verified that, on the one hand the mechanics behind rollover are complex and difficult to model precisely; on the other it was verified that tripped rollover can clearly occur at low speeds and with little or no steering input.

This thesis then addressed metrics - the static stability factor, the tilt table ratio, and the side pull test - which are proposed measures of resistance to smooth surface rollover. These metrics approximate the maximum lateral acceleration that a vehicle can withstand in a steady turn without rollover.

A notable finding is that the critical sliding velocity CSV, which has been proposed as the basis of government rulemaking, is independent of the roll moment of inertia, and in fact depends only on the track and cg height. Furthermore, while side pull testing and tilt table testing are mainly dependent on the aspect ratio T/2h, CSV is shown to vary widely with h given constant T/2h. Finally, an extension of the CSV analysis to include sideslope indicated that sideslope is very important, with downward slopes decreasing CSV and upward slopes increasing CSV.

The furrow-trip analysis led to the finding that, for small furrow length, the length of the furrow and the characteristics of the vehicle are sufficient to determine the minimum lateral velocity for rollover. The particular force generation mechanism of the furrow/tire interaction did not appear to be important.

In view of the fact that the literature indicates that most fatal rollover accidents are multiple-quarter-turn events, the curb-trip and furrow-trip analyses were extended to determine the minimum lateral velocity to elicit a two-quarter-turn rollover. Notable findings from this analysis are that (a) two-quarter-turn minimum velocities are about twice as high as one-quarter-turn velocities, (b) two-quarter-turn velocities may order vehicles differently than one-quarter-turn velocities, and (c) a key factor in two-quarter-turn velocities may be the height of the roof of the vehicle. This result should call into question the use of one-quarter-turn measures such at tilt table ratio, static pull test, and CSV for use as the sole indicator of the likelihood of

any particular vehicle being involved in fatal single vehicle rollover accidents.

The final chapter addressed the sensitivity of various measures of rollover resistance to small parameter changes. The analysis indicated, as expected, that T and h are very important. These are followed, in the case of transient maneuvers, by suspension damping, which in the case of a tripped maneuver may be about 15 percent, as important. Smaller effects, say in the range of about 5 percent as important as T and h, are the overturning moment of the tires and the roll gain of the suspension.

BIBLIOGRAPHY

[1] John Hinch, Scott Shadle, and Terry Klein. "NHTSA's Rollover Rulemaking Program - Results of Testing and Analysis". *SAE 920581*, 1992.

[2] K. A. Stonex. "Roadside Design for Safety.". In *Highway Research Board Proceedings, Vol. 39*, pages 120–156, 1960.

[3] R. N. Kemp and I. D. Neilson. "The Overturning of Cars as a Result of Severe Braking". Technical Report RRL LR 103, Road Research Laboratory, Ministry of Transport, 1967.

[4] J. E. Ford and J. E. Thompson. "Vehicle Rollover Dynamics Prediction by Mathematical Model". *SAE 690804*, 1969.

[5] G. M. Mackay and I. D. Tampen. "Field Studies of Rollover Performance". *SAE 700417*, 1970.

[6] Dennis Larson and J. B. Liljedahl. "Simulation of Sideways Overturning of Wheel Tractors on Side Slopes". *SAE 710709*, September 1971.

[7] Philip V. Hight, Arnold W. Siegel, and Alan M. Nahum. "Injury Mechanisms in Rollover Collisions". *SAE 720966*, 1972.

[8] R. A. Wilson and R. R. Gannon. "Rollover Testing". *SAE 720495*, 1972.

[9] Ian S. Jones. *Road Accident Studies with Particular Reference to the Handling and Stability Characteristics of Cars.* PhD thesis, University of London, 1973.

[10] Ian S. Jones. "The Mechanics of Rollover as the Result of Curb Impact". *SAE 750461*, 1975.

[11] W. Goldsmith. *Impact.* E. Arnold, London, 1960.

[12] Raymond R. McHenry. "Speed Estimates in Vehicle Rollovers". Technical Report Calspan Report No. ZQ-5639-V-1, Calspan Corporation, Buffalo, NY, January 1976.

[13] D. Bickerstaff. "The Handling Properties of Light Trucks". *SAE 760710*, 1976.

[14] Roy S. Rice, David J. Segal, and Ian S. Jones. "Development of Vehicle Rollover Maneuver", Volume I. Technical Report DOT-HS-6-01382, Calspan Corporation, Buffalo, NY, June 1978.

[15] Roy S. Rice, David J. Segal, and Ian S. Jones. "Development of Vehicle Rollover Maneuver", Volume II, Executive Summary. Technical Report DOT-HS-6-01382, Calspan Corporation, Buffalo, NY, June 1978. Final Report.

[16] Yasuhiko Fujiwara. "An Analysis on Vehicle Behavior in Overturning. In *Second International Technical Conference on Experimental Safety Vehicles*, 1979?

[17] R. H. Macmillan. *Dynamics of Vehicle Collisions.* Inderscience Enterprises Ltd., La Motte Chambers, St Helier, Jersey, Channel Islands, U.K., 1983. Special Publication SP5.

[18] A. C. Malliaris, Robert M. Nicholson, James H. Hedlund, and Stanley R. Scheiner. "Problems in Crash Avoidance and in Crash Avoidance Research". *SAE 830560*, 1983.

[19] Douglas R. Brown, Rickey L. Stansifer, and Dennis A. Guenther. "Scene Tripping as a Causal Factor in Vehicular Rollovers". In *Proceedings of the Canadian Multidisciplinary Road Safety Conference III*, London, Ontario, May 1984.

[20] K. F. Orlowski, R. T. Bundorf, and E. A. Moffatt. "Rollover Crash Tests - The Influence of Roof Strength on Injury Mechanics". *SAE 851734*, 1985.

[21] N. DeLeys and C. Brinkman. "Rollover Potential of Vehicles on Embankments, Sideslopes, and other Roadside Features". *SAE 870234*, 1987.

[22] Theodore J. Rosenthal, Henry T. Szostak, and R. Wade Allen. "User's Guide and Program Description for a Tripped Roll Over Vehicle Simulation". Technical Report DOT-HS-807-140, U. S. Department of Transportation, National Highway Traffic Safety Administration, July 1987.

[23] Kenneth W. Terhune. "A Study of Light Truck and Passenger Car Rollover and Ejection in Single-Vehicle Crashes". Technical report, Franklin Research Center, Arvin/Calspan Corporation, Buffalo, NY, May 1988. Calspan Report No. 7636.

[24] Andrzej G. Nalecz, Alan C. Bindemann, and Cleve Bare. "Sensitivity Analysis of Vehicle Tripped Rollover Model". Technical Report DOT-HS-807-300, University of Missouri-Columbia, 1988.

[25] Andrzej G. Nalecz, Alan C. Bindemann, and Howell K. Brewer. "Dynamic Analysis of Vehicle Rollover". In *Twelfth International Technical Conference on Experimental Safety Vehicles*, Göteborg, Sweden, 1989.

[26] K. F. Orlowski, E. A. Moffatt, R. T. Bundorf, and M. P. Holcomb. "Reconstruction of Rollover Collisions". *SAE 890857*, 1989.

[27] D. J. Segal and M. T. McGrath. "Analytical Study for Evaluation of Rollover Test Devices". Technical Report DOT–HS–805648, U. S. Department of Transportation, 1980.

[28] R. Young and H. Scheuerma. "Test for Vehicle Rollover Procedure". Technical Report DOT-HS-800–615, U. S. Department of Transportation, 1971.

[29] W. Riley Garrott, Michael Monk, and Jeffrey Chrstos. "Vehicle Inertial Parameters – Measured Values and Approximations". *SAE 881767*, 1988.

[30] Craig Winn. "Illustrations of Vehicle Rollover Mechanisms". NHTSA Rollover Subcommittee Presentation, July 1989.

[31] James Bernard, Jay Shannan, and Martin Vanderploeg. "Vehicle Rollover on Smooth Surfaces". *SAE 891991*, 1989.

[32] Peter Mengert, Santo Salvatore, Robert DiSario, and Robert Walter. "Statistical Estimation of Rollover Risk". Technical Report DOT–HS–807–446, U. S. Department of Transportation, National Highway Traffic Safety Administration, August 1989. Final Report.

[33] T. M. Thomas, N. K. Cooperrider, S. A. Hammoud, and P. F. Woley. "Real World Rollovers–A Crash Test Procedure and Vehicle Kinematics". In *Twelfth International Technical Conference on Experimental Safety Vehicles*, Göteborg, Sweden, 1989.

[34] Daniel Cohen, Kennerly Digges, and R. Hunter Nichols. "Rollover Crashworthiness Classification and Severity Indices". In *Twelfth International Technical Conference on Experimental Safety Vehicles*, Göteborg, Sweden, 1989.

[35] E. A. Harwin and Lloyd Emery. "The Crash Avoidance Rollover Study: A Database for the Investigation of Single Vehicle Rollover Crashes". In *Twelfth*

International Technical Conference on Experimental Safety Vehicles, Göteborg, Sweden, 1989.

[36] Neil K. Cooperrider, Terry M. Thomas, and Selim A. Hammoud. "Testing and Analysis of Vehicle Rollover Behavior". *SAE 900366*, 1990.

[37] E. A. Harwin and H. K. Brewer. "Analysis of the Relationship Between Vehicle Rollover Stability and Rollover Risk Using the NHTSA CARDfile Accident Database". *J Traffic Med*, 18(3):109–122, 1990.

[38] David N. Wormley and David S. Inouye. "Assessment of Light Weight Vehicle Rollover Research Test Requirements". Technical Report Contract DTRS-57-88-C-00078, Center for Transportation Studies, Massachusetts Institute of Technology, August 1990. Final Report, Prepared for U. S. Department of Transportation, Transportation Systems Center, In Support of National Highway Traffic Safety Administration.

[39] Ian S. Jones and Maria B. Penny. "Engineering Parameters Related to Rollover Frequency". *SAE 900104*, 1990.

[40] Gary J. Heydinger, W. Riley Garrott, Jeffrey P. Chrstos, and Dennis A. Guenther. "A Methodology for Validating Vehicle Dynamics Simulations". *SAE 900128*, 1990.

[41] Kenneth W. Terhune. "Contributions of Vehicle Factors and Roadside Features to Rollover in Single–Vehicle Crashes, Task 2 of Project "Crash Avoidance Research–Stability and Control" ". Technical Report DOT-HS-807-735, Arvin/Calspan Corporation, Buffalo, NY, March 1991.

[42] A. C. Malliaris and J. H. DeBlois. "Pivotal Characterization of Car Rollovers". In *13th International Technical Conference on Experimental Safety Vehicles*, Paris, France, November 1991.

[43] K. Digges and S. Klisch. "Analysis of the Factors Which Influence Rollover Crash Severity". *ESV Paper No. 91–S6–O–05*, 1991.

[44] Louise A. Obergefell, Ints Kaleps, and Arnold K. Johnson. "Prediction of Occupant's Motion During Rollover Crashes". *SAE 861876*, 1986.

[45] R. Wade Allen, Henry T. Szostak, Theodore J. Rosenthal, David H. Klyde, and Keith J. Owens. "Characteristics Influencing Ground Vehicle Lateral/Directional Dynamic Stability". *SAE 910234*, 1991.

[46] R. Wade Allen, Henry T. Szostak, Theodore J. Rosenthal, David H. Klyde, and Keith J. Owens. "Vehicle Dynamic Stability and Rollover". Technical Report No. 1268-1, National Highway Traffic Safety Administration, 1992. Contract No: NHTSA DTNH22-88-C-07384.

[47] Gary J. Heydinger, W. Riley Garrott, and Jeffrey P. Chrstos. "The Importance of Tire Lag on Simulated Transient Vehicle Response". *SAE 910235*, 1991.

[48] R. Wade Allen, Theodore Rosenthal, and Henry Szostak. "Steady State and Transient Analysis of Ground Vehicle Handling". *SAE 870495*, 1987.

[49] R. Wade Allen, Theodore Rosenthal, David Klyde, Keith Owens, and Henry Szostak. "Validation of Ground Vehicle Computer Simulations Developed for Dynamics Stability Analysis". *SAE 920054*, 1992.

[50] Jeffrey Chrstos and Dennis Guenther. "The Measurement of Static Rollover Metrics". *SAE 920582*, 1992.

[51] C. B. Winkler, K. L. Campbell, and C. E. Mink. "Variability in Center of Height Measurement". *SAE 920050*, 1992.

[52] Terry Klein. "A Statistical Analysis of Vehicle Rollover Propensity and Vehicle Stability". *SAE 920584*, 1992.

[53] W. Riley Garrott and Gary Heydinger. "An Investigation, Via Simulation, of Vehicle Characteristics that Contribute to Steering Maneuver Induced Rollover". *SAE 920585*, 1992.

[54] W. Riley Garrott. "The Variation of Static Rollover Metrics With Vehicle Loading and Between Similar Vehicles". *SAE 920583*, 1992.

[55] C. B. Winkler, S. E. Bogard, and K. E. Campbell. "Repeatability of the Tilt-Table Test Method". *SAE 930832*, 1993.

[56] S. E. Bogard, C. B. Winkler, and K. L. Campbell. "Sensitivity Analysis of the Tilt Table Methodology". Technical Report MVMA Project No. 11303, The University of Michigan Transportation Research Institute, April 1992.

[57] Chris Clover, Jon McLaughlin, Jim Bernard, and Steve Vardeman. "Sensitivity Analysis of a Tilt Table Test Procedure". Technical Report AAMA Project No. ISU 9219-C2137B, Iowa Center for Emerging Manufacturing Technology, Iowa State University, Ames, IA, November 1993.

[58] James E. Bernard and Chris L. Clover. "Validation of Computer Simulations of Vehicle Dynamics". *SAE 940231*, 1994.

[59] Andrzej G. Nalecz and Zheng Lu. "Methodology for Tripped Vehicle Rollover Testing and Analysis of Experimental Results". *SAE 940225*, 1994.

[60] W. Riley Garrott. "Measured Vehicle Inertia Parameters - NHTSA's Data Through September 1992". *SAE 930897*, 1993.

[61] J. L. Meriam. *Mechanics - Second Edition, Part II - Dynamics.* John Wiley and Sons, Inc., New York, 1959. Pages 298-299.

[62] J. Stannard Baker. *Traffic Accident Investigation Manual.* The Traffic Institute, Northwestern University, 1975. Chp 6 (p. 102–104), Chp 9 (p. 225–228,232–233).

[63] Ian S. Jones. *The Effect of Vehicle Characteristics on Road Accidents.* Pergamon Press, New York, 1976.

APPENDIX A. VDANL DATA SET

Vehicle Parameters

```
MASS =  113
SMASS =  95
UMASSF =  9
UMASSR =  9
LENA =  4.05
LENB =  5.18
IXS =  250
IYS =  1700
IZZ = 2100
IXZ = 0
KSTR =  22.3
KSCF =  .00024
KSCB = 0
DLADV = 0
DYADV = 0
DNADV = 0
DENSITY = .00237
REFAREA = 22
CDX = .5
AEROVEL = 44
KTL = 1.4
KSF =  3300
KSDF =  180
KSR =  3300
KSDR =  160
TRWF =  4.67
TRWB =  4.56
HCG =  2.12
KBS =  6600
HBS =  .2
```

Drive Train Parameters

```
KDC = 0
KDF = 2.4
KDB = 2.4
KCP = 0
KCPF = 0
KCPB = 0
KRF = 0
KRB = 2
KE1 = 135
KE2 = .25
KE3 = -.0004
KE4 = 18.9
KE5 = -.15
KE6 = 0
KTC0 = 123
SR0 = 2.1
ENGINEI = .125
TRANSMISSIONI = 0
SHIFTTIME = 1
SPEEDK1 = 1
SPEEDK2 = 1
KVAL = 12
K0 = 16
EPVEL = .25
IDLE = 50
DIFFTYPE$ = LIMSLIP
DG1 = 15
DG2 = 10
DG3 = 1
DG4 = 1
```

(CONTINUED)
KTSF = 14000
KTSR = 16400
KRAS = 12000
KRADP = 700
TSPRINGR = 20000
HRAF = 1.5
HRAR = 1.5
HS = 2.29
IXUF = 38
IXUR = 36
KLT = .00016
XACC = -2.1
ZACC = 1.83
DRAGC = -.015
LENS = 6.4
LM = 1.125
KBTF = -1.2
KVB = 26.3
KMB = 0
KBPVL = 100
SWZ = 0.5
SWW = 44
KCF = 0
LSO = 0
KLAGV = 25

Tire Parameters

TWIDTH = 8
KA0 = 0
KA1 = 15.52
KA2 = 6787
KA3 = 1.11
KA4 = 1000000
KA = .05
KMU = .234
TPRESS = 30
KB1 = -.000061
KB3 = 1.01
KB4 = 0
KGAMMA = .9

(CONTINUED)
DG5 = .006
DG6 = -200
DG7 = 0
DG8 = 0
DG9 = 0
DG10 = 0
NUMGEAR% = 4
DOWNSHIFT = 25
KGR1 = 3.5
KT1 2 = 46
KT2 2 = 108
KGR 2 = 2.25
KT1 3 = 72
KT2 3 = 168
KGR 3 = 1.5
KT1 4 = 108
KT2 4 = 252
KGR 4 = 1

(CONTINUED)
CSFZ = 16
MUNOM = .92
FZTRL = 2180
KK1 = -.00016
RR = 1.2
TIRE = BIAS
C1 = .535
C2 = 1.05
C3 = 1.15
C4 = .8
G1 = 1
G2 = 1

Suspension Parameters

SUSPENSIONF = SOLID AXLE
SUSPENSIONR = SOLID AXLE
HF = 0
HR = 0
LF = -1.4
LR = 1.3
KSAF = 1
KSAR = 1
BF = 0
BR = 0
CF = 0
CR = 0
DF = 0
DR = 0
EF = 0
ER = 0
KSLF = 0
KSLR = 0
LSAF = 1000
LSAR = 1000
KSADF = 0
KSADR = 0
KSAD2F = 0
KSAD2R = 0
KACK = .25

Driver Parameters

TAUA = .4
TAUR = .05
KY = .1
KR = 10.0
TL = .1
KPSI = 75
ZN = .5
WN = 20
KA = 0.1
KPSI2 = 750
TL2 = .6
KA2 = 2.5
KDELB11 = 2.05
KDELB12 = 1
KBETAD1 = 0
KBETAD2 = 2.75
KCDELT = 120
KBDSW = 1.00
THLAG = .25
BETA0 = .3491
ONTIME = 35
TMAX = 2
KDELB2 = .25
KBDDSW = 0.00

APPENDIX B. NHTSA DATA WITH TTR VALUES

Model Year	Vehicle Make	Vehicle Model	Track Width Front (m)	Track Width Rear (m)	Track Width Avg (m)	C.G. Height (m)	Static Stabil Factor	Tilt Table Ratio	TTR (T/2H)
1986	Buick	Century Estate	1.505	1.454	1.480	0.554	1.335	1.121	0.839
1981	Chevrolet	C-20 pickup	1.676	1.670	1.673	0.685	1.221	1.149	0.941
1984	Chevrolet	Caprice Classic	1.575	1.626	1.600	0.573	1.396	1.147	0.822
1983	Chevrolet	Cavalier	1.410	1.403	1.407	0.551	1.276	1.123	0.880
1991	Chevrolet	K1500 pickup	1.613	1.615	1.614	0.732	1.103	1.068	0.968
1991	Chevrolet	K1500 pickup	1.613	1.615	1.614	0.706	1.144	1.097	0.959
1990	Chevrolet	Lumina APV	1.492	1.549	1.521	0.626	1.215	0.979	0.806
1990	Chevrolet	Lumina APV	1.492	1.549	1.521	0.719	1.057	0.864	0.817
1990	Chevrolet	Lumina APV	1.492	1.549	1.521	0.674	1.128	1.009	0.894
1990	Chevrolet	Lumina APV	1.492	1.549	1.521	0.677	1.123	0.984	0.876
1990	Chevrolet	Lumina APV	1.492	1.549	1.521	0.698	1.089	0.901	0.828
1990	Chevrolet	Lumina APV	1.492	1.549	1.521	0.679	1.120	1.017	0.908
1990	Chevrolet	Lumina APV	1.492	1.549	1.521	0.667	1.140	1.036	0.909
1989	Chevrolet	S-10 Blazer	1.448	1.403	1.426	0.650	1.096	0.991	0.904
1991	Dodge	Caravan	1.524	1.575	1.549	0.638	1.214	1.052	0.866
1992	Dodge	Caravan	1.524	1.581	1.553	0.634	1.225	1.054	0.860
1991	Dodge	Caravan	1.524	1.575	1.549	0.635	1.220	1.047	0.858
1991	Dodge	Caravan	1.524	1.575	1.549	0.637	1.216	1.031	0.848
1992	Dodge	Caravan	1.518	1.575	1.546	0.659	1.173	1.054	0.898
1992	Dodge	Caravan	1.524	1.575	1.549	0.643	1.205	1.033	0.858
1992	Dodge	Caravan	1.524	1.575	1.549	0.654	1.184	1.032	0.872
1989	Dodge	Dynasty LE	1.461	1.461	1.461	0.533	1.370	1.136	0.830
1989	Dodge	Raider	1.410	1.422	1.416	0.661	1.071	0.931	0.870
1989	Dodge	Raider	1.410	1.422	1.416	0.683	1.036	0.883	0.852
1989	Dodge	Raider	1.410	1.422	1.416	0.721	0.982	0.823	0.839
1989	Dodge	Raider	1.410	1.422	1.416	0.691	1.025	0.859	0.838

ModelVehicle Year	Make	Vehicle Model	Track Width Front (m)	Rear (m)	Avg (m)	C.G. Height (m)	Static Stabil Factor	Tilt Table Ratio	TTR (T/2H)
1987	Dodge	Ram B-150	1.727	1.657	1.692	0.903	0.937	0.780	0.833
1987	Dodge	Ram B-150	1.727	1.657	1.692	0.858	0.986	0.846	0.858
1987	Dodge	Ram B-150	1.727	1.657	1.692	0.777	1.089	0.974	0.895
1987	Dodge	Ram B-150	1.727	1.657	1.692	0.847	0.999	0.814	0.815
1991	Dodge	Ram D-150	1.702	1.638	1.670	0.708	1.180	0.993	0.842
1991	Dodge	Ram D-150	1.702	1.638	1.670	0.669	1.248	1.048	0.840
1991	Dodge	Ram D-150	1.702	1.638	1.670	0.651	1.283	1.083	0.844
1991	Dodge	Ram D-150	1.702	1.638	1.670	0.677	1.234	1.032	0.837
1991	Dodge	Ramcharger	1.715	1.645	1.680	0.782	1.073	0.983	0.916
1991	Dodge	Ramcharger	1.715	1.645	1.680	0.743	1.130	1.055	0.934
1991	Dodge	Ramcharger	1.715	1.645	1.680	0.783	1.073	0.960	0.895
1991	Dodge	Ramcharger	1.715	1.645	1.680	0.803	1.046	0.935	0.894
1986	Ford	Aerostar XL	1.562	1.524	1.543	0.695	1.110	0.945	0.851
1988	Ford	E150 Club Wag XLT	1.765	1.702	1.734	0.770	1.126	1.078	0.957
1992	Ford	Explorer Sport	1.486	1.486	1.486	0.680	1.092	0.886	0.811
1991	Ford	Explorer XL	1.499	1.499	1.499	0.683	1.097	0.882	0.804
1991	Ford	Explorer XL	1.486	1.486	1.486	0.686	1.083	0.874	0.807
1991	Ford	Explorer XL	1.486	1.486	1.486	0.744	0.999	0.765	0.765
1991	Ford	Explorer XL	1.486	1.486	1.486	0.721	1.030	0.797	0.774
1991	Ford	Explorer XL	1.486	1.486	1.486	0.718	1.034	0.816	0.789
1984	Ford	F150	1.702	1.689	1.695	0.739	1.147	1.061	0.926
1984	Ford	F250	1.670	1.638	1.654	0.744	1.111	1.024	0.922
1991	Ford	Festiva	1.403	1.403	1.403	0.520	1.348	1.013	0.752
1991	Ford	Festiva	1.403	1.403	1.403	0.525	1.338	1.028	0.768
1991	Ford	Festiva	1.403	1.403	1.403	0.536	1.309	0.981	0.750
1991	Ford	Festiva	1.403	1.403	1.403	0.512	1.370	0.997	0.728
1991	Ford	Ranger	1.410	1.379	1.394	0.598	1.167	0.995	0.853
1992	Ford	Ranger	1.410	1.372	1.391	0.622	1.119	0.969	0.866
1991	Ford	Ranger	1.435	1.403	1.419	0.636	1.117	0.985	0.882
1991	Ford	Ranger	1.435	1.403	1.419	0.631	1.124	0.977	0.869
1991	Ford	Ranger	1.435	1.410	1.422	0.624	1.140	0.989	0.868
1991	Ford	Ranger	1.435	1.403	1.419	0.635	1.117	0.990	0.886
1991	Ford	Ranger	1.435	1.403	1.419	0.629	1.129	1.012	0.897
1991	Ford	Ranger	1.410	1.359	1.384	0.623	1.110	0.991	0.892
1992	Ford	Ranger	1.435	1.403	1.419	0.629	1.127	0.961	0.852
1991	Ford	Ranger	1.435	1.403	1.419	0.622	1.142	0.999	0.875
1988	Ford	Taurus	1.568	1.524	1.546	0.532	1.453	1.192	0.820
1991	Geo	Metro	1.359	1.340	1.349	0.511	1.320	1.128	0.854

Model Year	Vehicle Make	Vehicle Model	Track Width Front (m)	Track Width Rear (m)	Track Width Avg (m)	C.G. Height (m)	Static Stabil Factor	Tilt Table Ratio	TTR (T/2H)
1991	Geo	Tracker LSI	1.397	1.403	1.400	0.613	1.142	0.978	0.857
1991	Geo	Tracker LSI	1.397	1.403	1.400	0.639	1.095	0.896	0.818
1991	Geo	Tracker LSI	1.397	1.403	1.400	0.659	1.063	0.864	0.813
1991	Geo	Tracker LSI	1.397	1.403	1.400	0.638	1.097	0.920	0.838
1991	Geo	Tracker LSI	1.397	1.403	1.400	0.597	1.173	1.057	0.901
1991	GMC	Sierra C-10 1500	1.593	1.621	1.607	0.682	1.178	1.071	0.909
1991	GMC	Sierra C-10 1500	1.593	1.621	1.607	0.705	1.139	1.046	0.918
1991	GMC	Sierra SLE 1500	1.581	1.621	1.601	0.709	1.129	1.052	0.932
1991	GMC	Sierra SLE 1500	1.581	1.621	1.601	0.695	1.151	1.078	0.937
1990	GMC	Suburban 1500	1.727	1.651	1.689	0.768	1.099	0.991	0.902
1991	Honda	Accord LX	1.480	1.480	1.480	0.510	1.450	1.124	0.775
1991	Honda	Accord LX	1.480	1.480	1.480	0.504	1.467	1.184	0.807
1991	Honda	Accord LX	1.480	1.480	1.480	0.510	1.450	1.122	0.774
1991	Honda	Accord LX	1.480	1.480	1.480	0.511	1.447	1.122	0.776
1991	Isuzu	Amigo XL	1.461	1.467	1.464	0.653	1.122	1.016	0.906
1991	Isuzu	Rodeo	1.461	1.461	1.461	0.688	1.061	0.944	0.890
1991	Isuzu	Rodeo	1.461	1.473	1.467	0.693	1.058	0.929	0.878
1992	Isuzu	Rodeo	1.461	1.473	1.467	0.692	1.060	0.933	0.879
1991	Isuzu	Rodeo	1.448	1.448	1.448	0.679	1.066	0.959	0.900
1992	Isuzu	Rodeo	1.448	1.448	1.448	0.697	1.038	0.955	0.920
1991	Isuzu	Rodeo	1.448	1.448	1.448	0.662	1.093	0.937	0.857
1991	Isuzu	Rodeo	1.448	1.448	1.448	0.648	1.117	0.966	0.865
1991	Isuzu	Rodeo	1.448	1.448	1.448	0.645	1.123	0.947	0.843
1991	Isuzu	Rodeo	1.473	1.461	1.467	0.680	1.078	0.954	0.885
1991	Isuzu	Rodeo	1.448	1.448	1.448	0.694	1.044	0.937	0.898
1991	Isuzu	Rodeo	1.448	1.448	1.448	0.659	1.099	0.944	0.859
1991	Isuzu	U-15 pickup	1.461	1.461	1.461	0.628	1.162	1.087	0.935
1991	Mazda	MPV	1.549	1.543	1.546	0.665	1.162	1.063	0.915
1991	Nissan	Pathfinder	1.473	1.448	1.461	0.684	1.068	0.930	0.871
1990	Oldsmobile	Cutlass Calais	1.422	1.410	1.416	0.517	1.368	1.142	0.834
1991	Oldsmobile	Cutlass Calais	1.422	1.410	1.416	0.525	1.349	1.137	0.843
1991	Oldsmobile	Cutlass Calais	1.422	1.410	1.416	0.533	1.328	1.125	0.847
1991	Oldsmobile	Cutlass Calais	1.422	1.410	1.416	0.534	1.325	1.129	0.852
1991	Oldsmobile	Cutlass Calais	1.422	1.410	1.416	0.536	1.322	1.127	0.852
1991	Oldsmobile	Cutlass Calais	1.422	1.410	1.416	0.531	1.334	1.133	0.849
1991	Oldsmobile	Cutlass Calais	1.422	1.410	1.416	0.541	1.310	1.123	0.857
1990	Oldsmobile	Cutlass Calais	1.422	1.410	1.416	0.526	1.345	1.139	0.846
1991	Oldsmobile	Cutlass Calais	1.422	1.410	1.416	0.533	1.329	1.147	0.863

Model Year	Vehicle Make	Vehicle Model	Track Width Front (m)	Track Width Rear (m)	Track Width Avg (m)	C.G. Height (m)	Static Stabil Factor	Tilt Table Ratio	TTR (T/2H)
1990	Oldsmobile	Cutlass Calais	1.429	1.410	1.419	0.528	1.345	1.198	0.890
1992	Plymouth	Voyager	1.527	1.581	1.554	0.637	1.221	1.053	0.863
1991	Plymouth	Voyager	1.524	1.575	1.549	0.634	1.222	1.057	0.865
1991	Plymouth	Voyager	1.524	1.575	1.549	0.648	1.195	1.030	0.862
1991	Subaru	Justy GL	1.308	1.340	1.324	0.538	1.231	0.982	0.798
1989	Toyota	4Runner	1.518	1.499	1.508	0.699	1.079	1.008	0.934
1991	Toyota	Land Cruiser	1.588	1.588	1.588	0.757	1.049	0.953	0.909
1991	Toyota	Previa LE	1.575	1.562	1.568	0.638	1.229	1.026	0.835
1988	Yugo	GV	1.321	1.270	1.295	0.531	1.220	0.992	0.813

APPENDIX C. NHTSA DATA WITH CSV AND V2 CALCULATIONS

Vehicle Number	Track (m)	h (m)	T/2h (-)	Icg (kg-m^2)	Mass (kg)	RoofHt (m)	CSV (mph)	V2 Hinge	V2 Ice
# 1	1.397	0.506	1.380	404.	1239.7	1.35	12.09	20.17	21.98
# 2	1.398	0.533	1.311	381.	1251.5	1.37	11.35	19.04	20.87
# 3	1.480	0.554	1.336	551.	1518.6	1.38	12.01	19.70	21.53
# 4	1.525	0.553	1.379	672.	1496.3	1.38	12.92	21.12	22.89
# 5	1.525	0.539	1.415	578.	1492.3	1.38	12.96	20.86	22.67
# 6	1.525	0.553	1.379	628.	1500.9	1.38	12.77	20.73	22.52
# 7	1.525	0.560	1.362	605.	1491.8	1.38	12.54	20.32	22.13
# 8	1.525	0.546	1.397	582.	1506.3	1.38	12.78	20.61	22.38
# 9	1.525	0.552	1.381	619.	1496.3	1.38	12.77	20.71	22.50
# 10	1.525	0.555	1.374	623.	1506.3	1.38	12.70	20.61	22.40
# 11	1.407	0.543	1.296	431.	1261.9	1.38	11.41	19.33	21.16
# 12	1.603	0.671	1.194	705.	1895.8	1.77	10.93	19.61	21.80
# 13	1.648	0.736	1.120	962.	1797.9	1.87	10.83	20.40	22.65
# 14	1.648	0.741	1.112	1070.	1752.1	1.87	10.99	20.97	23.18
# 15	1.648	0.791	1.042	1267.	2173.8	1.83	10.20	19.32	21.46
# 16	1.648	0.703	1.172	878.	1870.9	1.77	11.14	20.01	22.14
# 17	1.632	0.700	1.166	694.	1853.2	1.77	10.72	19.07	21.24
# 18	1.629	0.654	1.245	1089.	1872.7	1.75	12.25	22.33	24.45
# 19	1.600	0.712	1.124	796.	2099.0	1.73	10.30	18.47	20.57
# 20	1.600	0.673	1.189	891.	1855.0	1.76	11.27	20.61	22.80
# 21	1.673	0.685	1.221	887.	2240.9	1.82	11.39	20.18	22.39
# 22	1.553	0.599	1.296	751.	1548.0	1.46	12.29	20.66	22.51
# 23	1.600	0.573	1.396	806.	1977.9	1.50	13.00	21.26	23.14
# 24	1.407	0.551	1.277	409.	1255.1	1.40	11.16	19.01	20.87
# 25	1.695	0.756	1.121	1076.	2259.5	1.86	10.73	19.57	21.76
# 26	1.614	0.732	1.102	856.	2148.4	1.80	10.19	18.66	20.83
# 27	1.614	0.706	1.143	850.	2002.8	1.82	10.66	19.64	21.86

#	28	1.521	0.626	1.215	822.	2152.9	1.63	11.03	19.62	21.70
#	29	1.521	0.719	1.058	910.	2150.7	1.63	9.72	17.76	19.77
#	30	1.521	0.660	1.152	728.	1574.3	1.68	10.74	19.89	22.00
#	31	1.521	0.674	1.128	727.	1652.3	1.63	10.44	18.97	21.01
#	32	1.521	0.677	1.123	764.	1724.9	1.68	10.40	19.25	21.33
#	33	1.521	0.698	1.090	895.	2176.5	1.62	9.97	18.06	20.05
#	34	1.521	0.679	1.120	761.	1728.5	1.68	10.36	19.16	21.26
#	35	1.521	0.667	1.140	726.	1648.7	1.69	10.55	19.52	21.65
#	36	1.336	0.539	1.239	344.	1285.9	1.49	10.41	18.74	20.78
#	37	1.419	0.640	1.109	555.	1589.3	1.65	9.77	18.46	20.61
#	38	1.374	0.665	1.033	523.	1458.3	1.64	9.07	17.72	19.86
#	39	1.372	0.634	1.082	646.	1392.1	1.61	9.90	19.48	21.58
#	40	1.419	0.664	1.069	580.	1728.5	1.67	9.36	17.86	20.03
#	41	1.426	0.650	1.097	604.	1789.3	1.65	9.63	18.11	20.26
#	42	1.379	0.570	1.210	380.	1201.2	1.56	10.47	19.19	21.29
#	43	1.419	0.573	1.238	436.	1466.4	1.61	10.70	19.42	21.54
#	44	1.377	0.554	1.243	401.	1276.0	1.56	10.75	19.67	21.75
#	45	1.422	0.610	1.166	560.	1605.2	1.61	10.28	19.03	21.11
#	46	1.422	0.690	1.030	749.	2301.6	1.53	9.00	16.41	18.34
#	47	1.422	0.638	1.114	659.	1830.5	1.59	9.87	18.28	20.34
#	48	1.618	0.709	1.141	772.	2038.2	1.85	10.49	19.28	21.56
#	49	1.463	0.550	1.330	469.	1219.7	1.32	12.04	19.57	21.34
#	50	1.441	0.583	1.236	410.	1237.9	1.39	10.87	18.22	20.06
#	51	1.323	0.520	1.272	307.	1026.1	1.33	10.84	18.61	20.43
#	52	1.394	0.489	1.425	360.	1295.0	1.26	12.22	19.41	21.11
#	53	1.303	0.510	1.277	265.	945.4	1.30	10.75	18.31	20.13
#	54	1.298	0.533	1.218	331.	1159.9	1.53	10.25	19.24	21.38
#	55	1.549	0.638	1.214	733.	1668.2	1.68	11.29	20.41	22.51
#	56	1.551	0.655	1.184	695.	1552.6	1.68	11.04	20.01	22.12
#	57	1.553	0.634	1.225	740.	1672.7	1.68	11.41	20.58	22.69
#	58	1.543	0.688	1.121	965.	1745.3	1.65	10.78	19.94	21.99
#	59	1.543	0.654	1.180	1101.	2203.7	1.61	11.18	20.10	22.09
#	60	1.549	0.635	1.220	743.	1667.7	1.66	11.37	20.43	22.53
#	61	1.543	0.684	1.128	832.	1547.6	1.67	10.80	20.04	22.10
#	62	1.549	0.664	1.166	756.	1532.6	1.68	11.03	20.23	22.31
#	63	1.549	0.637	1.216	741.	1665.0	1.68	11.33	20.52	22.62
#	64	1.546	0.659	1.173	693.	1503.6	1.70	10.97	20.15	22.27
#	65	1.549	0.643	1.205	801.	1753.0	1.68	11.27	20.45	22.55
#	66	1.549	0.654	1.184	740.	1654.1	1.68	11.04	20.04	22.12
#	67	1.549	0.642	1.206	816.	1580.7	1.68	11.51	21.12	23.22
#	68	1.547	0.633	1.222	815.	1592.5	1.68	11.65	21.36	23.46
#	69	1.429	0.515	1.387	380.	1098.2	1.36	12.32	20.40	22.22

#	70	1.508	0.625	1.206	608.	1496.3	1.57	11.03	19.47	21.47
#	71	1.508	0.599	1.259	509.	1278.7	1.65	11.49	20.71	22.81
#	72	1.508	0.627	1.203	792.	1845.5	1.55	11.08	19.55	21.50
#	73	1.530	0.632	1.210	586.	1771.1	1.71	10.79	19.41	21.59
#	74	1.500	0.608	1.234	592.	1744.4	1.69	10.99	19.92	22.09
#	75	1.513	0.543	1.393	614.	1649.2	1.45	12.66	20.95	22.83
#	76	1.461	0.533	1.371	560.	1559.4	1.40	12.29	20.43	22.28
#	77	1.462	0.532	1.374	472.	1233.4	1.39	12.45	20.74	22.53
#	78	1.422	0.511	1.391	398.	1058.3	1.38	12.52	21.10	22.94
#	79	1.422	0.519	1.370	395.	1022.5	1.40	12.37	21.10	22.94
#	80	1.422	0.517	1.375	418.	1129.5	1.37	12.33	20.72	22.51
#	81	1.422	0.526	1.352	471.	1273.7	1.34	12.10	20.14	21.91
#	82	1.378	0.694	0.993	650.	1523.6	1.85	8.95	19.12	21.56
#	83	1.416	0.661	1.071	583.	1736.7	1.83	9.38	18.89	21.30
#	84	1.416	0.683	1.037	684.	1964.3	1.79	9.13	18.27	20.63
#	85	1.416	0.721	0.982	750.	2198.7	1.77	8.63	17.30	19.59
#	86	1.416	0.691	1.025	705.	2198.7	1.77	8.93	17.69	19.99
#	87	1.637	0.658	1.244	703.	1610.6	1.76	11.70	20.79	22.95
#	88	1.692	0.777	1.089	1216.	2047.7	2.00	10.75	20.89	23.26
#	89	1.670	0.669	1.248	860.	2050.0	1.76	11.73	20.49	22.63
#	90	1.670	0.651	1.283	797.	1903.5	1.77	12.06	21.05	23.19
#	91	1.680	0.743	1.131	1094.	2311.2	1.87	10.79	19.81	22.04
#	92	1.544	0.694	1.112	732.	1605.2	1.83	10.37	19.98	22.25
#	93	1.541	0.694	1.110	789.	1785.6	1.84	10.30	19.87	22.18
#	94	1.543	0.671	1.150	751.	1817.4	1.84	10.57	20.15	22.49
#	95	1.543	0.695	1.110	720.	1710.4	1.82	10.23	19.53	21.80
#	96	1.541	0.684	1.126	819.	1900.4	1.84	10.41	20.02	22.33
#	97	1.642	0.775	1.059	1104.	2418.6	1.86	10.01	18.75	20.95
#	98	1.445	0.698	1.035	597.	1478.2	1.73	9.34	18.31	20.51
#	99	1.448	0.729	0.993	569.	1709.5	1.74	8.75	17.05	19.23
#	100	1.441	0.726	0.992	573.	1727.6	1.74	8.73	17.05	19.24
#	101	1.449	0.734	0.987	559.	1780.6	1.70	8.64	16.55	18.68
#	102	1.699	0.818	1.039	1035.	2162.9	1.89	9.95	18.49	20.68
#	103	1.735	0.765	1.134	1289.	2256.8	2.02	11.20	21.27	23.66
#	104	1.724	0.791	1.090	1374.	2295.3	2.04	10.82	20.98	23.37
#	105	1.728	0.752	1.149	1294.	2057.7	2.06	11.51	22.35	24.81
#	106	1.735	0.792	1.095	1508.	2186.5	2.01	11.13	21.56	23.91
#	107	1.406	0.511	1.376	328.	1006.6	1.35	12.07	20.05	21.86
#	108	1.431	0.503	1.422	337.	1038.4	1.35	12.53	20.52	22.31
#	109	1.471	0.688	1.069	754.	2017.8	1.71	9.58	18.21	20.38
#	110	1.486	0.680	1.093	690.	1905.8	1.73	9.78	18.46	20.65
#	111	1.499	0.683	1.097	750.	1970.6	1.71	9.91	18.52	20.69

# 112	1.486	0.686	1.083	742.	1966.1	1.73	9.75	18.49	20.66
# 113	1.486	0.744	0.999	896.	2394.6	1.70	8.98	17.07	19.19
# 114	1.486	0.721	1.031	849.	2394.6	1.70	9.20	17.33	19.46
# 115	1.486	0.718	1.035	839.	2264.9	1.71	9.29	17.60	19.75
# 116	1.678	0.678	1.237	754.	1550.8	1.78	11.88	21.08	23.23
# 117	1.651	0.679	1.216	841.	1700.4	1.80	11.66	21.11	23.30
# 118	1.651	0.707	1.168	1154.	1918.0	1.80	11.53	21.35	23.54
# 119	1.651	0.711	1.161	818.	1718.5	1.80	11.06	20.05	22.25
# 120	1.651	0.724	1.140	1334.	2235.4	1.80	11.24	20.85	23.02
# 121	1.645	0.695	1.183	781.	1718.1	1.80	11.19	20.23	22.42
# 122	1.645	0.690	1.192	792.	1763.0	1.80	11.26	20.32	22.49
# 123	1.645	0.690	1.192	799.	1761.2	1.80	11.27	20.36	22.55
# 124	1.645	0.689	1.194	745.	1763.9	1.80	11.18	20.08	22.27
# 125	1.645	0.690	1.192	787.	1762.1	1.80	11.25	20.30	22.47
# 126	1.645	0.690	1.192	781.	1764.8	1.80	11.23	20.26	22.43
# 127	1.645	0.688	1.195	779.	1765.2	1.80	11.26	20.28	22.49
# 128	1.645	0.716	1.149	857.	1918.5	1.78	10.83	19.52	21.64
# 129	1.632	0.680	1.200	935.	1854.6	1.78	11.51	20.93	23.13
# 130	1.695	0.739	1.147	721.	1860.9	1.87	10.70	19.19	21.42
# 131	1.651	0.692	1.193	839.	1837.8	1.78	11.30	20.24	22.41
# 132	1.670	0.648	1.289	727.	1870.4	1.77	12.00	20.81	22.96
# 133	1.670	0.668	1.250	764.	1920.3	1.77	11.67	20.33	22.48
# 134	1.671	0.700	1.194	787.	1889.5	1.80	11.20	19.86	22.05
# 135	1.665	0.676	1.232	840.	1906.3	1.80	11.64	20.72	22.89
# 136	1.654	0.744	1.112	761.	1914.0	1.85	10.34	18.85	21.09
# 137	1.660	0.720	1.153	827.	2017.3	1.83	10.77	19.44	21.63
# 138	1.403	0.520	1.349	340.	1142.7	1.38	11.66	19.50	21.33
# 139	1.403	0.525	1.336	298.	919.1	1.42	11.69	19.98	21.88
# 140	1.403	0.536	1.309	347.	1198.9	1.36	11.26	18.68	20.52
# 141	1.403	0.512	1.370	349.	1198.9	1.36	11.81	19.54	21.37
# 142	1.595	0.556	1.434	686.	1741.2	1.44	13.30	21.25	23.09
# 143	1.449	0.529	1.370	408.	1256.0	1.37	12.08	19.79	21.61
# 144	1.464	0.532	1.376	453.	1469.1	1.37	12.08	19.57	21.38
# 145	1.612	0.545	1.479	688.	1898.1	1.42	13.61	21.25	23.06
# 146	1.383	0.633	1.092	441.	1237.9	1.60	9.60	18.23	20.35
# 147	1.383	0.649	1.065	560.	1428.3	1.61	9.49	18.31	20.42
# 148	1.383	0.645	1.072	649.	1723.1	1.57	9.50	18.00	20.04
# 149	1.394	0.598	1.166	424.	1353.5	1.61	10.09	18.77	20.87
# 150	1.391	0.622	1.118	434.	1443.3	1.63	9.62	18.07	20.24
# 151	1.419	0.636	1.116	412.	1430.6	1.61	9.59	17.61	19.69
# 152	1.419	0.631	1.124	423.	1431.5	1.63	9.70	17.93	20.05
# 153	1.422	0.624	1.139	434.	1432.0	1.67	9.86	18.46	20.65

# 154	1.419	0.635	1.117	422.	1436.9	1.63	9.63	17.82	19.94
# 155	1.419	0.629	1.128	410.	1413.4	1.61	9.70	17.81	19.91
# 156	1.384	0.623	1.111	441.	1501.8	1.63	9.51	17.93	20.08
# 157	1.419	0.629	1.128	476.	1566.2	1.64	9.76	18.15	20.29
# 158	1.419	0.622	1.141	508.	1650.1	1.65	9.89	18.45	20.59
# 159	1.386	0.615	1.127	404.	1361.7	1.63	9.67	18.18	20.35
# 160	1.546	0.563	1.373	573.	1419.3	1.44	12.67	20.79	22.63
# 161	1.542	0.550	1.402	541.	1449.6	1.43	12.79	20.77	22.60
# 162	1.546	0.532	1.453	554.	1489.5	1.40	13.29	21.23	23.07
# 163	1.430	0.546	1.310	474.	1201.6	1.39	11.84	20.16	21.99
# 164	1.492	0.560	1.332	635.	1777.5	1.37	11.97	19.45	21.24
# 165	1.486	0.578	1.285	539.	1630.6	1.40	11.40	18.71	20.52
# 166	1.486	0.581	1.279	526.	1630.1	1.40	11.30	18.54	20.35
# 167	1.486	0.569	1.306	560.	1703.1	1.38	11.58	18.83	20.64
# 168	1.349	0.511	1.320	253.	814.8	1.33	11.37	19.26	21.10
# 169	1.400	0.613	1.142	418.	1157.6	1.65	10.09	19.22	21.41
# 170	1.400	0.639	1.095	475.	1447.8	1.61	9.54	17.93	20.01
# 171	1.400	0.659	1.062	492.	1451.0	1.61	9.29	17.58	19.64
# 172	1.400	0.638	1.097	469.	1376.6	1.62	9.61	18.15	20.25
# 173	1.400	0.597	1.173	398.	1080.1	1.67	10.40	19.94	22.15
# 174	1.626	0.663	1.226	954.	1764.8	1.75	11.90	21.62	23.74
# 175	1.599	0.793	1.008	1128.	2407.8	1.91	9.50	18.59	20.90
# 176	1.708	0.838	1.019	1207.	2426.8	1.99	9.83	18.84	21.13
# 177	1.419	0.672	1.056	640.	1712.6	1.70	9.39	18.29	20.48
# 178	1.607	0.682	1.178	737.	1851.8	1.78	10.88	19.67	21.87
# 179	1.607	0.705	1.140	779.	1990.6	1.75	10.50	18.86	21.01
# 180	1.601	0.695	1.152	795.	1981.5	1.77	10.64	19.31	21.48
# 181	1.689	0.768	1.100	1244.	2563.3	1.88	10.54	19.46	21.67
# 182	1.480	0.510	1.451	541.	1730.8	1.34	12.82	20.34	22.13
# 183	1.480	0.504	1.468	476.	1411.6	1.37	13.12	21.18	22.97
# 184	1.480	0.510	1.451	540.	1710.4	1.34	12.84	20.38	22.17
# 185	1.480	0.511	1.448	541.	1730.8	1.34	12.79	20.32	22.09
# 186	1.378	0.519	1.328	250.	878.8	1.34	11.35	18.87	20.68
# 187	1.368	0.540	1.267	312.	938.6	1.36	11.04	18.94	20.75
# 188	1.362	0.539	1.263	383.	1262.4	1.33	10.85	18.31	20.10
# 189	1.368	0.558	1.226	476.	1414.3	1.33	10.69	18.19	19.98
# 190	1.368	0.555	1.232	404.	1180.3	1.36	10.78	18.57	20.38
# 191	1.481	0.687	1.078	784.	2062.7	1.75	9.70	18.58	20.80
# 192	1.464	0.653	1.121	543.	1613.8	1.68	9.90	18.42	20.55
# 193	1.337	0.514	1.301	334.	1118.6	1.49	11.11	20.06	22.12
# 194	1.461	0.688	1.062	690.	1865.9	1.68	9.49	17.95	20.08
# 195	1.467	0.693	1.058	712.	1909.0	1.68	9.48	17.90	20.02

# 196	1.467	0.692	1.060	713.	1905.8	1.68	9.50	17.92	20.04
# 197	1.448	0.679	1.066	671.	1855.0	1.68	9.48	18.01	20.14
# 198	1.448	0.697	1.039	699.	1912.6	1.65	9.25	17.49	19.57
# 199	1.448	0.662	1.094	658.	1848.7	1.65	9.71	18.17	20.27
# 200	1.448	0.648	1.117	678.	1832.3	1.65	9.97	18.67	20.77
# 201	1.448	0.645	1.122	661.	1842.3	1.65	9.98	18.61	20.73
# 202	1.467	0.680	1.079	678.	1867.3	1.68	9.63	18.09	20.21
# 203	1.448	0.694	1.043	651.	1821.0	1.67	9.27	17.59	19.67
# 204	1.448	0.659	1.099	634.	1813.3	1.65	9.73	18.15	20.27
# 205	1.397	0.677	1.032	701.	1660.0	1.82	9.31	19.35	21.77
# 206	1.397	0.724	0.965	802.	1958.4	1.79	8.67	18.00	20.28
# 207	1.397	0.702	0.995	718.	1813.8	1.82	8.89	18.49	20.87
# 208	1.461	0.628	1.163	515.	1601.1	1.68	10.21	18.85	21.04
# 209	1.461	0.657	1.112	527.	1467.8	1.61	9.90	18.13	20.19
# 210	1.473	0.671	1.098	651.	1783.8	1.59	9.81	17.79	19.80
# 211	1.473	0.660	1.116	586.	1485.5	1.60	10.09	18.44	20.47
# 212	1.473	0.660	1.116	614.	1565.3	1.60	10.08	18.40	20.44
# 213	1.473	0.665	1.108	599.	1568.0	1.59	9.97	18.12	20.14
# 214	1.473	0.702	1.049	612.	1802.0	1.58	9.30	16.83	18.82
# 215	1.476	0.685	1.077	584.	1730.8	1.63	9.54	17.46	19.49
# 216	1.476	0.694	1.063	608.	1880.9	1.60	9.37	16.94	18.96
# 217	1.476	0.669	1.103	547.	1577.5	1.63	9.80	17.91	19.97
# 218	1.448	0.678	1.068	619.	1523.6	1.61	9.65	18.08	20.11
# 219	1.448	0.648	1.117	462.	1702.7	1.56	9.59	17.01	19.00
# 220	1.448	0.684	1.058	746.	2021.0	1.55	9.44	17.19	19.14
# 221	1.585	0.675	1.174	811.	1991.0	1.68	10.84	19.22	21.30
# 222	1.302	0.607	1.072	362.	1196.6	1.70	9.09	18.48	20.85
# 223	1.302	0.630	1.033	387.	1269.2	1.70	8.77	17.95	20.30
# 224	1.334	0.579	1.152	378.	1407.5	1.79	9.67	19.52	22.07
# 225	1.407	0.664	1.059	486.	1390.7	1.82	9.32	18.89	21.31
# 226	1.459	0.701	1.041	592.	1473.7	1.82	9.41	18.80	21.15
# 227	1.473	0.637	1.156	480.	1355.8	1.83	10.30	19.99	22.41
# 228	1.467	0.632	1.161	502.	1469.6	1.82	10.28	19.90	22.29
# 229	1.467	0.597	1.229	431.	1317.2	1.83	10.83	20.79	23.25
# 230	1.467	0.663	1.106	541.	1616.5	1.80	9.77	18.90	21.20
# 231	1.567	0.548	1.430	617.	1637.8	1.41	13.12	20.91	22.72
# 232	1.410	0.527	1.338	323.	920.5	1.41	11.86	20.27	22.14
# 233	1.325	0.547	1.211	354.	1210.2	1.54	10.27	19.13	21.25
# 234	1.309	0.512	1.278	267.	902.8	1.37	10.85	19.03	20.91
# 235	1.546	0.665	1.162	759.	1926.2	1.78	10.63	19.79	22.00
# 236	1.427	0.559	1.276	444.	1301.4	1.39	11.27	19.01	20.84
# 237	1.427	0.554	1.288	449.	1296.8	1.39	11.40	19.22	21.08

# 238	1.410	0.558	1.263	443.	1301.4	1.39	11.12	18.92	20.76
# 239	1.414	0.550	1.285	436.	1305.9	1.39	11.29	19.11	20.94
# 240	1.583	0.565	1.401	717.	1750.3	1.45	13.03	21.08	22.94
# 241	1.461	0.547	1.335	522.	1437.4	1.39	11.98	19.89	21.75
# 242	1.461	0.541	1.350	514.	1410.2	1.39	12.12	20.12	21.96
# 243	1.461	0.684	1.068	706.	1990.1	1.68	9.49	17.89	20.02
# 244	1.417	0.663	1.069	657.	1555.3	1.67	9.68	18.84	20.99
# 245	1.332	0.544	1.224	409.	1228.4	1.54	10.60	19.87	21.97
# 246	1.392	0.601	1.158	514.	1410.2	1.56	10.24	18.97	21.02
# 247	1.392	0.605	1.150	491.	1438.8	1.56	10.07	18.59	20.63
# 248	1.391	0.585	1.189	454.	1431.0	1.56	10.31	18.83	20.89
# 249	1.392	0.600	1.160	454.	1423.8	1.54	10.06	18.31	20.35
# 250	1.430	0.531	1.347	343.	956.8	1.38	12.01	20.13	21.96
# 251	1.430	0.523	1.367	349.	970.4	1.38	12.21	20.46	22.27
# 252	1.415	0.692	1.022	801.	1528.1	1.84	9.58	20.26	22.65
# 253	1.389	0.593	1.171	522.	1387.5	1.57	10.40	19.43	21.49
# 254	1.389	0.612	1.135	603.	1579.8	1.52	10.09	18.60	20.61
# 255	1.389	0.631	1.101	760.	1980.2	1.50	9.79	17.98	19.95
# 256	1.540	0.586	1.314	991.	1888.1	1.46	12.63	21.47	23.33
# 257	1.416	0.517	1.369	411.	1278.2	1.35	12.00	19.83	21.62
# 258	1.416	0.525	1.349	405.	1240.6	1.35	11.84	19.61	21.40
# 259	1.416	0.533	1.328	419.	1305.0	1.35	11.62	19.22	21.04
# 260	1.416	0.534	1.326	421.	1302.7	1.35	11.61	19.23	21.04
# 261	1.416	0.536	1.321	424.	1305.0	1.35	11.57	19.21	20.97
# 262	1.416	0.531	1.333	424.	1305.9	1.35	11.69	19.35	21.16
# 263	1.416	0.541	1.309	423.	1305.4	1.35	11.46	19.01	20.82
# 264	1.416	0.526	1.346	434.	1333.1	1.35	11.81	19.53	21.37
# 265	1.416	0.533	1.328	433.	1358.0	1.35	11.61	19.21	21.02
# 266	1.419	0.528	1.344	454.	1403.4	1.35	11.78	19.48	21.26
# 267	1.469	0.535	1.373	480.	1278.7	1.37	12.41	20.40	22.21
# 268	1.467	0.533	1.376	503.	1361.7	1.39	12.40	20.53	22.37
# 269	1.467	0.535	1.371	568.	1577.1	1.36	12.31	20.12	21.91
# 270	1.467	0.539	1.361	498.	1316.8	1.38	12.30	20.36	22.17
# 271	1.467	0.544	1.348	497.	1316.8	1.38	12.18	20.15	21.99
# 272	1.355	0.522	1.298	367.	1240.2	1.51	11.11	19.99	22.07
# 273	1.454	0.543	1.339	511.	1203.9	1.35	12.30	20.49	22.28
# 274	1.458	0.534	1.365	470.	1169.9	1.34	12.45	20.48	22.27
# 275	1.554	0.637	1.220	740.	1674.1	1.66	11.36	20.37	22.45
# 276	1.549	0.634	1.222	768.	1726.2	1.66	11.39	20.46	22.54
# 277	1.549	0.648	1.195	855.	1813.3	1.68	11.23	20.46	22.57
# 278	1.486	0.507	1.465	375.	1256.0	1.18	12.89	19.15	20.76
# 279	1.411	0.548	1.287	435.	1285.9	1.35	11.33	18.93	20.74

# 280	1.413	0.533	1.326	402.	1165.3	1.35	11.72	19.55	21.34
# 281	1.471	0.549	1.340	536.	1496.3	1.40	12.01	19.91	21.72
# 282	1.402	0.521	1.345	335.	938.6	1.39	11.95	20.36	22.22
# 283	1.365	0.545	1.252	299.	1043.4	1.44	10.67	18.66	20.59
# 284	1.324	0.538	1.230	284.	958.1	1.40	10.46	18.50	20.40
# 285	1.422	0.541	1.314	338.	1035.2	1.28	11.53	18.59	20.29
# 286	1.305	0.600	1.087	331.	1007.5	1.66	9.33	18.77	21.08
# 287	1.308	0.595	1.099	309.	940.9	1.65	9.44	18.86	21.12
# 288	1.308	0.628	1.041	351.	1078.7	1.65	8.92	17.97	20.21
# 289	1.309	0.640	1.023	326.	1091.0	1.66	8.66	17.41	19.69
# 290	1.307	0.600	1.089	347.	1007.5	1.66	9.41	18.99	21.27
# 291	1.308	0.679	0.963	358.	1228.8	1.65	8.14	16.49	18.66
# 292	1.308	0.596	1.097	296.	936.3	1.67	9.37	18.80	21.10
# 293	1.308	0.593	1.103	262.	933.6	1.66	9.26	18.33	20.63
# 294	1.309	0.697	0.939	342.	1241.5	1.64	7.89	15.92	18.09
# 295	1.305	0.599	1.089	348.	1009.4	1.66	9.41	19.04	21.32
# 296	1.305	0.601	1.086	331.	1009.4	1.66	9.31	18.75	21.05
# 297	1.305	0.661	0.987	396.	1225.2	1.64	8.45	17.11	19.33
# 298	1.305	0.606	1.077	324.	978.5	1.66	9.25	18.64	20.95
# 299	1.305	0.601	1.086	326.	1010.3	1.66	9.29	18.68	20.96
# 300	1.305	0.602	1.084	324.	1007.5	1.66	9.27	18.63	20.91
# 301	1.420	0.750	0.947	774.	1791.1	1.78	8.60	17.71	19.95
# 302	1.420	0.719	0.987	361.	1592.0	1.80	8.31	16.33	18.66
# 303	1.420	0.779	0.911	841.	2348.8	1.66	8.08	15.88	17.94
# 304	1.508	0.699	1.079	571.	1675.9	1.71	9.62	17.80	19.95
# 305	1.464	0.549	1.333	462.	1319.0	1.35	11.90	19.40	21.19
# 306	1.443	0.549	1.314	429.	1116.4	1.39	11.85	20.00	21.83
# 307	1.448	0.535	1.353	511.	1402.5	1.31	12.13	19.69	21.41
# 308	1.448	0.526	1.376	449.	1183.9	1.34	12.43	20.43	22.20
# 309	1.360	0.514	1.323	300.	1066.5	1.33	11.26	18.80	20.61
# 310	1.415	0.543	1.303	324.	995.7	1.35	11.41	18.95	20.74
# 311	1.387	0.541	1.282	365.	1310.4	1.38	10.93	18.39	20.25
# 312	1.410	0.727	0.970	782.	1960.2	1.86	8.69	18.28	20.68
# 313	1.588	0.757	1.049	937.	2318.9	1.87	9.68	18.46	20.75
# 314	1.407	0.671	1.048	704.	1510.4	1.80	9.63	19.90	22.25
# 315	1.407	0.691	1.018	838.	1701.8	1.78	9.43	19.55	21.85
# 316	1.407	0.694	1.014	954.	2155.2	1.75	9.23	18.77	21.03
# 317	1.440	0.508	1.417	342.	1071.0	1.23	12.47	19.41	21.09
# 318	1.443	0.485	1.488	329.	1089.6	1.24	13.03	20.18	21.83
# 319	1.364	0.540	1.263	359.	1255.1	1.52	10.76	19.36	21.42
# 320	1.568	0.638	1.229	774.	1782.5	1.78	11.44	21.09	23.33
# 321	1.358	0.549	1.237	358.	1203.0	1.53	10.58	19.28	21.34

# 322	1.359	0.562	1.209	410.	1283.7	1.52	10.44	19.10	21.14
# 323	1.359	0.551	1.233	396.	1225.2	1.52	10.68	19.49	21.55
# 324	1.417	0.656	1.080	461.	1433.8	1.71	9.41	18.12	20.33
# 325	1.321	0.499	1.324	235.	856.5	1.50	11.15	20.20	22.31
# 326	1.396	0.567	1.231	476.	1468.2	1.46	10.72	18.81	20.76
# 327	1.464	0.531	1.379	485.	1500.0	1.41	12.18	20.11	21.94
# 328	1.295	0.530	1.222	251.	820.7	1.37	10.39	18.49	20.37
# 329	1.295	0.531	1.219	265.	924.1	1.40	10.27	18.40	20.33

APPENDIX D. NHTSA VEHICLE KEY

		Model Year	Make	Vehicle Model	Occupants	Ballast (N)	Drive Axle	Fuel Tank
Vehicle #	1	1984	Audi	Quattro 4000	0	0	4	F
Vehicle #	2	1986	BMW	325i	0	0	R	F
Vehicle #	3	1986	Buick	Century Estate	1	0	F	F
Vehicle #	4	1986	Buick	Electra	0	0	F	F
Vehicle #	5	1986	Buick	Electra	0	0	F	N/A
Vehicle #	6	1986	Buick	Electra	0	0	F	F
Vehicle #	7	1986	Buick	Electra	0	0	F	F
Vehicle #	8	1986	Buick	Electra	0	0	F	F
Vehicle #	9	1986	Buick	Electra	0	0	F	F
Vehicle #	10	1986	Buick	Electra	0	0	F	F
Vehicle #	11	1986	Buick	Skylark	0	0	F	F
Vehicle #	12	1991	Chevrolet	1500 Silverado	0	0	R	F
Vehicle #	13	1988	Chevrolet	Astro Van	1	0	R	F
Vehicle #	14	1988	Chevrolet	Astro Van	1	0	R	E
Vehicle #	15	1988	Chevrolet	Astro Van	6	0	R	F
Vehicle #	16	1982	Chevrolet	C-10 Blazer	0	0	R	F
Vehicle #	17	1988	Chevrolet	C-10 pickup	1	0	R	E
Vehicle #	18	1982	Chevrolet	C-10 pickup	0	0	R	F
Vehicle #	19	1987	Chevrolet	C-15 pickup	N/A Lt Ld		R	F
Vehicle #	20	1987	Chevrolet	C-15 pickup	0	0	R	F
Vehicle #	21	1981	Chevrolet	C-20 pickup	1	0	R	F
Vehicle #	22	1983	Chevrolet	Caprice	0	0	R	F
Vehicle #	23	1984	Chevrolet	Caprice Classic	1	0	R	F
Vehicle #	24	1983	Chevrolet	Cavalier	1	0	F	F
Vehicle #	25	1978	Chevrolet	K-10 Blazer	0	0	4	F
Vehicle #	26	1991	Chevrolet	K1500 pickup	3	0	4	F
Vehicle #	27	1991	Chevrolet	K1500 pickup	1	0	4	F

Vehicle #	28	1990	Chevrolet	Lumina APV	2	4226	F	F
Vehicle #	29	1990	Chevrolet	Lumina APV	2	4226	F	F
Vehicle #	30	1990	Chevrolet	Lumina APV	0	0	F	F
Vehicle #	31	1990	Chevrolet	Lumina APV	1	0	F	F
Vehicle #	32	1990	Chevrolet	Lumina APV	1	0	F	F
Vehicle #	33	1990	Chevrolet	Lumina APV	7	0	F	F
Vehicle #	34	1990	Chevrolet	Lumina APV	2	0	F	F
Vehicle #	35	1990	Chevrolet	Lumina APV	0	0	F	F
Vehicle #	36	1981	Chevrolet	Luv	0	0	R	F
Vehicle #	37	1984	Chevrolet	S-10 Blazer	0	0	4	F
Vehicle #	38	1984	Chevrolet	S-10 Blazer	0	0	R	F
Vehicle #	39	1983	Chevrolet	S-10 Blazer	0	0	R	F
Vehicle #	40	1992	Chevrolet	S-10 Blazer	0	0	4	F
Vehicle #	41	1989	Chevrolet	S-10 Blazer	1	0	4	F
Vehicle #	42	1986	Chevrolet	S-10 pickup	0	0	R	F
Vehicle #	43	1992	Chevrolet	S-10 pickup	0	0	4	F
Vehicle #	44	1991	Chevrolet	S-10 pickup	0	0	R	F
Vehicle #	45	1987	Chevrolet	S-10 Tahoe	0	0	4	F
Vehicle #	46	1987	Chevrolet	S-10 Tahoe	N/A	GVWR	4	F
Vehicle #	47	1987	Chevrolet	S-10 Tahoe	N/A	Lt Ld	4	F
Vehicle #	48	1992	Chevrolet	Sportside K-10 pi	0	0	4	F
Vehicle #	49	1987	Chrysler	LeBaron	0	0	F	F
Vehicle #	50	1985	Chrysler	LeBaron	0	0	F	F
Vehicle #	51	1979	Datsun	210	0	0	R	F
Vehicle #	52	1979	Datsun	280ZX	0	0	R	F
Vehicle #	53	1974	Datsun	B210	0	0	R	F
Vehicle #	54	1981	Datsun	pickup	0	0	R	F
Vehicle #	55	1991	Dodge	Caravan	1	0	F	F
Vehicle #	56	1988	Dodge	Caravan	1	0	F	E
Vehicle #	57	1992	Dodge	Caravan	1	0	F	F
Vehicle #	58	1987	Dodge	Caravan	N/A	Lt Ld	F	F
Vehicle #	59	1987	Dodge	Caravan	N/A	GVWR	F	F
Vehicle #	60	1991	Dodge	Caravan	1	0	F	F
Vehicle #	61	1987	Dodge	Caravan	0	0	F	F
Vehicle #	62	1988	Dodge	Caravan	0	0	F	F
Vehicle #	63	1991	Dodge	Caravan	1	0	F	F
Vehicle #	64	1992	Dodge	Caravan	1	0	F	F
Vehicle #	65	1992	Dodge	Caravan	1	0	F	F
Vehicle #	66	1992	Dodge	Caravan	1	0	F	F
Vehicle #	67	1990	Dodge	Caravan	0	0	F	F
Vehicle #	68	1989	Dodge	Caravan C/V	1	0	F	E
Vehicle #	69	1989	Dodge	Colt	1	0	F	E

Vehicle # 70	1987 Dodge	Dakota	N/A Lt Ld	R	F
Vehicle # 71	1987 Dodge	Dakota	0	0	R	F
Vehicle # 72	1987 Dodge	Dakota	N/A	GVWR	R	F
Vehicle # 73	1991 Dodge	Dakota	0	0	F	F
Vehicle # 74	1992 Dodge	Dakota	0	0	R	F
Vehicle # 75	1978 Dodge	Diplomat	0	0	R	F
Vehicle # 76	1989 Dodge	Dynasty LE	1	0	F	F
Vehicle # 77	1985 Dodge	Lancer	0	0	F	F
Vehicle # 78	1983 Dodge	Omni	1	0	F	F
Vehicle # 79	1983 Dodge	Omni	1	0	F	E
Vehicle # 80	1983 Dodge	Omni	2	0	F	F
Vehicle # 81	1983 Dodge	Omni	4	0	F	F
Vehicle # 82	1987 Dodge	Raider	0	0	4	F
Vehicle # 83	1989 Dodge	Raider	1	0	4	F
Vehicle # 84	1989 Dodge	Raider	4	0	4	F
Vehicle # 85	1989 Dodge	Raider	4	2335	4	F
Vehicle # 86	1989 Dodge	Raider	4	2335	4	F
Vehicle # 87	1981 Dodge	Ram	0	0	R	F
Vehicle # 88	1987 Dodge	Ram B-150	1	0	R	F
Vehicle # 89	1991 Dodge	Ram D-150	3	0	R	F
Vehicle # 90	1991 Dodge	Ram D-150	1	0	R	F
Vehicle # 91	1991 Dodge	Ramcharger	1	0	4	F
Vehicle # 92	1988 Ford	Aerostar	0	0	R	F
Vehicle # 93	1991 Ford	Aerostar	0	0	R	F
Vehicle # 94	1992 Ford	Aerostar	0	0	4	F
Vehicle # 95	1986 Ford	Aerostar XL	1	0	R	F
Vehicle # 96	1992 Ford	Aerostar, long	0	0	4	F
Vehicle # 97	1978 Ford	Bronco	0	0	4	F
Vehicle # 98	1987 Ford	Bronco II	0	0	R	F?
Vehicle # 99	1988 Ford	Bronco II	1	0	4	E
Vehicle # 100	1988 Ford	Bronco II	1	0	4	E
Vehicle # 101	1989 Ford	Bronco II XL	1	0	R	E
Vehicle # 102	1983 Ford	Bronco XLT	0	0	4	F
Vehicle # 103	1992 Ford	E150	0	0	R	F
Vehicle # 104	1985 Ford	E150	1	0	R	F
Vehicle # 105	1978 Ford	E150	0	0	R	F
Vehicle # 106	1977 Ford	E250	0	0	R	F
Vehicle # 107	1985 Ford	Escort	0	0	F	F
Vehicle # 108	1986 Ford	Escort XR3i	0	0	F	F
Vehicle # 109	1992 Ford	Explorer	0	N/A	R	F
Vehicle # 110	1992 Ford	Explorer Sport	1	0	4	F
Vehicle # 111	1991 Ford	Explorer XL	1	0	4	F

Vehicle # 112	1991 Ford	Explorer XL	1	0	4	F
Vehicle # 113	1991 Ford	Explorer XL	5	1268	4	F
Vehicle # 114	1991 Ford	Explorer XL	5	1268	4	F
Vehicle # 115	1991 Ford	Explorer XL	5	0	4	F
Vehicle # 116	1982 Ford	F100	0	0	R	F
Vehicle # 117	1987 Ford	F150	0	0	R	F
Vehicle # 118	1987 Ford	F150	0	Lt Ld	R	F
Vehicle # 119	1987 Ford	F150	0	0	R	F
Vehicle # 120	1987 Ford	F150	N/A	GVWR	R	F
Vehicle # 121	1987 Ford	F150	1	0	R	E
Vehicle # 122	1987 Ford	F150	1	0	R	F
Vehicle # 123	1987 Ford	F150	1	0	R	F
Vehicle # 124	1987 Ford	F150	1	0	R	F
Vehicle # 125	1987 Ford	F150	1	0	R	F
Vehicle # 126	1987 Ford	F150	1	0	R	F
Vehicle # 127	1987 Ford	F150	1	0	R	F
Vehicle # 128	1987 Ford	F150	3	0	R	F
Vehicle # 129	1987 Ford	F150	0	0	R	F
Vehicle # 130	1984 Ford	F150	1	0	4	F
Vehicle # 131	1990 Ford	F150	0	0	R	F
Vehicle # 132	1992 Ford	F150 Sport	0	0	R	F
Vehicle # 133	1992 Ford	F150 Sport	0	0	R	F
Vehicle # 134	1992 Ford	F150 XLT	0	0	R	F
Vehicle # 135	1991 Ford	F150 XLT Lariat	0	0	R	F
Vehicle # 136	1984 Ford	F250	1	0	R	F
Vehicle # 137	1973 Ford	F250	0	0	R	F
Vehicle # 138	1991 Ford	Festiva	4	0	F	F
Vehicle # 139	1991 Ford	Festiva	1	0	F	F
Vehicle # 140	1991 Ford	Festiva	4	556	F	F
Vehicle # 141	1991 Ford	Festiva	4	556	F	F
Vehicle # 142	1980 Ford	LTD	0	0	R	F
Vehicle # 143	1988 Ford	Mustang GL	0	0	R	F
Vehicle # 144	1988 Ford	Mustang GT	0	0	R	F
Vehicle # 145	1981 Ford	Ranchero	0	0	R	F
Vehicle # 146	1985 Ford	Ranger	0	0	R	F
Vehicle # 147	1985 Ford	Ranger	N/A	Lt Ld	R	F
Vehicle # 148	1985 Ford	Ranger	N/A	GVWR	R	F
Vehicle # 149	1991 Ford	Ranger	1	0	R	F
Vehicle # 150	1992 Ford	Ranger	1	0	R	F
Vehicle # 151	1991 Ford	Ranger	1	0	R	F
Vehicle # 152	1991 Ford	Ranger	1	0	R	F
Vehicle # 153	1991 Ford	Ranger	1	0	R	F

Vehicle # 154	1991 Ford	Ranger	1	0	R	F
Vehicle # 155	1991 Ford	Ranger	1	0	R	F
Vehicle # 156	1991 Ford	Ranger	1	0	R	F
Vehicle # 157	1992 Ford	Ranger	1	0	R	F
Vehicle # 158	1991 Ford	Ranger	1	0	R	F
Vehicle # 159	1992 Ford	Ranger XLT	0	0	R	F
Vehicle # 160	1988 Ford	Taurus	0	0	F	F
Vehicle # 161	1992 Ford	Taurus	0	0	F	F
Vehicle # 162	1988 Ford	Taurus	1	0	F	F
Vehicle # 163	1987 Ford	Tempo	0	0	F	F
Vehicle # 164	1987 Ford	Thunderbird LX	1	Lt Ld	R	F
Vehicle # 165	1987 Ford	Thunderbird LX	1	0	R	F
Vehicle # 166	1987 Ford	Thunderbird LX	1	0	R	F
Vehicle # 167	1987 Ford	Thunderbird LX	2	0	R	F
Vehicle # 168	1991 Geo	Metro	1	0	F	F
Vehicle # 169	1991 Geo	Tracker LSI	1	0	4	F
Vehicle # 170	1991 Geo	Tracker LSI	4	667	4	F
Vehicle # 171	1991 Geo	Tracker LSI	4	667	4	F
Vehicle # 172	1991 Geo	Tracker LSI	4	0	4	F
Vehicle # 173	1991 Geo	Tracker LSI	0	0	4	F
Vehicle # 174	1985 GMC	C-15 pickup	0	0	R	F
Vehicle # 175	1984 GMC	C-20 Suburban	0	0	R	F
Vehicle # 176	1982 GMC	C-20 Suburban	0	0	4	F
Vehicle # 177	1990 GMC	Jimmy ST	0	0	4	F
Vehicle # 178	1991 GMC	Sierra C-10 1500	1	0	R	F
Vehicle # 179	1991 GMC	Sierra C-10 1500	3	0	R	F
Vehicle # 180	1991 GMC	Sierra SLE 1500	1	0	R	F
Vehicle # 181	1990 GMC	Suburban 1500	1	0	4	F
Vehicle # 182	1991 Honda	Accord LX	5	200	F	F
Vehicle # 183	1991 Honda	Accord LX	1	0	F	F
Vehicle # 184	1991 Honda	Accord LX	5	0	F	F
Vehicle # 185	1991 Honda	Accord LX	5	200	F	F
Vehicle # 186	1983 Honda	Civic	0	0	F	F
Vehicle # 187	1986 Hyundai	Excel	0	0	F	F
Vehicle # 188	1987 Hyundai	Excel	1	Lt Ld	F	N/A
Vehicle # 189	1987 Hyundai	Excel	4	0	F	F
Vehicle # 190	1987 Hyundai	Excel	1	0	F	F
Vehicle # 191	1978 IH	Scout	0	0	4	F
Vehicle # 192	1991 Isuzu	Amigo XL	1	0	4	F
Vehicle # 193	1986 Isuzu	pickup	0	0	R	F
Vehicle # 194	1991 Isuzu	Rodeo	1	0	4	F
Vehicle # 195	1991 Isuzu	Rodeo	1	0	4	F

Vehicle # 196	1992 Isuzu	Rodeo	1	0	4	F
Vehicle # 197	1991 Isuzu	Rodeo	1	0	4	F
Vehicle # 198	1992 Isuzu	Rodeo	1	0	4	F
Vehicle # 199	1991 Isuzu	Rodeo	1	0	4	F
Vehicle # 200	1991 Isuzu	Rodeo	1	0	4	F
Vehicle # 201	1991 Isuzu	Rodeo	1	0	4	F
Vehicle # 202	1991 Isuzu	Rodeo	1	0	4	F
Vehicle # 203	1991 Isuzu	Rodeo	1	0	4	F
Vehicle # 204	1991 Isuzu	Rodeo	1	0	4	F
Vehicle # 205	1988 Isuzu	Trooper	0	0	4	F
Vehicle # 206	1988 Isuzu	Trooper	4	0	4	F
Vehicle # 207	1988 Isuzu	Trooper	2	0	4	F
Vehicle # 208	1991 Isuzu	U-15 pickup	1	0	4	F
Vehicle # 209	1986 Jeep	Cherokee	0	0	4	F
Vehicle # 210	1984 Jeep	Cherokee	2	1446	4	F
Vehicle # 211	1984 Jeep	Cherokee	0	0	4	F
Vehicle # 212	1984 Jeep	Cherokee	1	0	4	F
Vehicle # 213	1984 Jeep	Cherokee	1	0	4	F
Vehicle # 214	1984 Jeep	Cherokee	4	0	4	F
Vehicle # 215	1988 Jeep	Cherokee	2	0	4	F
Vehicle # 216	1988 Jeep	Cherokee	4	0	4	F
Vehicle # 217	1988 Jeep	Cherokee	0	0	4	F
Vehicle # 218	1987 Jeep	Cherokee	0	0	4	F
Vehicle # 219	1987 Jeep	Cherokee	N/A	Lt Ld	4	F
Vehicle # 220	1987 Jeep	Cherokee	N/A	GVWR	4	F
Vehicle # 221	1977 Jeep	Cherokee	0	0	4	F
Vehicle # 222	1981 Jeep	CJ-5	0	0	4	F
Vehicle # 223	1981 Jeep	CJ-5	1	0	4	F
Vehicle # 224	1975 Jeep	CJ-5 (modified)	0	0	4	F
Vehicle # 225	1983 Jeep	CJ-7	0	0	4	F
Vehicle # 226	1983 Jeep	CJ-7	0	0	4	F
Vehicle # 227	1987 Jeep	Wrangler	0	0	4	F
Vehicle # 228	1988 Jeep	Wrangler	2	0	4	F
Vehicle # 229	1988 Jeep	Wrangler	0	0	4	F
Vehicle # 230	1988 Jeep	Wrangler	4	0	4	F
Vehicle # 231	1992 Lincoln	Continental	0	0	F	F
Vehicle # 232	1986 Mazda	323	0	0	F	F
Vehicle # 233	1984 Mazda	B2000	0	0	R	F
Vehicle # 234	1979 Mazda	GLC	0	0	R	F
Vehicle # 235	1991 Mazda	MPV	1	0	4	F
Vehicle # 236	1987 Mercedes	190	0	0	R	F
Vehicle # 237	1987 Mercedes	190	0	0	R	F

Vehicle # 238	1987	Mercedes	190 E	0	0	R	F
Vehicle # 239	1987	Mercedes	190 E	0	0	R	F
Vehicle # 240	1984	Mercury	Grand Marquis	0	0	R	F
Vehicle # 241	1988	Nissan	Maxima	0	0	F	F
Vehicle # 242	1986	Nissan	Maxima	0	0	F	F
Vehicle # 243	1991	Nissan	Pathfinder	1	0	4	F
Vehicle # 244	1987	Nissan	Pathfinder	0	0	4	F
Vehicle # 245	1985	Nissan	pickup	0	0	R	F
Vehicle # 246	1989	Nissan	pickup	1	0	R	E
Vehicle # 247	1989	Nissan	pickup	1	0	R	E
Vehicle # 248	1989	Nissan	pickup	1	0	R	E
Vehicle # 249	1988	Nissan	pickup	1	0	R	E
Vehicle # 250	1987	Nissan	Sentra	0	0	F	F
Vehicle # 251	1987	Nissan	Sentra	0	0	F	F
Vehicle # 252	1987	Nissan	Van	0	0	R	F?
Vehicle # 253	1987	Nissan	XE King Cab	0	0	R	F
Vehicle # 254	1987	Nissan	XE King Cab	N/A	Lt Ld	R	F
Vehicle # 255	1987	Nissan	XE King Cab	N/A	GVWR	R	F
Vehicle # 256	1980	Oldsmobile	98	0	0	R	F
Vehicle # 257	1990	Oldsmobile	Cutlass Calais	1	0	F	F
Vehicle # 258	1991	Oldsmobile	Cutlass Calais	1	0	F	F
Vehicle # 259	1991	Oldsmobile	Cutlass Calais	1	0	F	F
Vehicle # 260	1991	Oldsmobile	Cutlass Calais	1	0	F	F
Vehicle # 261	1991	Oldsmobile	Cutlass Calais	1	0	F	F
Vehicle # 262	1991	Oldsmobile	Cutlass Calais	1	0	F	F
Vehicle # 263	1991	Oldsmobile	Cutlass Calais	1	0	F	F
Vehicle # 264	1990	Oldsmobile	Cutlass Calais	1	0	F	F
Vehicle # 265	1991	Oldsmobile	Cutlass Calais	1	0	F	F
Vehicle # 266	1990	Oldsmobile	Cutlass Calais	1	0	F	F
Vehicle # 267	1985	Oldsmobile	Cutlass Ciera	0	0	F	F
Vehicle # 268	1985	Oldsmobile	Cutlass Ciera	1	0	F	F
Vehicle # 269	1985	Oldsmobile	Cutlass Ciera	4	0	F	F
Vehicle # 270	1985	Oldsmobile	Cutlass Ciera	1	0	F	E
Vehicle # 271	1985	Oldsmobile	Cutlass Ciera	1	0	F	E
Vehicle # 272	1980	Plymouth	Arrow	0	0	R	F
Vehicle # 273	1985	Plymouth	Reliant	0	0	F	F
Vehicle # 274	1987	Plymouth	Sundance	0	0	F	F
Vehicle # 275	1992	Plymouth	Voyager	1	0	F	F
Vehicle # 276	1991	Plymouth	Voyager	1	0	F	F
Vehicle # 277	1991	Plymouth	Voyager	1	0	F	F
Vehicle # 278	1985	Pontiac	Fiero	0	0	R	F
Vehicle # 279	1989	Pontiac	Grand Am	1	0	F	E

Vehicle # 280	1985 Pontiac	Grand Am	0	0	F	F
Vehicle # 281	1978 Pontiac	LeMans	0	0	R	F
Vehicle # 282	1988 Pontiac	LeMans	0	0	F	F
Vehicle # 283	1984 Subaru	Brat	0	0	4	F
Vehicle # 284	1991 Subaru	Justy GL	1	0	F	F
Vehicle # 285	1987 Subaru	XT Coupe	0	0	F	F
Vehicle # 286	1988 Suzuki	Samurai	1	0	4	F
Vehicle # 287	1988 Suzuki	Samurai	0	0	4	F
Vehicle # 288	1988 Suzuki	Samurai	2	0	4	F
Vehicle # 289	1988 Suzuki	Samurai	2	0	4	F
Vehicle # 290	1988 Suzuki	Samurai	1	0	4	F
Vehicle # 291	1988 Suzuki	Samurai	4	0	4	F
Vehicle # 292	1988 Suzuki	Samurai	0	0	4	F
Vehicle # 293	1988 Suzuki	Samurai	0	0	4	F
Vehicle # 294	1988 Suzuki	Samurai	4	0	4	F
Vehicle # 295	1988 Suzuki	Samurai	1	0	4	F
Vehicle # 296	1988 Suzuki	Samurai	1	0	4	F
Vehicle # 297	1988 Suzuki	Samurai	4	0	4	F
Vehicle # 298	1988 Suzuki	Samurai	1	0	4	E
Vehicle # 299	1988 Suzuki	Samurai	1	0	4	F
Vehicle # 300	1988 Suzuki	Samurai	1	0	4	F
Vehicle # 301	1987 Toyota	4Runner	N/A Lt Ld		4	F
Vehicle # 302	1987 Toyota	4Runner	0	0	4	F
Vehicle # 303	1987 Toyota	4Runner	N/A GVWR+		4	F
Vehicle # 304	1989 Toyota	4Runner	1	0	4	F
Vehicle # 305	1987 Toyota	Camry	0	0	F	F
Vehicle # 306	1983 Toyota	Camry	0	0	F	F
Vehicle # 307	1983 Toyota	Camry	4	0	F	F
Vehicle # 308	1983 Toyota	Camry	1	0	F	F
Vehicle # 309	1976 Toyota	Corolla	0	0	R	F
Vehicle # 310	1987 Toyota	Corolla FX	0	0	F	F
Vehicle # 311	1982 Toyota	Cressida	0	0	R	F
Vehicle # 312	1979 Toyota	Land Cruiser	0	0	4	F
Vehicle # 313	1991 Toyota	Land Cruiser	1	0	4	F
Vehicle # 314	1987 Toyota	LE Van	0	0	R	F
Vehicle # 315	1987 Toyota	LE Van	N/A Lt Ld		R	F
Vehicle # 316	1987 Toyota	LE Van	N/A GVWR		R	F
Vehicle # 317	1986 Toyota	MR2	0	0	R	F
Vehicle # 318	1986 Toyota	MR2	0	0	R	F
Vehicle # 319	1989 Toyota	pickup	0	0	R	F
Vehicle # 320	1991 Toyota	Previa LE	1	0	R	F
Vehicle # 321	1988 Toyota	RN50 pickup	0	0	R	F

Vehicle # 322	1986	Toyota	RN50 pickup	2	0	R	F
Vehicle # 323	1986	Toyota	RN50 pickup	1	0	R	F
Vehicle # 324	1986	Toyota	RN60 pickup	0	0	4	F
Vehicle # 325	1971	Volkswagen	Beetle	0	0	R	F
Vehicle # 326	1991	Volvo	240	1	0	R	F
Vehicle # 327	1991	Volvo	740	1	0	R	F
Vehicle # 328	1987	Yugo	GV	0	0	F	F
Vehicle # 329	1988	Yugo	GV	1	0	F	F